Université d'Ottawa · University of Ottawa

Biochemical Properties of the Muscle-Specific Ca^{2+}/Calmodulin-Dependent Protein Kinase II β Isoform

George J. Chatzis

Thesis submitted in partial fulfillment
of the requirements for the degree of
Master of Science (Pharmacology)

Department of Cellular and Molecular Medicine
Faculty of Medicine
University of Ottawa
Ottawa, Ontario

Dedicated to my parents, Katerina and Ioannis Chatzis and to my grandparents Maria and Georgios Chatzis, for their love of education.

Abstract

Cytosolic calcium (Ca^{2+}) levels are critical for the control of muscle contraction and are tightly regulated by a variety of Ca^{2+} transport systems localized in various membranes. Ca^{2+} binding proteins such as calmodulin (CaM) and Ca^{2+}/CaM-dependent protein kinases (CaM Kinases) are believed to exert major regulatory control on Ca^{2+} activity. Previous studies in this lab led to the cloning of a cDNA encoding a CaM Kinase II β isoform from skeletal muscle that differed from the classical β isoform by the inclusion of three alternatively spliced exons in the variable domain which were enriched in proline residues.

A CaM Kinase, assumed to be localized in the sarcoplasmic reticulum (SR), has been implicated in the regulation of excitation-contraction (E-C) coupling. We hypothesized that this novel CaM Kinase II β isoform called SOCK (Son Of CaM Kinase) may be the CaM Kinase II isoform that regulates E-C coupling by being targeted to specific regions of the SR, whereby it phosphorylates critical Ca^{2+} transporting proteins such as the ryanodine (RyR) and dihydropyridine (DHPR) receptors in response to changes in Ca^{2+} levels. In order to gain insight into the sub cellular distribution of this CaM Kinase II isoform in skeletal muscle, sub cellular membrane fractions were isolated from skeletal muscle by centrifugation on a discontinuous sucrose gradient. Western blots performed on these fractions indicated that the CaM Kinase II isoforms including SOCK and the CaM Kinase II anchoring protein αKAP had similar cofractionated with the ryanodine receptor (RyR1)-calcium release channel (RyR1). Furthermore, the CaM Kinase II β isoform detected with a CaM Kinase II β specific antibody (Cbβ-1) consisted of a polypeptide with an apparent molecular weight of 73 kDa corresponding to the size

predicted from the cDNA sequence of SOCK. The 60/58 kDa neuronal CaM Kinase II β isoforms were not detected in skeletal muscle fractions. Double-immunohistochemical staining of skeletal muscle sections performed with RyR1 and CaM Kinase II β-specific monoclonal antibodies revealed an overlapping striated pattern of immunofluorescence. This indicates that both proteins are in close proximity to each other in the terminal cisternae of the SR.

Since our results demonstrated that SOCK co-localizes with RyR1 in the SR, we postulated that this kinase might regulate excitation-contraction coupling by phosphorylating key proteins involved in this process. Recombinant SOCK was found to phosphorylate the RyR1, DHPR α_{1S} and DHPR β_{1A} subunits in *in vitro* assays. A comparison of the substrate specificity of the endogenous CaM Kinase II isoforms in skeletal muscle SR was determined with kinase assays using purified triads. The DHPR α_{1S} and DHPR β_{1A} subunits of the L-type Ca^{2+} channel, but not the RyR1 were phosphorylated in a Ca^{2+}/CaM-dependent manner.

The proline rich insert of SOCK implied that this region may interact with proteins that contain SH3 domains, potentially targeting proteins in tyrosine kinase and MAP kinase signaling pathways to the terminal cisternae of the SR. The three alternatively spliced exons in SOCK contain three proline rich tandem repeats with multiple P-X-X-P consensus sequences of SH3 binding domains. The specific P-X-X-P sequences encoded by the third exon were homologous to sequences in proteins known to bind the SH3 domains of Grb2 and Src. Investigation of the association of SOCK with SH3 domains was determined by immunoprecipitating Grb2 and Src from solubilized membrane fractions and detecting the presence of SOCK in Western blot analysis. SOCK

was specifically detected in Grb2 and Src immunoprecipitates, but was not detected when the Grb2 and Src specific antibodies were neutralized with blocking peptides. Overlay experiments with biotinylated SH3 domains indicated that the SH3 domain of Src and the N-terminal SH3 domain of Grb2 specifically associate with sequences encoded by exons P1 and P3, but not with the sequence encoded by exon P2. Furthermore, the association of these SH3 domains with SOCK were found to significantly decrease the phosphorylation of the CaM Kinase II specific substrate Auto Camtide II as determined in *in vitro* CaM Kinase II assays. Attempts to identify the minimal Grb2/Src binding sites using site directed mutagenesis indicated that multiple P-X-X-P motifs in P1 and P3 may be responsible for the binding.

These results suggest that SOCK represents the CaM Kinase II β isoform in skeletal muscle. Targeting of SOCK to the SR may serve in the regulation of E-C coupling via phosphorylation of the DHPR α_{1S} and DHPR β_{1A} subunits of the L-type Ca^{2+} channel and possibly the RyR1. The association of the proline rich region of SOCK with SH3 domains may serve to integrate Ca^{2+} and tyrosine kinase signaling pathways by targeting kinases such as Src or adapter proteins like Grb2 to the E-C coupling apparatus.

Acknowledgements

I would like to thank my supervisor, Dr. Balwant S. Tuana for allowing me to pursue exciting research in his laboratory and for supporting me over the past few years. His open-mindedness allowed me to expand my problem-solving skills and grow as a scientist. Special thanks to Drs. Stephen Gee, Anthony Gramolini, Bernard Jasmin, Anthony Krantis, Sam Kacew, John Leddy, Stephen Lee, Jean-Marc Renaud and William Staines, for their suggestions and assistance throughout this project. I would especially like to thank Maysoon Salih for teaching me the ways of molecular biology and for assisting me in overcoming experimental challenges. Maysoon, you have the 'golden-touch', even King Midas would want to clone your hands! I also wish to thank the members of our lab for their assistance, support and companionship: Rosa Guzzo, Serdal Sevinc, Kevin Wong, Thanya Ganendran and Paul Wielowieyski. I would also like to thank the numerous people who made Ottawa feel like home and science fun: John Lunde (For Respecting My Limits!), Abdel Basset Elzaghalai (For keeping me awake on graveyard shifts at the lab!), Rosa Guzzo (The sister I never had!), Wadih Matar (For being Wadih!), Kambiz Musave and Joe Chakkalakal (For the smooth mix of science, beer and house music to the break of dawn!), Mark Stocksley (For the smooth mix of science and beer!) Jen Thompson (For the positive Chi!), Ian Sutcliffe (For encouraging me!), Ian Laquian, Andreanne Bonhomme, Dan Katachi, Sam Qutob, Neena Kushwaha, Lambro Pezoulas and Kostas Karagiozis. Finally a special thanks to my parents Ioannis and Katerina Chatzis, my grandparents Maria and Georgios Chatzis and Anastasia and Konstantine Parasidis and also to Annie Aubry who have supported and encouraged me in so many ways.

TABLE OF CONTENTS

LIST OF TABLES

LIST OF FIGURES

LIST OF ABREVIATIONS

AKAP	cAMP-dependent kinase anchoring protein
AMP	Adenosine monophosphate
AP	action potential
ATP	Adenosine triphosphate
AV	atrioventricular
βAR	beta adrenergic receptor
BCA	bicinchoninic acid
bp	base pair
BSA	bovine serum albumen
CaM	Calmodulin
CaM K	Ca^{2+}/CaM-dependent protein kinase
CFA	complete Freund's adjuvant
CHAPS	3-([cholamidpropyl]-dimethylaminio)-2-hydroxyl-1-propanesulfonate
CICR	calcium induced calcium release
CREB	cAMP response element binding protein
DAG	diacylglycerol
DHP	Dihydropyridine
DMSO	Dimethyl sulfoxide
DTT	Dithiothreitol
EAD	early-after depolarization
E-C	excitation-contraction
ECL	enhanced chemiluminescence
EDTA	ethylene-diamine-tetra-acetic acid
EF-2	elongation factor-2
EGTA	ethyleneglycol-bis(β-aminoethyl ether)-N,N'-tetraacetic acid
EPSP	excitatory post-synaptic potential
ET	endothelin
FITC	fluorescien isothiocyanate

GST	glutathione-S-transferase
HEPES	4-(2-hydroxyethyl)-1-piperazineethanesulfonate
HRP	horse radish peroxidase
IFA	incomplete Freund's adjuvant
IgG	immunoglobulin G
IgM	immunoglobulin M
IPTG	isopropyl-1-thio-β-D-galactopyranoside
IP_3	inositol triphosphate
LTD	long term depression
LTP	long term potentiation
MLCK	myosin light chain kinase
MOPS	3-[N-Morpholine]propanesulfonic acid
NLS	nuclear localization signal
NO	nitric oxide
NP-40	Nonidet P-40
nt	nucleotide
PAGE	polyacrylamide gel electrophoresis
PBS	phosphate buffered saline
PCR	polymerase chain reaction
PIPES	piperazine-N,N'-bis(ethanesulfonic acid)
PIP_2	phosphatidylinositol 4,5-bisphosphate
PKA	cAMP-dependent protein kinase
PKC	protein kinase C
PLC	phospholipase C
PMSF	phenylmethylsulfonyl fluoride
P_o	open probability
PPD	p-Phenylenediamine
PVDF	polyvinyl dinitro-fluoride
RACK	receptor for activated C kinase
RPM	revolutions per minute
RyR	ryanodine receptor

SA	sinoatrial
SDS	sodium dodecyl sulfate
SE	succinimidyl ester
SH3	Src homology three
SOCK	son of CaM kinase
SR	sarcoplasmic reticulum
TBS	tris buffered saline
T_m	melting temperature
Tris	Tris(hydroxymethyl)aminomethane
Triton-X-100	octylphenol ethylene oxide condensate
T-tubule	transverse-tubule
Tween 20	polyoxyethylene sorbitan monolaurate

CHAPTER 1 INTRODUCTION

1.1 General

The human body contains approximately 650 muscles, which constitute about 35% - 40% of the female and male body weight, respectively. The purpose of muscle is to contract and generate force. Contraction of muscle is a vital component of many biological processes such as locomotion, blood circulation, digestion, respiration and visual acuity.

The development of the light microscope led to the classification of muscle into two types, striated and smooth. The microscope revealed the characteristic striated pattern of alternating light and dark bands in skeletal and cardiac muscle, which was absent in smooth muscle. Skeletal muscle, as the name implies, is connected to the skeleton of bones. Contraction of these muscles results in the motion of bones as well as the maintenance of gait or pusture via muscle tone. Movement of the body is voluntary and under conscious control, so skeletal muscle is innervated by the somatic nervous system.

A single skeletal muscle cell is known as a muscle fiber. Each muscle fiber is formed during embryonic development by the fusion of a number of undifferentiated, mono-nucleated cells known as myoblasts. Fusion of myoblasts leads to the formation of multinucleated cells known as myotubes (Ontell and Kezeka, 1984). As the proteins required for contraction are expressed, the myotubes grow in diameter and length, pushing the nuclei to the periphery and ensuring unobstructed end-to-end spanning of the contractile machinery. The process of muscle differentiation is completed by the time of birth and the fibers continue to grow as the neonate grows.

The striated pattern of skeletal and cardiac muscle results from the presence of thick and thin protein filaments in the cytoplasm, which are organized into cylindrical bundles known as myofibrils. The myofibrils are typically 1 μm wide (Vender et al., 1994). The myofibril is built from a bundle of several hundreds protein filaments in parallel and arranged in a repeating pattern (Figure 1.1). One unit of this repeating pattern is termed a *sarcomere* and represents the minimal contractile unit of skeletal and cardiac muscle. The dark band in the middle of each sarcomere contains the thick filaments composed almost entirely of the contractile protein myosin and is termed the *A band*. Two sets of thin filaments flank and partially overlap the thick filaments. The thin filaments are composed mainly of the contractile protein actin which is in close association with the regulatory proteins troponin and tropomyosin and together form the *I band* (Vander et al. 1994). An *A band* and two half *I bands* comprise the sarcomere and are demarcated by the Z line, which is composed largely of α-actinin and forms a network of interconnecting proteins that anchor one side of the thin filaments (Pollack, 1990) (figure 1.1).

Shortening of a muscle fiber is a result of the tension generated by the interaction of myosin with actin. Myosin is composed of a long tail and a globular head that contains an actin binding site and an enzymatic ATPase site that hydrolyzes ATP to ADP and inorganic phosphate. Hydrolysis of ATP yields 7 kcal/mol of energy that can be used to perform work. When a muscle is at rest, the ATPase site of myosin has already hydrolyzed ATP and is prepared to do work. Depolarization of the plasma membrane triggers the release of Ca^{2+} from the SR into the sarcoplasm. Cytosolic Ca^{2+} binds to troponin C, causing the tropomyosin strands to

Figure 1.1 Myofibril Structure Illustrating Thick and Thin Filament Organization of the Sarcomere

Myofibrils are composed of alternating bands of thick and thin filaments. One unit of this repeating structure is called a sarcomere, contained within two Z lines. Two sets of thin actin filaments flank each Z line. The I band represents regions in the thin filaments that do not overlap with thick filaments. The thick myosin filaments are contained within the A band and the H zone represents the region in which thin filaments do not overlap thick filaments. The H zone and I band decrease in length as contraction pulls the two sets of thin filaments toward the M line.

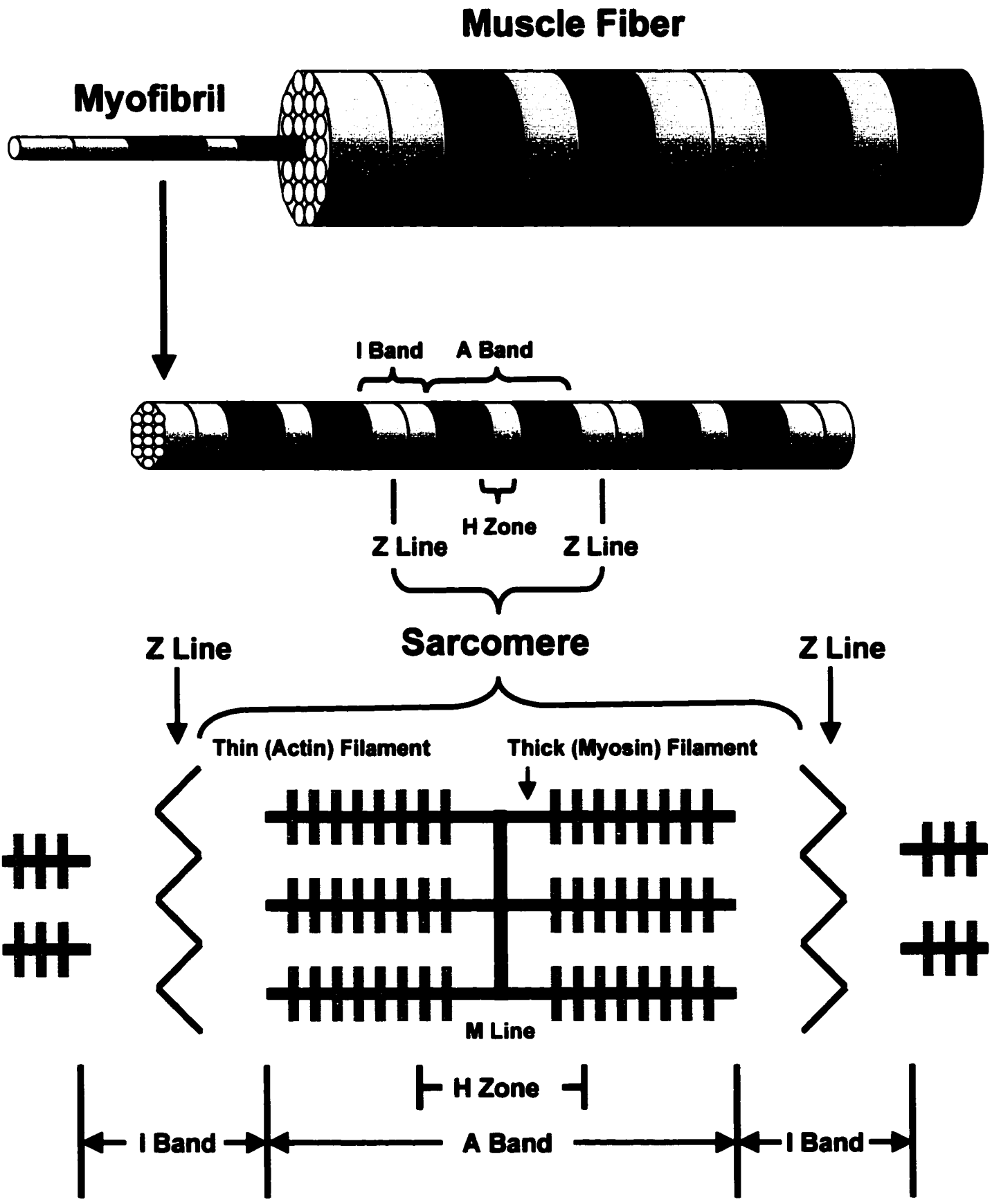
Muscle Fiber
Myofibril
I Band
A Band
H Zone
Z Line
Z Line
Sarcomere
Z Line
Z Line
Thin (Actin) Filament
Thick (Myosin) Filament
M Line
H Zone
I Band
A Band
I Band

shift, thereby exposing the myosin-binding sites on the actin filaments. The globular head of myosin can now bind to actin, forming actin-myosin cross-bridges. Myosin pulls on actin, drawing the thin filaments closer to the M line. Another ATP must bind to the ATPase site in order to break the myosin-actin cross-bridge and hydrolysis of ATP provides the energy for the next power stroke. These events are called cross-bridge cycling and will continue to shorten the sarcomere as long as Ca^{2+} and ATP are available. When cytosolic Ca^{2+} levels decrease and release from troponin C, the tropomyosin complex shifts and re-blocks the myosin binding sites of actin, thus inhibiting further cross-bridge cycling and returning the muscle fiber to a state of relaxation.

Cardiac muscle displays properties associated with both skeletal and smooth muscle, yet it is considered as a class unto itself as it possesses unique physical, biochemical and electrical properties. Cardiac muscle is striated like skeletal muscle and composed of cells with one centrally located nucleus like smooth muscle. The coordinated contraction of cardiac muscle is required to generate enough force to pump blood throughout the body. This coordinated contraction is due in part to the connectivity of cardiac cells via gap junctions which allows for the flow of electrical charge to adjacent cells. This flow of electrical charge propagates the action potential throughout the heart. The initial depolarization starts in a small cluster of auto depolarizing pacemaker cells in the sinoatrial (SA) node of the right atrium, which spreads through the gap junctions, resulting in the depolarization and contraction of the atria. Another group of pacemaker cells at the atrioventricular (AV) node, located at the atrial-venticular boarder, propagate the depolarization through a high speed conducting system called the bundle of His, which then triggers ventricular contraction in a coordinated manner by the

branched network of Purkinje fibers. Innervation of the heart by both sympathetic and parasympathetic branches of the autonomic nervous system at the SA node speeds up or slows down the auto-depolarization of these pacemaker cells and modulates the cardiac output based on systemic oxygen demands.

Smooth muscle cells are spindle-shaped and unlike skeletal muscle, the precursor cells of smooth-muscle do not fuse during development and therefore there is a single centrally located nucleus (Vander et al., 1994). The major contractile proteins are myosin and actin as in skeletal muscle, but troponin and tropomyosin are not present in smooth muscle. Initiation of smooth muscle contraction requires myosin phosphorylation as opposed to the conformational change of actin's myosin binding sites in skeletal and cardiac muscle, hence the lack of troponin and tropomysosin. The thin filaments are anchored to the plasma membrane as well as to cytoplasmic structures known as dense bodies, which function like the Z lines in skeletal muscle. Although lacking a highly organized contractile aparatus, the thick and thin fibers in smooth muscle tend to run diagonally across the spindle shaped cells (Vander et al., 1994). Contraction of the thick and thin filaments pull on the plasma membrane resulting in a more round shape. Thus the contraction of parallel-organized spindle shaped smooth muscle cells results in shortening in one dimension. Autonomic innervation of smooth muscle by the sympathetic and parasympathetic branches can alter the rate and force of contraction, which spreads through gap junctions to adjacent smooth muscle cells.

1.2 Striated Muscle Excitation-Contraction Coupling Machinery

Skeletal and cardiac muscles are required to be very fast, yet highly accurate and responsive during contraction. In order to achieve such performance characteristics,

skeletal and cardiac muscle have evolved a unique control mechanism for regulating the cytoplasmic Ca^{2+} concentration, which in turn regulates force development by the contractile machinery.

Contraction of striated muscle provides one of the most well studied examples of calcium signaling. All cells need to maintain specific concentrations of solutes in their cytoplasm, which are significantly different from those found in the extracellular solution. Muscle cells are insulated from extracellular solutes by means of the sarcolemma, a phospholipid bilayer, which prevents the entry of macromolecules and ions (Opie, 1991). Embedded within the sarcolemma are proteins which function as ion channels, transporters and pumps, allowing for the controlled flow of molecules in and out of the cell. A selectively permeable membrane is a critical component of electrically excitable cells like neurons and muscle, as it allows for the maintenance of an electrochemical gradient. This electrochemical gradient creates a potential difference that can be used to do work, such as the contraction of muscles. The process that couples the depolarization of the sarcolemma to the release of calcium from intracellular stores resulting in the contraction of muscle fibers is called excitation-contraction coupling (E-C coupling).

The entry of sodium ions (Na^+), following stimulatory events at the neuromuscular junction, initiates depolarization across the membrane of the sarcolemma (Ebashi, 1991). This change in electrical potential is propagated along the sarcolemma into invaginations referred to as transverse tubules or T-tubules. The T-tubule membrane system runs perpendicular to the length of the muscle and penetrates deep into the muscle fibers. They contain an ion channel known as the L-type Ca^{2+} channel (also known as the

dihydropyridine receptor, DHPR), which acts as a voltage sensor that detects changes in electrochemical potential due to membrane depolarization (Leong and MacLennan, 1998a). The first step in E-C coupling is the detection of membrane depolorization and activation of the DHPR, which causes the channel to open and allow an influx of Ca^{2+}. Up until this point, the integrity of the electrochemical potential of Ca^{2+} has been maintained at 10 000 times more Ca^{2+} in the extracellular fluid than in the cytoplasm of the resting muscle cell. This concentration gradient is partly maintained by the Na^{+}-Ca^{2+} exchanger which pumps Ca^{2+} out of the cell in exchange for Na^{+}. Upon depolarization of the sarcolemma, the DHPR undergoes a conformational change that allows Ca^{2+} to enter along its concentration gradient into the cytoplasm, triggering Ca^{2+} release from the intracellular stores of the SR (Fabiato, 1983). The DHPR is also thought to directly associate with proteins in the SR, thereby facilitating the release of Ca^{2+} (Caswell and Brandt, 1989). This signal is transferred to the ryanodine receptor (RyR), also known as the Ca^{2+} release channel, that releases most of the Ca^{2+} required to initiate the cross-bridge cycling of the contractile proteins. The release of Ca^{2+} from the SR through the RyR is the second step of E-C coupling, as described in detail below (section 1.3). Contraction ensues almost instantaneously as a result of the release of Ca^{2+} from the RyR that binds to troponin C, un-blocking the myosin binding sites of actin, which allows for the initiation of cross-bridge cycling. The Ca^{2+} must be extruded in order for the muscle to return to a state of relaxation. The removal of cytosolic Ca^{2+} is accomplished by the Ca^{2+}-ATPase pump residing in the SR which uses the coupling of ATP hydrolysis to pump Ca^{2+} back into the sarcoplasmic reticulum and also by the Na^{+}-Ca^{2+} exchanger residing in the sarcolemma that uses the gradient of Na^{+} to pump Ca^{2+} out of the cell,

thus inhibiting cross-bridge cycling and terminating muscle contraction (MacLennan, 1985).

The DHPR can activate the release of intracellular calcium stores in one of two ways, depending on the muscle type. In cardiac muscle, the extracellular calcium entering into the sarcoplasm by the DHPR will bind to the RYR that is embedded in the terminal cisternae of the SR. This triggers the release of intracellular Ca^{2+} from the lumen of the SR in a process termed calcium induced calcium release (CICR) (Fabiato, 1983) (Figure 1.2A). In skeletal muscle, sarcolemma depolarization causes a conformational change in the DHPR, which acts primarily as a voltage sensor and weakly as a Ca^{2+} channel (Figure 1.2B). This conformational change directly interacts with the RYR and results in Ca^{2+} release from the SR in a protein-protein interaction dependent manner termed mechanical coupling (Leong and MacLennan, 1998b; Lu and Meissner, 1994). The main evidence that supports these two modes of inducing Ca^{2+} release comes from differences observed in stoichiometric ratios of RYR to DHPR in skeletal and cardiac muscle, differences in cardiac and skeletal muscle specific DHPR and RYR isoforms and a stringent requirement of extracellular calcium for RYR Ca^{2+} release in cardiac muscle. Experiments designed to investigate the stoichiometric ratios of DHPR to RYR revealed that for every DHPR in the T-tubules of skeletal muscle, there are two RYRs in the SR (Franzini and Jorgensen 1994; Bers and Stiffel 1993). In comparison, in cardiac muscle there are one tenth as many DHPRs as RYRs (i.e., 1 DHPR: 10 RyR1) (Bers and Stiffel, 1993). The RyR isoform of skeletal muscle has been shown to interact directly with the DHPR in immunoprecipitations from detergent solubilized triads (Marty et al., 1994). The cardiac RYR isoform has not been shown to exhibit such interactions with the

DHPR. Experiments with skinned skeletal and cardiac muscle fibers demonstrated that cardiac muscle contracts only if bathed in a solution of Ca^{2+}, while skeletal muscle contraction does not require this source of Ca^{2+}, but rather relies on intracellular Ca^{2+} stores (Melzer et al., 1995).

Dissection of the structural basis of the distinct coupling mechanisms of cardiac and skeletal muscle has been greatly assisted using mutant mouse lines termed *dysgenic* and *dyspedic*. Dysgenic and dyspedic mice have been engineered to lack both copies of the skeletal muscle RyR1 and DHPR α1 subunit, respectively (Adams et al., 1990; Buck et al., 1997). E-C coupling is ablated in skeletal muscle myocytes from these mice, but is rescued by transfection with the skeletal muscle DHPR α1 subunit or RyR1 isoform, respectively. Dysgenic skeletal myotubes transfected with the cardiac muscle DHPR α1 subunit resulted in cardiac muscle like CICR which is dependent on influx of extracellular Ca^{2+} (Tanabe et al., 1990a). Dysgenic skeletal muscle myotubes transfected with chimeras between skeletal and cardiac muscle DHPR α1 subunits, indicated that the cytoplasmic loop between the II and III transmembrane repeats is a critical determinant of skeletal muscle type E-C coupling. This presumably happens via the physical association between the two channels demonstrated in co-immunoprecipitation experiments of skeletal DHPR and RyR and not in cardiac muscle (Tanabe et al., 1990b). These findings correlate well with the requirement of extracellular Ca^{2+} for the activation of the RYR in cardiac muscle, versus skeletal muscle's direct interaction between the DHPR and RyR.

Figure 1.2 Comparison of CICR induced E-C Coupling in Cardiac Muscle and the Direct Activation of E-C Coupling in Skeletal Muscle

The voltage gated DHPR in cardiac muscle acts primarily as a Ca^{2+} channel, allowing extracellular Ca^{2+} to enter into the cytosol, which binds to and activates the Ryanodine receptor (A). The release of Ca^{2+} from one RyR activates adjacent ryanodine receptors in the process of Ca^{2+}-induced Ca^{2+} release. The DHPR in skeletal muscle acts primarily as a voltage sensor and weakly as a Ca^{2+} channel. The DHPR associates with the Ryanodine receptor and directly triggers Ca^{2+} release through the RyR, which can activate Ca^{2+} release from uncoupled Ryanodine receptors (B).

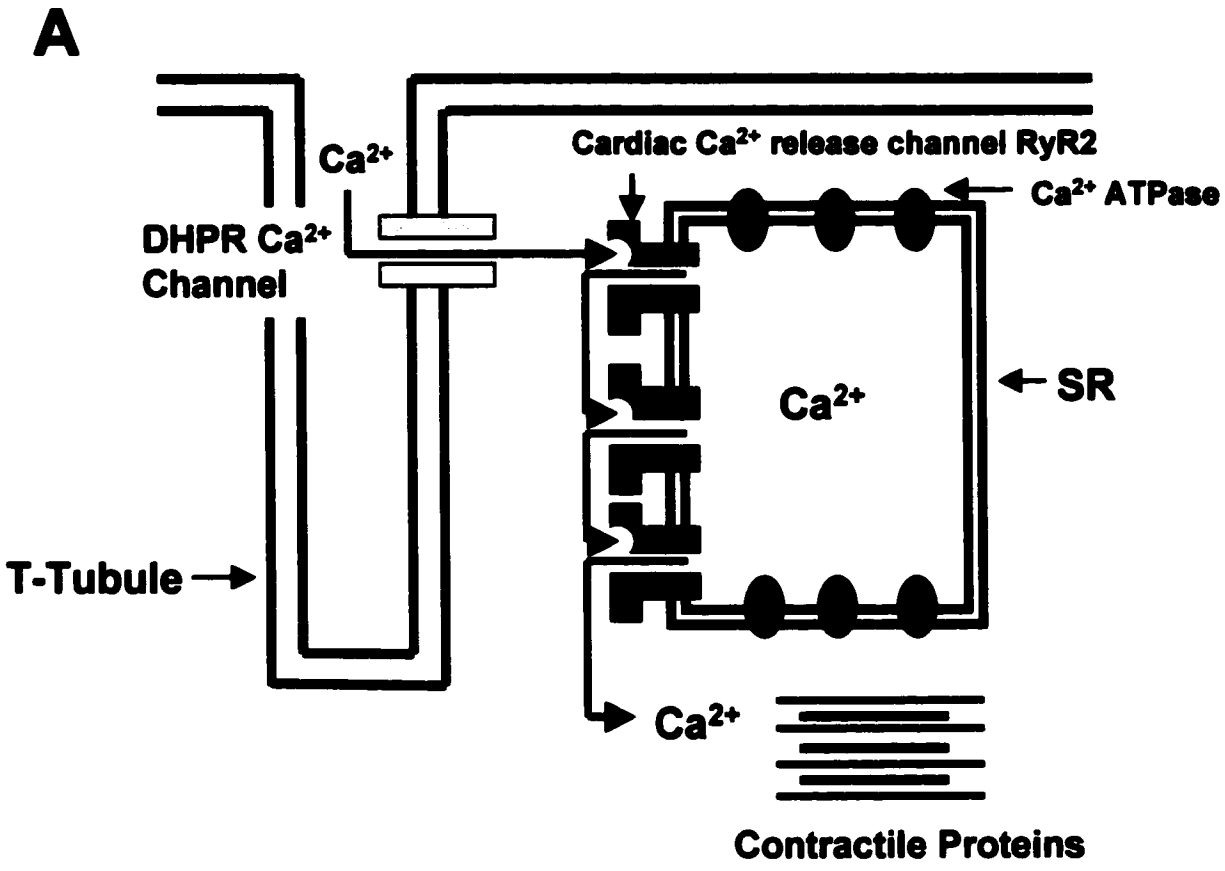
A
Ca2+
Cardiac Ca2+ release channel RyR2
Ca2+ ATPase
DHPR Ca2+
Channel
SR
Ca2+
T-Tubule
Ca2+
Contractile Proteins

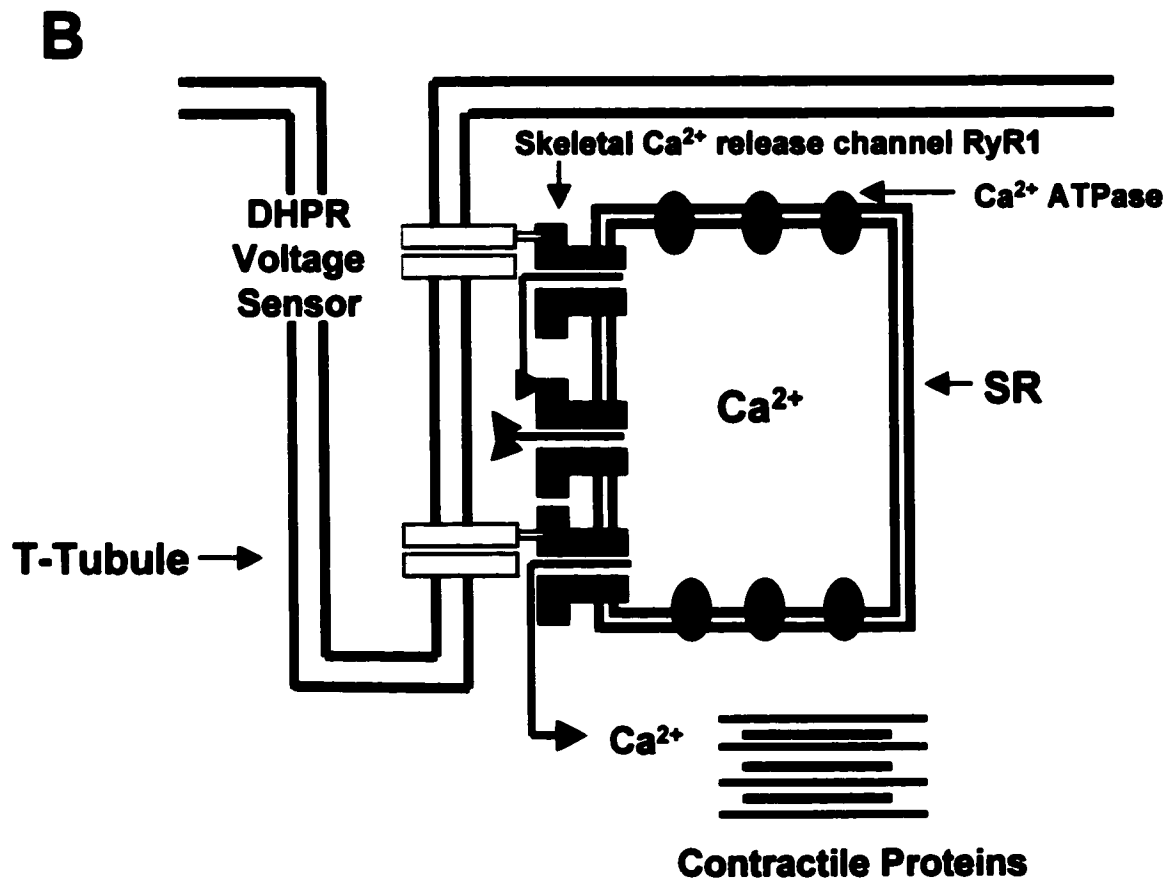
B
Skeletal Ca2+ release channel RyR1
Ca2+ ATPase
DHPR
Voltage
Sensor
SR
Ca2+
T-Tubule
Ca2+
Contractile Proteins

It has been shown that when cardiac DHPRs sense a voltage change, there is a rapid increase of extracellular Ca^{2+} influx into the sarcoplasm while in skeletal muscle, the DHPR Ca^{2+} influx is slow and comparatively minimal (Lamb and Walsh, 1987 Field et al., 1988).

Unlike Ca^{2+} release, Ca^{2+} re-uptake into the SR is constitutively active and requires coupling of the energy of ATP hydrolysis to cause Ca^{2+} transport. The Ca^{2+} - ATPase pump in the SR generates a thousand-fold concentration gradient of Ca^{2+} across the SR in resting muscle. This happens by actively pumping Ca^{2+} out of the cytoplasm and back into the lumen of the SR. Low cytosolic Ca^{2+} levels are required for muscular relaxation, which ensure Ca^{2+} is removed from the troponin C and tropomyosin complex. At the molecular level however, this pumping is approximately 10^5 times slower than release, which reflects the limitations of ATP coupled Ca^{2+} transport (MacLennan et al., 1997). In particular, two Ca^{2+} ions are transported back into the SR and two protons are expelled for every ATP hydrolyzed (MacLennan et al, 1997). The cell makes up for a relatively slow rate of Ca^{2+} re-uptake by providing a vast number of Ca^{2+}-ATPases, accounting for two thirds of SR proteins (MacLennan et al., 1985). The Ca^{2+}-ATPases reside primarily along the longitudinal SR where they are in close proximity to the muscle fibers, which allows for uniform Ca^{2+} removal from the cytoplasm (MacLennan et al., 1985). The function of these three proteins, DHPR, RYR and Ca^{2+}–ATPase become points of regulation by ions, binding proteins and by phosphorylating kinases.

1.3 Molecular Regulation of E-C Coupling

Ca^{2+} is the physiological regulator of contraction in muscle. Without it, contraction is not possible. The DHPR, RYR and Ca^{2+}–ATPase regulate the levels of cytosolic Ca^{2+} and thus contraction. Inorganic ions, small molecular compounds, multiple protein interactions as well as covalent modification via phosphorylation by protein kinases regulate the activities of the DHPR, RYR and Ca-ATPase.

The DHPR or L-type Ca^{2+} channel exists as a multimeric complex of α_1, α_2, β, δ and γ in a 1:1:1:1:1 ratio in skeletal muscle, while the cardiac L-type Ca^{2+} channel does not have a γ-subunit (Catterall, 1991; Striessnig, 1999) (Figure 1.3). The α_1 subunit of skeletal muscle (α_{1S}), has an overall homology of 66% with the cardiac α_{1C} subunit (Mikami et al., 1989). In skeletal and cardiac muscle the DHPR is arranged as a tetrad or diad, respectively, in the T-tubule membrane (Rios et al., 1993). The α1 subunit acts as the functional Ca^{2+} pore of the DHPR, while the α2, β, δ and γ subunits act to modify channel properties (Striessnig, 1999). Secondary structure analysis predicted the α1 subunit to have four hydrophobic domains, each containing six transmembrane segments (S1-S6) (figure 1.4). The fourth transmembrane segment S4, has positively charged residues regularly arranged on one side of the helix in each domain, enabling this segment to undergo voltage-dependent conformational changes (Garcia et al., 1997). Leucine zipper motifs in the S4-S5 regions also affect activation.

The segment between transmembrane segments S5-S6 lines the pore of the Ca^{2+} channel and confers selectivity of the DHPRs for divalent over monovalent cations. This selectivity is thought to be due to a Ca^{2+} binding site in the pore composed of four glutamate residues (Yang et al., 1993). Mutation of specific glutamate residues in this

Figure 1.3 Subunit composition of the L-type Ca^{2+} channel

The L-type Ca^{2+} channel in skeletal muscle is composed of five subunits in a 1:1:1:1:1 ratio. The α_1 subunit forms the ion pore of the channel while the α_2, β, γ and δ subunits associate with the α_1 subunit via non-covalent interactions. The α_2 and δ subunits are disulphide linked and are derived from proteolytic processing of a common precursor protein. The α_1 subunit contains binding sites for Ca^{2+} and CaM that influence the inward Ca^{2+} current when occupied.

Extracellular

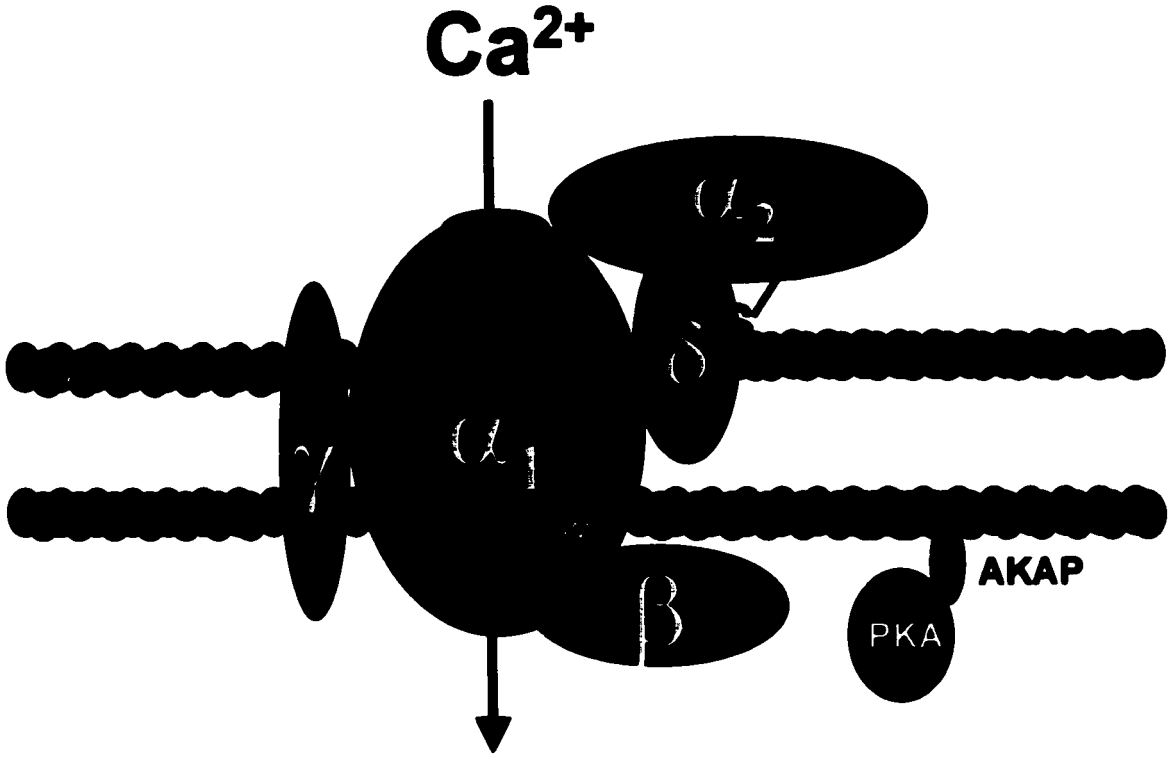

Cytoplasm

Figure 1.4 Secondary Structure of the DHPR α_1 subunit

The DHPR α_1 subunit is composed of four hydrophobic domains each containing six transmembrane segments (S1-S6). S4 contains positively charged residues enabling this segment to undergo voltage-dependent conformational changes. The sequences between S5 and S6 line the pore of the Ca^{2+} channel and confer selectivity of the channel to divalent cations. The cytoplasmic linker between S1 and S2 forms association with the DHPR β subunit. The cytoplasmic linker between S2-S3 in the DHPR α_1 subunit associates with RyR1 and is critical for skeletal muscle type E-C coupling. A high affinity Ca^{2+} binding site (EF hand motif) and a CaM binding site (IQ motif) are located on the cytoplasmic carboxy terminus.

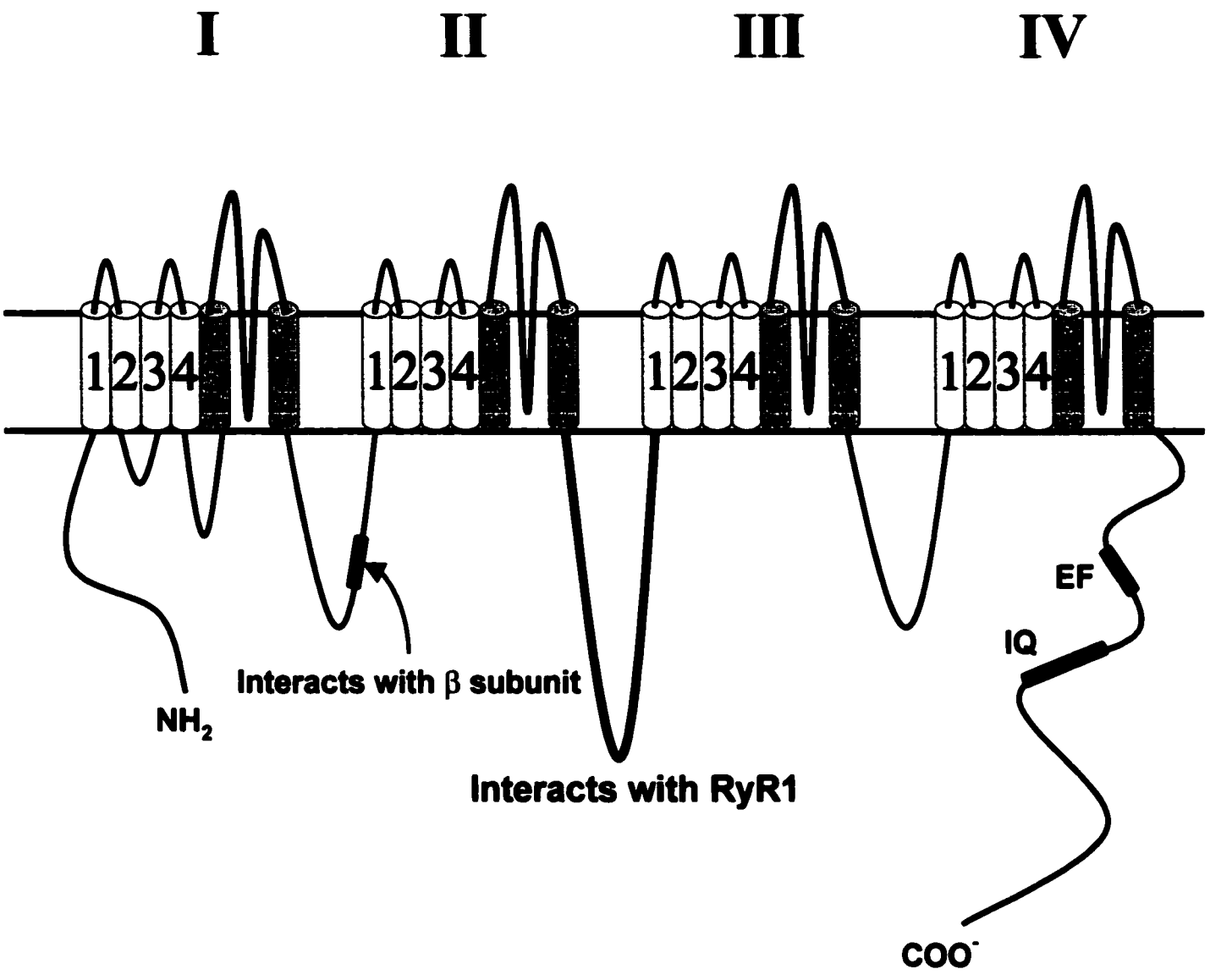
Extracellular
I
II
III
IV
1234
1234
1234
1234
EF
IQ
Interacts with β subunit
NH2
Interacts with RyR1
COO-
Intracellular

region alters the selectivity of the channel, making it more permeable to monovalent cations like Na^+ (Sather et al., 1993).

The α2 and δ subunits are linked by disulphide bonds and are derived from the proteolytic processing of a single precursor protein (De Jongh et al., 1990). The extracellular hydrophilic α_2 peptide interacts with one or more extracellular portions of α_1, while the transmembrane helix of the δ peptide anchors the subunit in the plasma membrane (Gurnett et al., 1997). This association is non-covalent, and can be dissociated upon solubilizaton of the channel with the detergents CHAPS and Triton X-100 (Takahashi et al., 1987). These subunits have been implicated in modifying the gating properties and affecting the expression levels of the DHPR (Singer et al., 1991; Bangalore et al., 1996). The β subunit interaction with α1 subunit of the DHPR is a result of a 30-200 amino acid stretch in the β subunit interacting with the cytoplasmic linker between repeats I and II (S1 and S2) in the α1 subunit of the DHPR (Pragnell et al., 1994). Targeting of the DHPR to the T-Tubules in the sarcolemma is thought to be directed by the β subunit (Chien et al., 1995). In addition, regulation of the α_1 subunit by the presence of β subunit has been shown by enhancement of ionic current and charge movement through the channel. Ca^{2+} dependent inactivation is also shown in the presence of the β subunit (Kamp, et al., 1996; Zong et al., 1994).

Ca^{2+} ions and the Ca^{2+}/CaM complex, have been shown to alter the gating of the DHPR by facilitating Ca^{2+} entry upon membrane depolarization and also leading to Ca^{2+} and CaM-dependent inactivation of the channel (Zuhlke, 1999). Upon activation of the α_1 subunit there is an influx of extracellular Ca^{2+}. The inward Ca^{2+} current (I_{Ca}) is

positively enforced in a process called facilitation, which is a positive feedback mechanism that augments inward Ca^{2+} current of L-type Ca^{2+} channels (Dzurha, 2000). Despite extensive biophysical analysis, the molecular basis of autoregulation remains unclear. A putative Ca^{2+} binding EF-hand motif (high affinity Ca^{2+} binding motif) and a nearby consensus CaM-binding isoleucine-glutamine (IQ) motif in the carboxy terminus of the $\alpha 1$ subunit have been implicated in the L-type Ca^{2+} channel (Zuhlke et al., 1998; de Leon, et al., 1995).

Recently, a Ca^{2+} and CaM-dependent kinase (CaM Kinase II) has been implicated in the facilitation of early-after depolarizations of the L-type Ca^{2+}channel (Dzhura et al., 2000; Anderson et al., 1998). A constitutively active CaM Kinase IIα isoform that did not need the presence of Ca^{2+}/CaM for activation was engineered by the aforementioned authors. Treatment of the L-type Ca^{2+} channel in excised inside-out patches with this kinase (in solutions with Ba^{2+} instead of Ca^{2+}), stimulated facilitation even when CaM or the effects of Ca^{2+} from intracellular stores was not present. In light of this, the observed positive and negative regulation by Ca^{2+} and CaM may be a result of activation of CaM Kinase II and subsequent phosphorylation of the L-type Ca^{2+} channel on a yet to be defined target.

Phosphorylation of DHPR subunits has already been shown to be an important mechanism affecting the gating properties of the channel. Activation of cAMP-dependent protein kinase (PKA) or protein kinase C (PKC), leads to activation of the L-type calcium channel. Both of these kinases are activated as a result of signaling events at the plasma membrane. Stimulation of the β adrenergic receptor (βAR) by epinephrine results in the activation of the heterotrimeric G proteins, which are coupled to the

channel. This triggers G_s to stimulate adenyl cyclase (AC) activity, increasing cellular levels of cAMP and activating PKA. The α_1 and β subunits contain multiple consensus sequences for serine phosphorylation by PKA (5 putative sites in α_1 and 3 in β). Of these, Ser-1928 of the α_1 subunit and Ser-478/Ser479 of the β subunit are phosphorylated *in vivo* (De Jongh et al., 1996; Haase et al., 1996). Phosphorylation at these sites results in upregulation of the L-type Ca^{2+} channel I_{Ca} and point mutations of these serines prevents channel activation by PKA (Gao et al., 1997; Bunemann et al., 1999). An anchoring protein (AKAP) is inserted into the T-tubule system, targeting PKA to the L-type Ca^{2+} channel (Johnson et al., 1994). When PKA is prevented from binding to AKAP by competition with peptides derived from one of the interaction sites in AKAP, its regulation of the skeletal and cardiac muscle L-type Ca^{2+} channels is blocked (Johnson et al., 1994; Gao et al., 1997).

PKC regulates the L-type Ca^{2+} channel in cardiac muscle, however the substrates for PKC and the underlying molecular mechanisms of this regulation remain largely unknown. Multiple G_q protein-coupled receptors, which include endothelin (ET), α_1 adrenergic and angiotensin II receptors, trigger signaling cascades leading to activation of PKC. Activated G_q stimulates phospholipase C (PLC), which hydrolyzes phosphatidylinositol 4,5-bisphosphate (PIP_2), generating inositol triphosphate and diacylglycerol (DAG) (Berridge, 1997). Activation of PKC involves translocation of the enzyme to specific targets. A specific PKC isozyme PKCε translocates to the T-tubule membrane and interacts with a specific anchoring protein referred to as RACK (receptors for activated C kinase)(Huang et al., 1997; Mochly et al., 1998). The α_{1C} and β_2 subunits of cardiac L-type Ca^{2+} channel are substrates of PKC (Puri et al., 1997). Phosphorylation

of the L-type Ca^{2+} channel by PKC leads to an increase, followed by a gradual decrease, in I_{Ca} (Singer et al., 1992).

Regulation of Ca^{2+} release from the RyR in the SR involves many mechanisms of regulation. The RyR has been purified, cloned and sequenced from a variety of species, and several isoforms have been identified. Mammalian tissues express three isoforms, known as RyR1, RyR2 and RyR3 (Zorzato et al., 1990; Otsu et al., 1990; and Hakamata et al., 1992). They are comprised of approximately 5000 amino acids with a molecular weight of about 560 kDa and are encoded by three different genes. RyR1 and RyR2 are expressed predominately in skeletal muscle and in cardiac muscle respectively (Marks et al, 1989, and Nakai et al., 1990). RyR3 has a wide tissue distribution including skeletal and cardiac muscle but it is known as the brain RyR isoform based on its initial identification (Ledbetter et al., 1994). A RyR holoreceptor is comprised of a homotetramer which has a quarterfoil shape and a size of 22-27nm on each side (Inui et al., 1987; Wagenknecht et al., 1989) (figure 1.5). Divalent inorganic ions like Ca^{2+} and Mg^{2+}can affect RyR activity. Ca^{2+} has major importance in the regulation of the RyR and is thought to be the physiological channel activator because other ligands cannot activate the channel in the absence of Ca^{2+} or they require Ca^{2+} for maximum effect. The RyR displays a biphasic response to Ca^{2+}, which is shown by the bell shaped relationship between Ca^{2+} release and extravessicular Ca^{2+} concentration (Chamberlain *et al.*, 1984). It has been suggested that RyR has a high affinity Ca^{2+} binding site occupied at low Ca^{2+} concentrations (50% activation at 0.5 μM) which stimulates Ca^{2+} release and a low affinity Ca^{2+} binding site occupied at higher Ca^{2+} concentrations (50% inhibition at 0.15 mM) which inhibits Ca^{2+} release (Chamberlain et al., 1984). This dual mode of Ca^{2+}

Figure 1.5 Structure of RyR holoreceptor and accessory proteins

The Ryanodine receptor is comprised of a homotetramer organized in a quarterfoil shape. A 12 kDa protein FKBP-12 binds to each RyR monomer. There are numerous Ca^{2+} and CaM binding sites on each RyR monomer which are thought to affect Ca^{2+} release through the Ryanodine receptor. Triadin is a glycoprotein that associates with the ryanodine receptor and resides primarily in the lumen of the SR but crosses into the cytosol via a transmembrane sequence. The Ca^{2+} binding protein, calsequestrin, associates with triadin in the lumen of the SR.

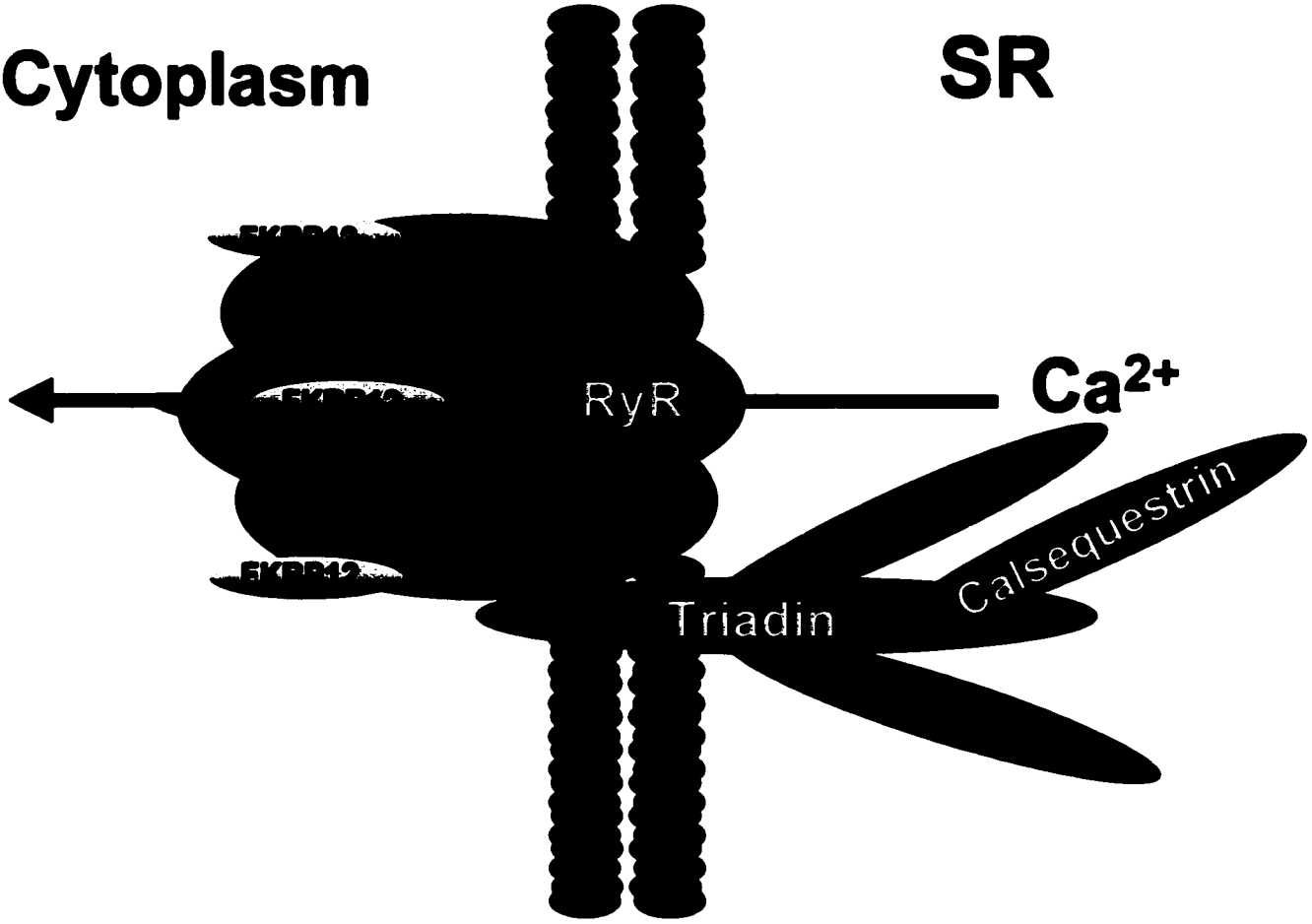
Cytoplasm
SR
RyR
Ca2+
Calsequestrin
Triadin

regulation of RyR activity allows for positive feedback initially and then negative feedback when Ca^{2+} levels reach a critical threshold.

In skeletal muscle, the initiation of Ca^{2+} release from the SR is dependent on the direct association and conformational changes of the DHPR and is not dependent on the entry of Ca^{2+} to stimulate Ca^{2+} release. Some Ca^{2+} enters through the DHPR and would be expected to bind to the high affinity Ca^{2+} binding sites and activate the RyR but this is not the case in skeletal muscle. It appears that Mg^{2+} (which has an inhibitory effect on resting muscle RyR activity) competes with Ca^{2+} for the Ca^{2+} binding sites on the RyR. The Ca^{2+} inhibitory site of skeletal muscle RyR1 has a greater affinity for Mg^{2+} compared to cardiac muscle RyR2. This is one explanation given in the literature as to why skeletal muscle does not exhibit CICR type activation of the RyR (Coronado et al., 1994; Pessah et al., 1985). Mg^{2+} competes with Ca^{2+} at both activation and inhibition sites, yet the affinity of Mg^{2+} at the activation site is 40 to 1000 times lower than Ca^{2+} binding. Furthermore, Mg^{2+} binding does not activate either RyR1 or RyR2 as does Ca^{2+} (Meissner et al., 1986). In contrast, the affinity of the inhibitory site is virtually identical for Ca^{2+} and Mg^{2+}, with the binding of Mg^{2+} just as effective at inhibiting RyR function as Ca^{2+} (Laver et al., 1997).

It is important to note that although the Ca^{2+} and Mg^{2+} affinity for the inhibitory site is the same, this affinity is less in cardiac muscle RyR2 as compared to skeletal muscle RyR1 (Silverman et al., 1994). As a result of this difference, a rise in myoplasmic Ca^{2+} concentration to 1μM could be expected to activate some Ca^{2+} release channels, which in turn would be reinforced by opening adjacent channels to nearly maximal levels in cardiac muscle. In contrast, the skeletal RyR1 isoform would be greatly inhibited by

the presence of 1mM Mg^{2+} due to the stronger binding affinity for the Ca^{2+} inhibitory site. Mg^{2+} binding can only occur when the RyR is unphosphorylated, as is demonstrated by experiments in which PKA and CaM Kinase II phosphorylation of the RyR blocks Mg^{2+} binding (Hain et al., 1994). The voltage sensor activation of the RyR by DHPR must be able to overcome the inhibitory effect of Mg^{2+} in skeletal muscle, possibly by lowering the affinity of the release channels for Mg^{2+} (Lamb 2000). Although the initial activation of RyR is not dependent on the entry of Ca^{2+} through the DHPR, one half of the RyR1 channels are not coupled to DHPR and must be activated by other means. It is thought that after Ca^{2+} levels rise from activation of the DHPR-coupled RyR1 channels, the effect of the Mg^{2+} bound to the inhibitory binding site on nearby RyR1s is removed by stimulation of the RyR1 channels (that are uncoupled to DHPRs) at the high affinity Ca^{2+} binding sites by Ca^{2+}. This is a form of CICR in skeletal muscle, however this can only occur after RyR1 receptors that are coupled to DHPR are activated mechanistically as described above.

Small molecules such as adenine nucleotides and nitric oxide (NO) alter the activity of the RyR. Adenine nucleotides like adenosine monophosphate (AMP), adenosine diphosphate (ADP) and cyclic AMP, activate the release of Ca^{2+} in cardiac and skeletal muscle, even at low Ca^{2+} concentrations and in the presence of Mg^{2+} (Meissner and Henderson, 1987). NO inhibits RyR in skeletal and heart muscle, inhibiting both the rate of Ca^{2+} release from the SR and the open probability (P_o) of the channel (Meszaros et al., 1996; Zahradnikova et al., 1997). This inhibition causes depression of contractile force, and because the major form of the NO synthase in muscle is of the Ca^{2+}/CaM-dependent type, this regulation may represent another feedback loop in Ca^{2+} signaling.

Accessory proteins bind to the RyR and affect its activity in positive and negative ways, also serving to ensure proper functioning of the RyR channel. CaM binds to RyR and has a dual mode of regulation on RyR activity. CaM activates the channel by increasing the P_o in a dose dependent manner at sub micromolar Ca^{2+} levels (Tripathy et al., 1995). At high concentration of free Ca^{2+} (1.0 μM) CaM inhibits channel activity (Fuentes et al., 1994). In single channel experiments performed with skeletal or cardiac RyR channels, 2 μM CaM reversibly decreased channel P_o and this effect was Ca^{2+}-dependent. There are two to six tentative binding sites for CaM per RyR monomer, indicating that CaM can have different effects based on binding location. The molecular basis of CaM-dependent regulation of the RyR remains largely undefined.

FK506-binding protein FKBP12 (FKBP12.6 in cardiac) is another relatively small protein (12 kDa in skeletal and 12.6 kDa in cardiac muscle) which has important effects on the proper function of the RyR in skeletal and cardiac muscle. Each RyR monomer has one FKBP12 protein attached to it constitutively (Jayaraman et al., 1992). This interaction helps maintain proper channel gating from fully open to fully closed state and to synchronize the release of Ca^{2+} from all four RyR monomers. In planar lipid bilayers, skeletal-muscle RyRs stripped of FKBP12 display long lasting subconductance states (Timerman et al., 1993; Brilliantes et al., 1994). Subconductance is defined as the incomplete closure or opening of the RyR. Proteins in the lumen of the SR also play important roles in RyR function.

Calsequestrin is the primary Ca^{2+} binding protein in the lumen of SR and has been found to bind up to 40 moles of Ca^{2+} per mole of protein electrostatically via stretches of acidic amino acids (Niki et al., 1996). The high capacity and low affinity for

Ca^{2+} is a biochemical feature of calsequestrin that ensures free levels of Ca^{2+} in the lumen are low during muscle relaxation but are easily released upon activation of the RyR. High levels of free luminal Ca^{2+} have been shown to inhibit SR function by inhibiting the Ca^{2+} ATPase pump (Mitchell et al., 1988). Calsequestrin is linked to the RyR via a glycoprotein triadin which is primarily in the lumen of the SR but also spans the SR membrane and projects into the cytosol (Guo et al., 1995). Triadin has been shown to have a regulatory role on the activity of RyR. Phosphorylation of triadin by CaM Kinase II inhibits Ca^{2+} release from the RyR (Damiani, 1995). Groh et al.(1999) demonstrated that the cytoplasmic tail of triadin has a functional interaction with the RyR, as determined by immunoprecipitation and inhibition of this interaction leading to a decrease in Ca^{2+} release from the SR. Phosphorylation of triadin by CaM Kinase II also resulted in the inhibition of Ca^{2+} release from the SR (Damiani, 1995).

Phosphorylation of RyR1 and RyR2 is another mode of regulating Ca^{2+} release from the SR. The RyR has been demonstrated to be a substrate for PKA, PKC, PKG and Cam Kinase II. The RyR2 incorporates 1 mol of phosphate per mol of tetramer when treated with PKA, PKC or PKG. This led to an increase in ryanodine binding of 10%-30%. (Takasago, 1991). Ryanodine binding is an indication of RyR activity that increases in relation to the release of Ca^{2+}. CaM Kinase II phosphorylation of the RyR may have two opposing effects on RyR activity in E-C coupling, explained in detail in section 1.4.

In skeletal muscle, the DHPR interacts with the RyR via the cytoplasmic loops between transmembrane domains II and III of DHPR and a 40 amino acid sequence in

RyR1 (Leong and MacLennan, 1998). This protein-protein interaction is critical for skeletal muscle type E-C coupling.

Ca^{2+} re-uptake in the SR is an active process performed by the Ca^{2+}-ATPase pump. The Ca^{2+}-ATPase pump has two isoforms, a fast twitch muscle specific isoform SERCA1 and cardiac and slow twitch skeletal muscle isoform SERCA2 (MacLennan et al., 1997). The Ca^{2+} pump resides in the longitudinal SR. In cardiac and slow-twitch skeletal but not in fast twitch skeletal muscle the Ca^{2+}-ATPase is regulated by phospholamban (Simmerman and Jones, 1998). Phospholamban inhibits the Ca^{2+} pump by reducing its affinity for Ca^{2+}, which is critical for the speed of cardiac muscle relaxation. Phospholamban is phosphorylated by PKA or Cam Kinase II after β-adrenergic stimulation, causing phospholamban to dissociate from the Ca^{2+} pump and thereby restoring the active pumping of Ca^{2+} through the Ca^{2+}-ATPase pump (Lindemann and Watanabe, 1985). The cardiac and slow twitch SERCA2 isoform is phosphorylated by an endogenous CaM Kinase II isoform, resulting in a two-fold increase in Ca^{2+} transport activity (Hawkins et al., 1994). The ATP binding site of the Ca^{2+}-ATPase pump is required for energetic coupling of calcium re-uptake and a Ca^{2+} binding site must also be occupied for the Ca^{2+} pump to function (MacLennan et al., 1997).

1.4 Role of CaM Kinase and Muscle Function

Although intracellular Ca^{2+} is the physiologic regulator of E-C coupling, it also plays an important role in long-term changes by regulating signaling pathways that involve PKC as well as Ca^{2+}/CaM-dependent kinases. The diverse effects of Ca^{2+} as a

chemical messenger have been observed in a multitude of cellular mechanisms such as secretion, carbohydrate metabolism, cell cycle progression, gene expression and neuronal plasticity (Means and Dedman, 1980). Ca^{2+} can bind directly to target molecules or it can bind to CaM, a cytoplasmic Ca^{2+} binding protein, thus forming a complex that can then bind and activate affected molecules. CaM can bind up to four Ca^{2+} ions in a coordinated fashion and appears to be the most common modulator/mediator of intracellular Ca^{2+} signals. Conformational changes accompanied by Ca^{2+} binding to CaM results in an α-helical configuration which is required for the binding of the Ca^{2+}/CaM complex to other enzymes. (Means and Dedman, 1980; O'Neil and DeGrado, 1990).

The Ca^{2+}/CaM complex has been shown to be a potent activator of a large family of protein kinases called Ca^{2+}/CaM-dependent protein kinases (CaM kinases). CaM kinases share common structural features and generally have a variable domain at the N-terminus followed by a highly conserved catalytic and regulatory domains (50-60% identity), followed by another variable domain and an association domain at the C-terminus (Schulman, 1993). Although there are some similar features in the CaM kinase family, they may differ in how they are activated by CaM, regulated by autophosphorylation, localized with, as well as in their substrate specificity (Nairn and Picciotto, 1991).

The Ca^{2+}/CaM-dependent protein kinases can either be multifunctional or they may be dedicated to a single function and phosphorylate only one or two substrates. Dedicated CaM kinases include myosin light chain kinase (MLCK), elongation factor 2 kinase (EF-2 Kinase) and phosphorylase kinase. MLCK is a well-studied enzyme which plays an integral role in regulating smooth muscle EC coupling by phosphorylating the

regulatory light chain myosin II (Stull et al., 1998). MLCK phosporylation of the light chain of myosin II enables interaction between myosin and actin, which initiates smooth muscle cross-bridge cycling and contraction (Ogaki et al., 1999). In skeletal and cardiac muscle, MLCK is thought to modulate contractility by increasing the sensitivity of the contractile elements to activation by Ca^{2+} as a result of myosin light chain phosphorylation (Moore et al., 1994).

Another dedicated CaM kinase, EF-2 kinase (CaM kinase III) is a ubiquitous protein kinase that phosphorylates and inactivates eukaryotic translational elongation factor-2 (EF-2). This modulates the rate of polypeptide chain elongation during translation via a transient inhibition of protein synthesis (Pavur et al., 2000).

Phosphorylase kinase has been implicated in the regulation of glycogen metabolism as it phosphorylates glycogen phosphorylase resulting in its activation and glycogen breakdown (Brushia and Walsh, 1999). Work by Polishchuk et al (1994) has also implicated phosphorylase kinase in the regulation of glycogen biosynthesis at the SR membrane system via phosphorylation and inhibition of glycogen synthase.

Other CaM Kinases are multifunctional as they can phosphorylate a number of different substrates. These include CaM Kinase I, II and IV, which are involved in numerous cellular activities. Such activities include the metabolism of carbohydrates, lipids and amino acids, the synthesis and release of neurotransmitters, the regulation of ion channels, cytoskeletal proteins, gene expression, cell growth and proliferation (Walaas and Greengard, 1991). CaM Kinases I and IV display unique regulatory properties as their activity depends heavily on phosphorylation at Thr 177 and Thr 196 respectively by a Ca^{2+}/CaM-dependent protein kinase I kinase (CaM Kinase I Kinase or

CaM KK) (Haribabu et al, 1995 and Lee and Edelman, 1994). CaM KK in turn is regulated in a multimodal fashion as it requires Ca^{2+}/CaM for activation and is inhibited by phosphorylation at Thr 108 by cAMP-dependent protein kinase (PKA) (Matsushita and Nairn, 1999). Long term effects can be elicited upon the activation of CaM Kinase I and CaM Kinase IV via transcription activation by phosphorylating activating transcription factor-1 (ATF-1) and/or the cAMP response element binding protein (CREB) in response to elevated levels of free Ca^{2+} (Sun et al., 1996).

Of all the multifunctional CaM Kinases, CaM Kinase II (CaM KII) is the best characterized kinase (Braun and Schulman, 1995). CaM Kinase II is made up of products from a multi-gene family. These consist of four isoforms (isozymes), referred to as (α, β, γ and δ), which are encoded by four separate genes (Schulman, 1993). Each gene may give rise to several isoforms by alternative splicing. Thus, the gene encoding α gives rise to α and α_B , while β can encode β, β', their embryonal counterparts β_e, β'_e , β_3 in pancreas and β_4 in skeletal and cardiac muscle. Finally, γ can encode γ_A, γ_B, γ_C, while δ encodes at least six different isoforms (Bennet and Kennedy, 1987; Benson et al., 1991; Tombes and Krystal, 1997; Edman and Schulman, 1994; Uriquidi and Ashcroft, 1994; Chatzis and Tuana, 1999; Mayer et al., 1993; Nghiem et al., 1993; Schworer et al., 1993). Each gene product of the four members (α, β, γ and δ) share three highly conserved domains: an N-terminal catalytic domain, a central autoregulatory domain and a C terminal association domain. Tobimatsu and Fujisawa (1989) have shown that CaM Kinase II classes share approximately 80-90% identity across these core domains. There are two variable domains, one is located at the extreme N-terminus while the other (a larger variable domain) resides between the regulatory and association domains.

The catalytic domain at the N-terminus (a.a 11-260) contains the conserved sub-domains that are characteristic of protein kinases, namely an ATP binding domain and a catalytic domain which transfers one phosphate from the bound ATP to a substrate (Hanks et al., 1988). Amino acids 260-320 constitute the auto-regulatory domain which serves as a point for activation via the CaM binding domain as well as auto-inhibition via a pseudo-substrate which binds the catalytic domain when CaM is not present, rendering the enzyme inactive (Schulman and Lou, 1989). Autophosphorylation of multiple threonine and serine residues in the autoregulatory domain is another way of regulating CaM Kinase II function. An association domain at the C-terminus allows for assembly of a holo-enzyme complex. The variable domain between the association and regulatory domains is a site that constitutes the main difference between different CaM Kinase II family members and is expressed via the alternative splicing of exons in a tissue specific manner.

The binding of Ca^{2+}/CaM to CaM Kinase II enhances ATP affinity for the kinase and stimulates autophosphorylation on multiple threonine and serine residues, which results in changes in the state of enzyme activity. Phosphorylation of Thr 287 in CaM Kinase II β (286 in α) results in CaM trapping, a phenomenon which maintains the activity of CaM Kinase II by keeping the CaM complex attached to the enzyme even after Ca^{2+} levels have dropped below threshold (Schulman, 1992). In this autonomous Ca^{2+} independent state of activity, the question arises as to what events cause the de-activation of CaM Kinase. Experiments have been done which demonstrate that autophosphorylation within the CaM binding domain on residues Thr 305 or Thr 306 is sufficient to block CaM binding and restore CaM Kinase II to its inactive state (Patton et

al., 1990; Hanson and Schulman, 1992; Colbran and Soderling, 1990). It has also been demonstrated that phosphorylation of Ser 314 in this region had no effect on CaM binding.

CaM Kinase II forms a holoenzyme complex with its association domain, forming a hub and spoke arrangement with the slightly hydrophobic C-terminus (association domain) at the hub and the N-terminus (catalytic domain) radiating outward. A large holoenzyme of 6-12 subunits can be comprised of a homomultimer or a heteromultimer, with each subunit binding CaM and exhibiting kinase activity (Schulman, 1993). Examination of the holoenzyme by use of electron microscopy suggests that the 12 sub units are arranged as stacked hexameric rings with a diameter of approximately 100Å (Woodgett et al., 1983).

The CaM Kinase II multi-gene family is an important functional element of Ca^{2+} signaling, which display diverse effects in many cellular activities and events in a multitude of tissues. In the brain, CaM Kinase II accounts for up to 2% of cellular protein in the hippocampus and on average, comprises 0.25% of total brain protein (Erondu and Kennedy, 1985). CaM Kinase II regulates the exocytosis of neurotransmitters via phosphorylating Synapsin I, which then dissociates from synaptic vessicles and thereby facilitates neurotransmitter release (Schiebler et al., 1986). Neurotransmitter synthesis is also dependent on CaM Kinase II, which can phosphorylate the rate limiting enzyme tyrosine hydroxylase in catecholamine biosynthesis, at amino-acids Ser19 and Ser40 (Campbell et al., 1986). CaM Kinase II is a good candidate for the storage mechanism involved in memory, which is electrically explained as activity-dependent synaptic modifications such as long-term potentiation (LTP). LTP is a long-lasting increase of the

post-synaptic potential following an afferent tetanization or long-term depression (LTD) (Lisman, 1994; Colbran et al., 1989). In this model of neuronal plasticity, CaM Kinase II is thought to contribute to the increased post-synaptic responsiveness observed in LTP. This occurs via phosphorylation of the hippocampal AMPA receptor (glutamate receptor) GluR1, which enhances the inward current through post-synaptic glutamate receptors, resulting in larger excitatory post-synaptic potentials (EPSPs) (McGlade-McCulloh et al., 1993; Tan et al., 1994). Once induced, LTP can persist for several weeks in rats (DeJonge and Racine, 1985).

Although CaM Kinase II function in skeletal and cardiac muscle is not as well characterized as in the brain, much can be said about its involvement in the regulation of ion channels. A CaM-dependent kinase has been implicated in the regulation of skeletal and cardiac muscle E-C coupling which is localized to the SR membrane system (Tuana and MacLennan, 1984; Kim and Ikemoto, 1986) (Figure 1.6). It has been shown that phosphorylation of SR proteins regulates changes in receptor/channel function (Xu et al., 1997). Recently, an anchoring protein called α-KAP has been isolated and found to contain a hydrophobic sequence composed of the association domain of CamKII-α with a few hydrophobic residues added (Ulrich Bayer et al., 1998). This protein is thought to target and anchor the CaM Kinase II isoforms to the SR membrane system, allowing for localized interactions with various SR proteins.

In skeletal and cardiac SR, CaM Kinase II has been shown to phosphorylate multiple proteins such as the RyR, Ca^{2+}-pump, phospholamban and possibly the DHPR. Cardiac RyR2 was shown to incorporate between 2-4 moles of P_i (incorporated phosphate) per mole of RyR tetramer after treatment with CaM Kinase II (Hohenegger

and Suko, 1993; Takasago et al., 1991). The functional consequence of cardiac RyR2 phosphorylation by CaM Kinase II has been shown to have two opposing effects. One finding indicates a decreased affinity for ryanodine and decreased channel P_o due to the reduced lifetime of the open channel (Takasago et al., 1991; Lokuta et al., 1995). Another finding indicates an increased P_o after treatment of cardiac RyR2 with CaM Kinase II (Witcher et al., 1991). Yet, another study provides evidence that CaM Kinase II may have multiple actions; phosphorylation by exogenous CaM Kinase II made the channel insensitive to Mg2+ inhibition (which activates RyR2), whereas phosphorylation by endogenous CaM Kinase II, presumably at a different site, produced channel inhibition (Hain et al., 1995).

Skeletal RyR1 phosphorylation by CaM Kinase II is even more controversial. Suko et al (1993), discovered exogenous CaM Kinase II phosphorylated RyR1 *in vitro* with a stoichiometry ranging from 0.3-0.9 moles P_i per receptor monomer at Ser-2843. Other evidence exists which suggests there is minimal phosphorylation of RyR1 by CaM Kinase II and questioned its physiological relevance (Strand et al., 1993). Functional studies have also provided controversial results, because RyR1 phosphorylation by CaM Kinase II resulted in either channel activation (Herrmann-Frank and Varsanyi, 1993), channel inactivation (Wang and Best, 1992) or no effect (Chu et al, 1990). Hain et al (1994) employed the same experimental conditions used in cardiac SR to test the effect of CaM Kinase II on skeletal RyR1 function. Their results indicated that skeletal muscle RyR1 responds the same way as cardiac RyR2 does to CaM Kinase II phosphorylation i.e. exogenous CaM Kinase II removed Mg^{2+} inhibition (activation of RyR1) while

Figure 1.6 Comparison of CaM Kinase II β and SOCK

All Cam Kinase II isoforms are composed of an N-terminal kinase domain, a central regulatory domain, a variable domain and an association domain at the C-terminus. The cDNA of SOCK differs from the cDNA of CaM Kinase II β by the addition of three alternatively spliced exons in the variable domain that encode for proline-rich sequences and are designated as exons P1, P2 and P3. The cDNA encoding SOCK shares over 90% identity with the cDNA encoding CaM Kinase II β when comparing sequences other than the alternatively spliced exons.

CaM Kinase II β 60 kDa

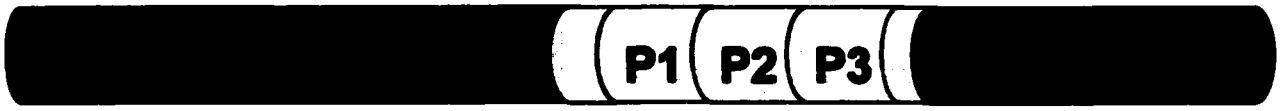

Son Of CaM Kinase II (SOCK) 73 kDa

endogenous CaM Kinase II blocked the channel, presumably by direct phosphorylation of RyR1 (Hain et al., 1994).

CaM Kinase II also regulates the Ca^{2+}-ATPase pump via two modes of action, either by directly phosphorylating the pump or via phosphorylation of the regulatory protein phospholamban. The cardiac and slow twitch skeletal muscle Ca^{2+}-ATPase pump (SERCA2), but not the fast twitch skeletal muscle Ca^{2+}-ATPase pump (SERCA1), undergo phosphorylation by CaM Kinase II (Hawkins et al., 1994). SERCA2 phosphorylation results in stimulation of the V_{max} of ATP hydrolysis and Ca^{2+} transport (Xu et al., 1993; Toyofuku et al., 1994). Phospholamban is a protein, which binds to and inactivates the Ca^{2+}-ATPase pump. Phosphorylation of phospholamban by CaM Kinase II after β-adrenergic stimulation was found to decrease phospholamban's affinity for the Ca^{2+}-pump. In so doing it relieves the inhibition and restores the activity of SERCA2 (James et al., 1989; Sasaki et al., 1992).

The cardiac L-type Ca^{2+} current (I_{Ca}), is known to be modulated by a variety of agents including hormones, neurotransmitters and drugs (Anderson et al. 1994). CaM Kinase II is thought to mediate the Ca^{2+}-induced enhancement of I_{Ca} in mammalian cardiac myocytes by a mechanism, which is likely to involve the direct phosphorylation of the L-type Ca^{2+} channel or an associated regulatory protein (Anderson et al., 1994). A recombinant constitutively-active CaM Kinase II α has been shown to increase 'facilitation', which is a positive feedback mechanism that augments inward Ca^{2+} currents of L-type Ca^{2+} channels in response to increased intracellular Ca^{2+} concentrations (Dzhura et al., 2000). Treatment of rabbit ventricular myocytes with KN-93 (a water-soluble CaM Kinase II inhibitor) significantly depressed early after

depolarizations (EADs) and implicates CaM Kinase II in the induction of EADs (Anderson et al., 1998). EADs depolarize the oscillations in the action potential (AP) that occur during repolarization (January and Moscucci, 1992). EADs are clinically important because they may initiate lethal arrhythmias associated with long QT intervals, including Torsades de Pointes (Roden et al., 1996).

1.5 Statement of the Problem:

A CaM Kinase has been implicated in the regulation of E-C coupling in skeletal and cardiac muscle. A number of studies indicate that proteins involved in E-C coupling are phosphorylated in a Ca^{2+} and CaM-dependent manner, with effects on the uptake and release of Ca^{2+} from the SR (Wang and Best, 1992; Hain et al., 1994; Dzhura et al., 2000; Anderson et al., 1998). The exact isoform responsible for this regulation remains to be clearly defined. Work in this lab led to the cloning of a cDNA encoding a muscle specific CaM Kinase II β isoform which differed from the brain isoform by the addition of three alternatively splices exons, which encoded proline rich sequences (Leddy, 1999). Proline rich sequences have been shown to act as modules, which direct the association of a protein with Src tyrosine kinase homology 3 (SH3) domains. The interaction of SH3 domains (found in tyrosine kinases like Src or in adapter proteins in tyrosine kinase signaling pathways like Grb2) with proline rich motifs in proteins are believed to be critical for the transmission of signaling cascades initiated at the plasma membrane (Pawson, 1995).

The purpose of this study was to further characterize at the biochemical and molecular level, the subcellular localization, substrate specificity and protein-protein

interactions with SH3 domains of a muscle specific CaM Kinase II β isoform called SOCK (Son Of CaM Kinase). The molecular characterization of SOCK led to the identification of SOCK as a protein targeted to the terminal cisternae of the SR that directly phosphorylated E-C coupling machinery. Identification of SH3 domain containing proteins that associate with the proline rich region of SOCK was also investigated. This may implicate SOCK as an integrator of Ca^{2+} and tyrosine kinase signaling cascades at the level of SH3 domains.

2. Materials and Methods

2.1 Subcellular Fractionation of Rabbit Skeletal Muscle:

Subcellular fraction of skeletal muscle was achieved as described by Chu *et al* (1988). New Zealand white rabbits were sacrificed with an overdose of sodium-pentabarbitol and the fast twitch skeletal muscle from the back and hind limbs were excised and placed on ice. In order to reduce proteolytic degradation all procedures were carried out at 4°C and protease inhibitors were used in all solutions, with final concentrations of 1 mM benzamidine, 1 mM iodoacetamide, 0.5 μM pepstatin, 0.5 μM leupeptin and 1 mM phenylmethane sulfonyl fluoride (PMSF). The membrane fractionation experiment was replicated using muscle collected from different animals and all Western blots were performed at least three times with each fractionation experiment.

Approximately 50 g of skeletal muscle from rabbit hind limb and back were homogenized in 250 ml of muscle homogenization buffer (10 mM HEPES pH 7.4, 5 mM EDTA, 1.2 mM EGTA, 10% sucrose, 1mM PMSF, 0.5 μM leupeptin and 0.5 μM pepstatin) with 4 x 30 second bursts in a Sorvall homogenizer, followed by 2 x 30 second bursts in a Brinkman polytron homogenizer at 20 000 rpm (figure 2.1). The homogenate was then subjected to two low speed centrifugations, 5000 x g for 10 min and 11 000 x g for 20 min in a Beckman JA-20 rotor. The supernatant was filtered through 8 layers of cheesecloth then KCl was slowly added at 4°C to a final concentration of 0.5 M and the final mixture was stirred for 45 minutes. The salt washed membranes were sedimented by ultracentrifugation for one hour at 192 000 x g (42 000 rpm in 42.1 Ti Beckman rotor).

The cytosolic supernatant identified as S3 was saved and the crude microsomal pellet was resuspended in 60 ml of gradient buffer (4 mM HEPES pH 7.4, 0.4 M KCl, 26 % (wt/wt) sucrose, 0.5 μM leupeptin and 0.5 μM pepstatin). The microsomes were

Figure 2.1 Skeletal Muscle Membrane Fractionation Procedure

Homogenized rabbit fast twitch skeletal muscle was subjected to discontinuous centrifugation at 5000 x g, the pellet (P1) was discarded and the supernatant (S1) was centrifuged at 11 000 x g. The supernatant (S2) was filtered through cheesecloth and subjected to a salt wash in 0.5 M KCl to remove aggregated contractile proteins. Following this, S2 was ultracentrifuged at 190 000 x g to sediment crude microsomes. The crude membranes were resuspended in 25% sucrose gradient buffer and layered on to a discontinuous sucrose gradient consisting of 45%, 38%, 34% and 32% sucrose cushions. The crude microsomes were overlayed with a cushion of 15% sucrose and centrifuged in overnight. Five membrane fractions were collected at each interface of the sucrose cushions consisting of different subcellular membrane fractions. The membrane fractionation experiments were replicated in muscle collected from different animals and all Western blots were performed at least three times for each antibody.

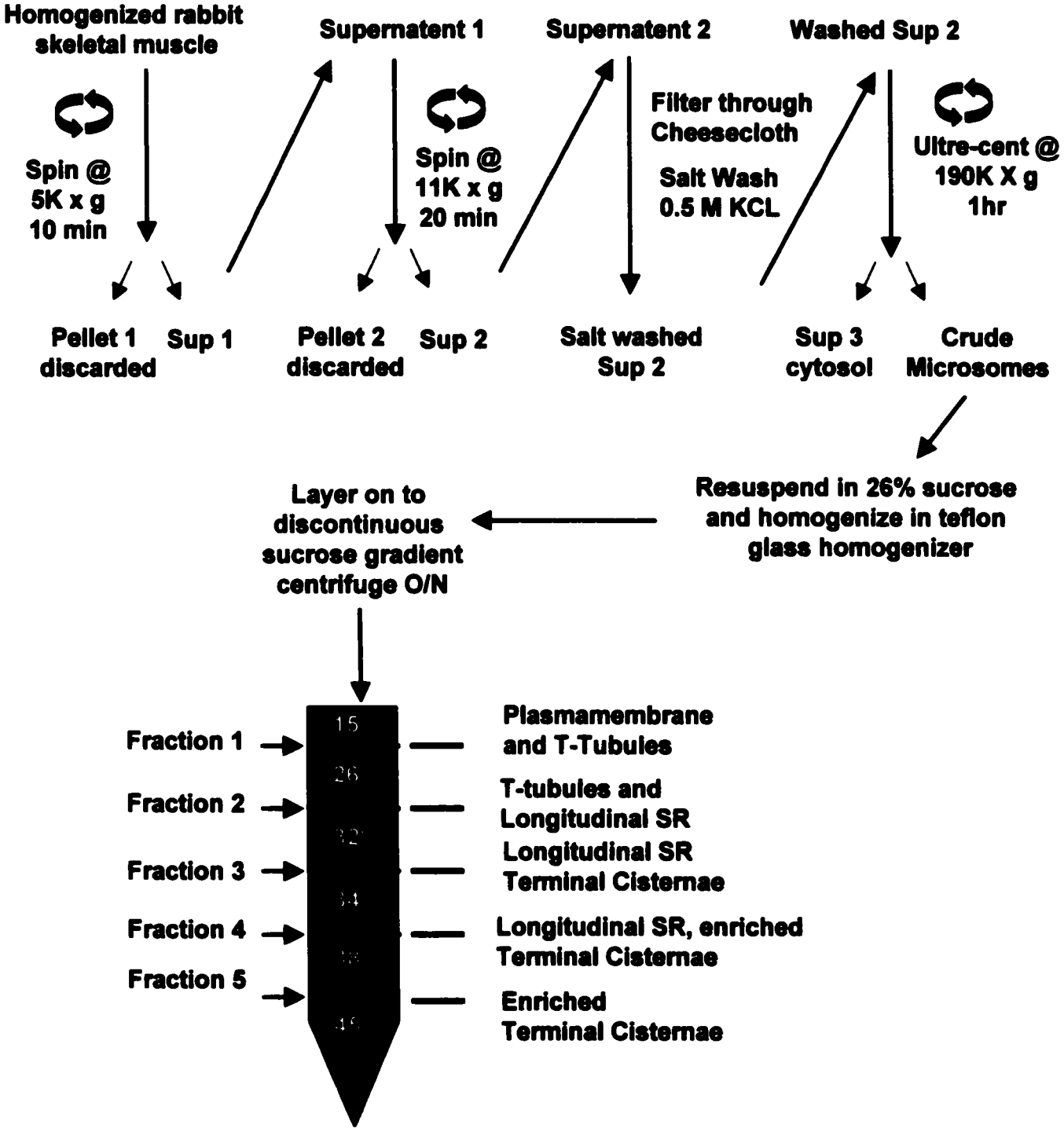
Homogenized rabbit skeletal muscle
Spin @ 5K x g 10 min
Pellet 1 discarded
Sup 1
Supernatent 1
Spin @ 11K x g 20 min
Pellet 2 discarded
Sup 2
Supernatent 2
Filter through Cheesecloth
Salt Wash 0.5 M KCL
Salt washed Sup 2
Washed Sup 2
Ultre-cent @ 190K X g 1hr
Sup 3 cytosol
Crude Microsomes
Resuspend in 26% sucrose and homogenize in teflon glass homogenizer
Layer on to discontinuous sucrose gradient centrifuge O/N
Fraction 1
Fraction 2
Fraction 3
Fraction 4
Fraction 5
15
26
32
34
38
42
Plasmamembrane and T-Tubules
T-tubules and Longitudinal SR
Longitudinal SR Terminal Cisternae
Longitudinal SR, enriched Terminal Cisternae
Enriched Terminal Cisternae

dispersed with 15 strokes in a Teflon™ dounce homogenizer at 2500 rpm. From this mixture, 10 ml of the crude microsomes was layered on top of a sucrose step gradient consisting of 7 ml each of 32%, 34% and 38% sucrose and 4 ml of 45% sucrose. A total of 6 gradients were prepared. The crude microsome samples were overlaid with 3-4 ml of 15% sucrose in gradient buffer and the gradients were centrifuged for 16 hours at 22 000 rpm/4°C in an SW28 Beckman rotor. The proteins were collected from each interphase (fractions F1 to F5), diluted to 10% sucrose and ultra-centrifuged for 45 min at 192 000 x g (42000 rpm in Beckman 42.1 rotor). The pellets were resuspended with muscle homogenization buffer and dispersed with 5 strokes in a Teflon™ dounce homogenizer at 2500 rpm. Determination of protein concentrations in the samples were made possible with the use of a BCA® protein assay kit (PIERCE) using bovine serum albumin as standard.

2.2 Western Blot Analysis

The Laemmli buffer system (Laemmli, 1970) was used to make polyacrylamide SDS gels, electrophoresis buffer and electroblot buffer. Mini-gels were prepared with 1 mm thickness consisting of 10% or 7% polyacrylamide for the resolving portion of the discontinuous gel. The 7% gels were used to resolve large proteins like RyR1 (560 kDa), which do not migrate in the 10% gels. The stacking gel was composed of 4% polyacrylamide and was used for both 7% and 10% polyacrylamide gels. Protein samples were resuspended in an equal volume of 2X SDS loading buffer (supplemented with bromophenol blue to see the samples when loading) and boiled for 5 minutes before loading onto the polyacrylamide SDS gels. Electophoresis was performed with the BioRad

Mini Protein II system at a low voltage (60 V), until the dye front migrated to the resolving gel. At this point the voltage was increased to 100 volts and electrophoresis continued until the dye front migrated out the bottom of the resolving gel. The proteins were electroblotted onto PVDF membrane (Amersham Pharmacia) with a BioRad TransBlot apparatus in a buffer containing Tris 25 mM, pH 7.2, glycine 190 mM and 20% methanol. Proteins were routinely electroblotted at 30 V overnight except when probing for the RyR, which due to its large molecular weight required a voltage of 85 volts over night for complete transfer. To assess the quality of the electroblotted proteins, the membranes were stained with Ponceau S. The blots were blocked in TBS-T (tris buffered saline, pH 7.2 with 0.1% Tween 20 detergent added) supplemented with 3-5% carnation skim milk powder. Following this the blots were washed for 3 x 10 minutes with TBS-T pH 7.2. Primary antibodies were diluted in TBS-T 3-5% skim milk powder. Monoclonal antibodies anti-RyR1 (Upstate), anti-CaM Kinase II-β Cbβ-1 (Gibco), anti-DHPR-β_1 (Upstate), anti-DHPR-α_1 (Upstate) and anti-Grb2 (Transduction Labs) were used at a 1:4000 dilution. The monoclonal anti-GST antibody (Santa Cruz) was used at 1:15 000 dilution. Monoclonal anti-Src (Upstate) was used at 1:2000. The affinity purified polyclonal rabbit antibodies, RU16 (broad CaM Kinase II antibody) and anti-SOCK were used at 1:4000. The primary antibodies were incubated with the membranes for either 1.5 hours at room temperature or overnight at 4°C. The primary antibodies were then decanted and the membranes were washed for 4 x 15 minutes with TBS-T at room temperature. Secondary antibodies were conjugated to the enzyme horse-radish peroxidase (HRP). The goat anti-mouse-HRP (Amersham Pharmacia) was used to detect monoclonal antibodies and was used at a 1:5000 dilution for all the monoclonal antibodies with the exception of anti-GST which required the secondary

antibody to be diluted 1:15 000 in order for a clean signal to be observed. The goat anti-rabbit-HRP (Amersham Pharmacia) was used at 1: 4000 dilution for all the rabbit polyclonal antibodies. The secondary antibodies were incubated with the membranes for 1 hour at room temperature followed by a 6 x 15 minute wash with TBS-T. To visualize the immunoreactivity of the primary antibodies, 3 ml of enhanced chemilumnescent reagent, ECL (NEN) was incubated with the membranes for 1 minute at room temperature. The HRP conjugated secondaries catalyze a reaction with the ECL which produces light. The blots were exposed to Kodak BioMax® MR film for periods of 10 seconds to 5 minutes, and were subsequently developed in a Kodak film developer.

2.3 Single and Double Immunohistochemical Staining of Skeletal Muscle Sections

In order to visualize the localization of skeletal muscle membrane proteins, immunohistochemical staining was performed on sections of skeletal muscle. Longitudinal sections of rat gastrocnemius muscle were obtained with a Microm cryostat (Heidelberg) from muscles embeded in paraffin which provided 12 μm sections suitable for analysis by immunohistochemistry. The sections were placed onto Super Frost/Plus slides (Fisher Brand), transferred to a moist chamber at room temperature and washed 2 x 15 min with buffer A (0.5% BSA, 0.15% glycine in PBS, pH 7.4).

Sections were blocked with buffer A, supplemented with 5% horse serum (Jackson ImmunoResearch) for 20 minutes at room temperature. After blocking, the sections were incubated for 1 hour at room temperature with the following primary antibodies: anti-CaMKII-β Cbβ-1 (IgG2b, Gibco BRL) used at 1:200 dilution in Buffer A and anti-RyR-XA7B6 (IgM, Upstate) used at 1:100 dilution in Buffer A. In a series of experiments, a

combination of the above antibodies was diluted as indicated for double immunohistochemical staining. The prepared sections were washed 3 x 15min with Buffer A prior to the addition of the fluorochrome labeled secondary antibodies.

Due to the fact that both primary antibodies are mouse monoclonals, while being of different immunoglobulin (Ig) classes (IgG2b vs. IgM), secondary antibodies where selected which would react only with the specific Ig class to minimize any cross reactivity. Fluorescein (FITC)- conjugated AffiniPure goat anti-mouse IgG (subclassses 1 + 2a +2b + 3) and Fc_γ fragment specific (Jackson ImmunoResearch) was diluted 1:100 in Buffer A. However, the Cy™3-conjugated AffiniPure goat ant-mouse IgM, μ chain specific (Jackson ImmunoResearch) was diluted 1:800 in Buffer A. Secondary antibodies were incubated with the sections for 1 hour at room temperature in the dark. The sections were washed three x 15min in PBS, coverslipped with Antifade PPD (p-Phenylenediamine) mounting media (0.1% PPD/glycerol) and examined using a Zeiss Axiophot microscope and images captured with a Sony Power HAD 3CCD colour video camera.

2.4 Purification of CaM Kinase II from the Brain and Skeletal Muscle

Ten rat brains were homogenized in 5 volumes of brain homogenization buffer (10 mM HEPES pH 7.4, 1% Triton X-100, 10% sucrose (wt/wt), 1 mM PMSF, 0.5 μM leupeptin and 0.5 μM pepstatin) with 4 x 30-second bursts in a polytron homogenizer. The homogenate was centrifuged at 10 000 x g for 10 minutes in a Beckman JA-20 rotor and Beckman Avanti™ J-25 centrifuge. The pellet was discarded and the supernatent was ultra-centrifuged at 100 000 x g in a 42.1 Ti Beckman rotor and Beckman Optima™ L-90K

Ultracentrifuge for 1 hour at 4°C. After this step, the pellet was again discarded and the supernatant, consisting of diluted cytoplasm, was adjusted to 1 mM $CaCl_2$ with a 100 mM $CaCl_2$ stock solution.

Purification of calmodulin binding proteins was accomplished by adding 150 µl of Calmodulin Sepharose® 4B (Pharmacia cat#17-0529-01) to the sample, followed by end-over-end rotation for 2 hours at 4°C. The sepharose beads were separated from the solution by centrifugation in a table-top centrifuge (Fisher Scientific, Centrific™ centrifuge) at 4000 rpm for 1 min. The supernatent was discarded and the beads were washed 3 x 5 minutes in homogenization buffer supplemented with 1mM $CaCl_2$. The calmodulin binding proteins were eluted by adding 1 ml of brain homogenization buffer that contained 5 mM EDTA and 5 mM EGTA, and using end-over-end rotation for 1 hour at 4°C. The EDTA and EGTA were removed by dialysis carried-out overnight in a Slide-A-Lyzer® (5000 MWCO, Pierce) against 2 L of 10 mM Hepes pH 7.4, supplemented with 10% sucrose to maintain the initial volume.

Skeletal muscle CaMKII was purified from detergent solubilized Fraction 4 and Fraction 5 from the skeletal muscle membrane fractionation experiment as described by Tuana and MacLennan, 1988. The heavy SR membranes were solubilized with membrane solubilization buffer (10 mM HEPES pH 7.4, 2% Triton X-100, 0.6 M KCl, 10% sucrose (wt/wt), 1 mM PMSF, 0.5 µM leupeptin and 0.5 µM pepstatin) with rotation at 4° C for 2 hours. The insoluble membranes were separated from solubilized proteins by ultra-centrifugation carried out at 100 000 x g in a 42.1 Ti Beckman rotor and Beckman Optima™ L-90K Ultracentrifuge for 1 hour at 4°C. As before, the pellet was discarded and the supernatant was adjusted to 1 mM $CaCl_2$ with a 100 mM $CaCl_2$ stock solution.

Purification of CaM Kinase and other calmodulin binding proteins was accomplished by the addition of 150 µl of calmodulin Sepharose® 4B (Pharmacia cat#17-0529-01) to the solubilized membranes and all steps pursuant to this were performed as above.

2.5 Expression and Purification of GST-Fusion Proteins

The cDNAs of the muscle and brain-specific CaM Kinase II β isoforms were subcloned into a GST expression vector and were purified using the GST® fusion protein system (Amersham Pharmacia). The pGEX-Kg vector was used and all cDNAs were either subcloned from existing vector/constructs or PCR products were digested with the appropriate restriction endonucleases and ligated into the vector. A total of 10 fusion proteins were purified corresponding to full length SOCK, full length CaM Kinase II β as well as protein domains of the proline rich region of SOCK, Q2A (all three proline rich tandem repeats), proline rich exon 1 - P1, proline rich exon 2 - P2, proline rich exon 3 - P3, Src-SH3 (obtained from Dr. John Bell, University of Ottawa) Grb2 N-SH3, Grb2-SH2 and Grb2 C-SH3 (Grb2 constructs were provided by Dr. Anthony Pawson, University of Toronto). Table 1 provides detailed information about each construct.

Table 2.1: GST-Fusion Protein Expression Constructs

Construct	Expressed protein	MCS orientation	Predicted Molecular Size of GST Fusion
GST	Glutathione S Tranferase	Bam HI EcoR1	26 kDa
GST-SOCK	Full cDNA of muscle specific CamKII-β isoform	Bam HI EcoR1	99 kDa
GST-CaMKII-β	Full cDNA of brain specific CamKII-β isoform	Bam HI EcoR1	86 kDa
GST-Q2A	All three proline rich tandem repeats of SOCK	Bam HI EcoR1	39 kDa
GST-P1	Exon 1 of the proline rich region of SOCK	Bam HI EcoR1	30 kDa
GST-P2	Exon 2 of the proline rich region of SOCK	Bam HI EcoR1	29 kDa
GST-P3	Exon 3 of the proline rich region of SOCK	Bam HI EcoR1	32 kDa
GST-Src SH3	SH3 Domain of Src kinase	Bam HI EcoR1	34 kDa
GST-N-SH3	N-terminal SH3 domain of Grb2	Bam HI EcoR1	33 kDa
GST-SH2	SH2 domain of Grb2	Bam HI EcoR1	37 kDa
GST-C-SH3	C-terminal SH3 domain of Grb2	Bam HI EcoR1	33 kDa

Due to the high GC content in the cDNA of SOCK, a special strain of *E. coli* called CodonPlus™-RP BL21 (Stratagene) was required to correct for the codon bias between the GC-rich sequences of SOCK and that of *E. coli*. The CodonPlus™-RP cells contain a ColE1 compatible plasmid that encodes extra copies of the argU and proL tRNA genes which rescues expression of genes restricted by either AGG/AGA arginine codons or the CCC codon for proline. In order for the expression of full-length recombinant SOCK, the extra tRNAs for arginine and proline are required. Codon bias has been found to cause problematic expression of heterologous genes from GC-rich genomes like in mammals when expressed in *E. coli* hosts. Biased codon usage refers to the relative differences in the occurrence of specific codons for a given amino acid between the genomes of different species. For example, the codons AGG and AGA for arginine and the codon CCC for proline are rarely used in bacterial genes which is reflected by the relatively low abundance and expression of their respective tRNA species as compared to mammalian genomes (Andersson and Kurland, 1990; Carstens et al., 2000). It has been suggested that clusters or more than average us of AGG/AGA or CCC codons in a cDNA can reduce both the quantity and quality of the synthesized protein during forced high level expression in bacteria (Kane, 1995). Analysis of the deduced amino acid sequences encoded by the cDNA for SOCK for the presence of AGA/AGG arginine and CCC proline codons led to the identification 10 AGA, 10 AGG and 19 CCC codons with 4 tandem AGG-AGG/AGA-AGG pairs. Most of these codons are contained within the exons encoding the proline rich region of SOCK. Translation of tandem AGG-AGG or AGA-AGA sequences in bacteria, has been found to result in 50% ribosomal frameshift (in the +1 direction), ribosomal hop or premature translation termination when the ribosomes read through these tandem

arginine codons (Spanjaard and Duin, 1988). If this phenomenon is present during the translation of SOCK, this may explain the observed truncated products of SOCK that are most likely due to premature translational stops due to the presence of 4 tandem AGG-AGG/AGA-AGA codon pairs. For example, if considering the 50% probability for a +1 frameshift occurring at each of the tandem arginine codons (determined by Spanjaard and Duin, 1988), the possibility of translating the full-length product is approximately 6%. This does not take into account the contribution of the CCC proline codons or single AGG/AGA codons to translation errors. Biased codon usage is observed with other codons other than arginine and proline, which may also explain the multiple protein products observed in affinity purified recombinant CaM Kinase II β. A putative role for the effect on translation arising due to codon bias between bacterial genes with high and low codon bias, is that this allows for efficient translation of genes with low codon bias which are usually genes important for bacterial replication such as structural proteins.

The isolation of GST-SOCK and GST-CaM Kinase II β was accomplished by following an optimized expression and purification scheme, which ensured soluble expression of the heterologous full-length kinases. Cultures were seeded with single colonies taken from LB agar plates and grown overnight in a 30ml volume of Rich LB media (1.6% Tryptone, 1.2% Yeast extract, 0.5% NaCl and 2% glucose with Ampicillin, 100 μg/ml and chloramphenicol, 40 μg/ml), placed in 50mL Falcon tubes. Holes were burnt in the caps of the tubes for proper aeration.

For each kinase, five falcon tubes were seeded with one colony from a LB agar plate. The following day, the bacterial cultures were centrifuged for 10 minutes at 5000 rpm in a Beckman JA18 rotor (Beckman Avanti™ J-25 centrifuge) in 50 ml Falcon tubes. The

supernatant was discarded and the pellets were vortexed before being resuspended in 30 ml fresh rich LB media supplemented with the appropriate antibiotics. Aliquots of 5ml were added to thirty falcon tubes containing 30 ml of rich LB media with ampicillin and chloramphenicol. The cultures were grown at 37°C/250-rpm in an Innova 400 incubator (New Brunswick Scientific) until an optical density (A_{595} nm) of 0.5-0.6 was reached. The tubes were then placed in a -20°C room and chilled to 5°C.

Fusion protein synthesis was induced by adding 17 µl of 100 mM IPTG into each Falcon tube (0.05 mM IPTG). The cultures were grown at 28°C/250 rpm for four hours before collecting the bacteria by centrifugation in a Beckman JA18 rotor for 10 minutes at 5000 rpm. The pellets were vortexed and resuspended with 100 ml of lysis buffer (PBS, pH 7.4, 1% Triton® X-100, 5% glycerol, 0.8% NaCl). The pellets were resuspended in a total of 100 ml lysis buffer for SOCK and 100 ml for CaM Kinase II β. The tubes were flash frozen in liquid nitrogen and stored at -80°C until ready to proceed with the batch purification.

The bacteria were thawed in a water bath at room temperature and then placed on ice. After, the bacteria were lysed by adding lysozyme to 0.1 mg/ml (Boehringer Mannheim) and incubated for 30 minutes on ice with occasional shaking. The bacterial lysate was sonicated for one minute (2 times 30-second bursts) using a 60 Sonic Dismembrator sonicator (Fisher Scientific). The tubes were centrifuged in a Beckman JA 20 rotor and Beckman Avanti™ J-25 centrifuge for 20 min at 20 000 x g, 22 °C. The GST-fusion proteins were affinity purified on glutathione sepharose 4B® (Amersham Pharmacia). The glutathione sepharose® 4B was equilibrated with lysis buffer for 10 minutes before 500 µl was added to each Falcon tube. Tubes were rotated end-over-end at

room temperature for 1.5 hrs. The beads were separated from the solution with a ten second pulse at 4000 rpm in a table top centrifuge (Eppendorf 5417C) and were washed 3 x 5 minutes with lysis buffer with rotation at room temperature. The beads were finally washed twice in Purification wash buffer (PBS, pH 7.4, 0.5% NP-40, 5% glycerol, 0.8% NaCl) and transferred to 1.5 mL eppendorf tubes. GST-fusion proteins were eluted by adding 1ml of elution buffer (PBS, pH 9.5, 50 mM glutathione, 0.5% NP-40, 5% glycerol, 0.8% NaCl) and rotating the tubes at room temperature for 2 hours. The purified kinases were analysed with Western blots using an anti-GST monoclonal Ab (Santa-Cruz biotech). All other GST-fusion proteins were purified as above with the exception of growing the cultures in 1L buffled flasks.

A total of 2 μg of GST-SOCK and GST-CaM Kinase II β as well as 30 μg of sarcoplasmic reticulum and brain homogenate were separated on 10% polyacrylamide SDS gels and electroblotted on to PVDF membrane. Western blots were performed with RU16 at a dilution of 1:2000 in TBS-T and Cbβ-1 at a dilution of 1:2000 in TBS-T and the reaction was visualized with ECL® (NEN) after exposure to Kodak BioMax® MR film and development in a Kodak X-ray film developer.

2.6 Activity of Recombinant SOCK and CaM Kinase II β

The CaM dependent protein kinase activity of purified recombinant GST-SOCK and GST-CaM Kinase II β was measured using a CaM Kinase II Assay kit (UPSTATE biotechnology cat# 17-135). This assay kit measures the ^{32}P incorporation into Auto Camtide II, a specific substrate peptide comprised of the amino acids KKALRRQETVDAL which is found in the protein synapsin I, a well-documented CaM Kinase II substrate. The

phosphorylation was performed according to the manufacturer's recommendation. Final kinase buffer concentrations were as follows: 20 mM MOPS, pH 7.2, 25 mM β-glycerol phosphate, 1 mM sodium orthovanadate, 1 mM dithiothreitol, 1mM $CaCl_2$, 1 mM EGTA, 15 mM $MgCl_2$, 100 μM Auto Camtide II, 0.4 μg Calmodulin, 125 μM ATP-cold/[γ-^{32}P] ATP (10 μCi/reaction) and 1 μM of GST-SOCK or GST-CaM Kinase II β. In a control reaction, 5 mM EGTA was added to determine the Ca^{2+} dependence of the enzymes.

Samples were incubated for 10 minutes at 30°C and the reaction was terminated with the addition of 20 μL of cold trichloroacetic acid. The peptide was separated from the residual [γ-^{32}P]-ATP by spotting 20 μL of the reaction sample onto numbered P81 phosphocellulose squares that were washed 3 x 5 min in 0.75% phosphoric acid and once in acetone before quantitation by liquid scintillation counting. All reactions were performed in duplicate and the results of the γ^{32}P incorporated into the peptide as determined with scintillation counts, were corrected for background counts obtained in the absence of added enzyme.

The effect of putative SOCK binding proteins on SOCK enzyme activity was compared in a set of parallel experiments. In these experiments, 10 μM of different GST fusion proteins (GST, GST-SH3 domain of Src, GST-SH3-N terminus of Grb2, GST-SH2 domain of Grb2 or GST-SH3-C terminus of Grb2) were added to the enzyme assay. Control experiments were performed to determine if the components of the GST elution buffer (PBS, pH 7.2, 10% glycerol, 0.5% NP-40 and 30 mM glutathione) had any effect on SOCK or CaM Kinase II β enzyme activity. These results represent the mean ± SDM for four experiments.

2.7 Purification of Triads from Rabbit Skeletal Muscle

Triad vesicles were obtained as described by Marty et al., 1994. New Zealand white rabbits were sacrificed and fast twitch skeletal muscle was collected and homogenized (as described in 2.1), with the homogenization buffer composed of, 20 mM PIPES pH 7.1, 150 mM KCL, 300mM sucrose, 2.5 mM EGTA. The homogenate was centrifuged at 4000 x g in a Beckman JA 20 rotor and Beckman Avanti™ J-25 centrifuge for 15 minutes, filtered through Whatman no. 4 paper and incubated for 1 hr at 4°C in the presence of 1 M NaCl. After a second centrifugation for 20 minutes at 10 000 x g using a Beckman JA 20 rotor and Beckman Avanti™ J-25 centrifuge the supernatent was discarded and the pellets were homogenized in buffer A (20 mM PIPES pH 7.1, 150 mM KCL, 300mM sucrose, 2.5 mM EGTA). The triad vesicles were collected by centrifugation at 17 000 x g for 40 minutes 4°C, washed twice and resuspended with buffer A without EGTA. Protein quantitation was performed with the BCA® protein assay kit (PIERCE), the triad vesicles were frozen in liquid nitrogen and stored at -80°C.

2.8 Phosphorylation of immunoprecipitated Ryanodine and Dihydropyridine Receptors by Recombinant SOCK

RyR and DHPR-α_{1S} and DHPR-β_{1A} sub-units were immunoprecipitated from solubilized triad structures composed of terminal cisternae and T-tubules as described by Marty et al., 1994. Triads (5 mg/ml) were diluted 1:1 in solubilization buffer (25 mM MOPS, pH 7.2, 1.6% CHAPS, 0.9 M NaCl 0.3 M sucrose and 50 μM EGTA) and rotated at 4°C for 2 hours. Particulate material was separated from solution by ultracentrifugation at 190 000 x g in a 60 Ty Beckman rotor and Beckman Optima™ L-90K Ultracentrifuge for 1

hour at 4°C. The supernatent was kept and aliquots of 1.0 mL were added to 1.5 mL eppendorf tubes. Immunoprecipitation of the RyR, DHPR α_{1S} and DHPR β_{1A} sub-units was performed with anti-RyR1, anti-DHPR α_{1S} and anti-DHPR β_{1A} specific monoclonal antibodies (Upstate Biotechnology) at 1:100 dilutions. The antibodies were incubated with the solubilized triads overnight at 4°C with rotation. On the following morning, the antigen-antibody complexes were precipitated by adding 30 µL of protein A/G Plus® agarose (Santa Cruz Biotech). The samples were incubated for 4 hours at 4°C with rotation. The protein A/G agarose slurry was separated from the solution by centrifugation and was washed 4 x 5 minutes with solubilization buffer diluted 1:1 in homogenization buffer. The immunoprecipitated proteins were subjected to a final equilibration wash in enzyme assay buffer (20 mM MOPS, pH 7.2, 25 mM β-glycerol phosphate, 1 mM sodium orthovanadate, 1 mM dithiothreitol and 0.3 M sucrose). Enzyme assays were performed as per the manufacturer's recommendation (Upstate CaM Kinase II enzyme assay kit) with the modification of 0.3 M sucrose to keep the receptors from aggregating. The total amount of GST-SOCK added was 100 ng and the reaction was incubated at 30°C for 10 minutes. After this, the tubes were placed on ice and washed 3 times with a 1:1 mix of solubilization buffer and skeletal muscle homogenization buffer to remove GST-SOCK. The protein A/G beads with the immunoprecipitated proteins were then suspended in 30 µL of 2 X SDS loading buffer and electrophoresed on 7% and 10% polyacrylamide gels. The RyR and DHPR-α_1 were resolved on a 7% polyacrylamide gel, and the DHPR-β_1 sub-unit was resolved on a 10% polyacrylamide gel. The proteins were electroblotted onto PVDF membrane and exposed to Kodak BIOMAX™ MS film overnight at -80°C and developed in a Kodak x-ray film developer.

2.9 Measurement of Ca^{2+}/Cam Dependent Activity of ^{32}P incorporation into proteins of the Sarcoplasmic Reticulum

Triads (5 mg/mL, as described in section 2.8), were incubated in conditions suitable for CaM Kinase activity. Final kinase buffer concentrations were as follows: 25 mM MOPS, pH 7.2, 10 mM β-glycerol phosphate, 1 mM sodium orthovanadate, 1 mM dithiothreitol, 1 mM $CaCl_2$, 0.25 mM EGTA, 15 mM $MgCl_2$, 2 μM calmodulin, 0.4 mM ATP-cold/[γ-^{32}P]-ATP (200 μCi/mL), 0.3 M sucrose. All samples were kept on ice until ready for incubation at 25°C for 5 minutes. Two sets of reactions were performed, one with Ca^{2+} and calmodulin and one without added Ca^{2+}. PKA and PKC specific peptide inhibitors were added to all samples (Upstate). Kinase activity was terminated by the addition of 5 mM EDTA and 5 mM EGTA and the membranes were diluted 1:1 with solubilization buffer (25 mM MOPS, pH 7.2, 1.6% CHAPS, 0.9 M NaCl 0.3 M sucrose and 50 μM EGTA) and rotated at 4°C for 2 hours. Particulate material was separated from solution by ultracentrifugation at 190 000 x g in a 60 Ty Beckman rotor and Beckman Optima™ L-90K Ultracentrifuge for 1 hour at 4°C. The proteins were immunoprecipitated and electrophoresed on SDS polyacrylamide gels as described above. The proteins were electroblotted onto PVDF membranes and exposed to Kodak BIOMAX™ MS film overnight at -80°C and developed in a Kodak x-ray film developer.

2.10 Immunoprecipitation of Src and Grb2 from Skeletal Muscle

The heavy SR enriched fraction F4 (see membrane fractionation section 3.1) was solubilized with an equal volume of muscle homogenization buffer (10 mM HEPES pH 7.4, 5 mM EDTA, 1.2 mM EGTA, 10% sucrose, 1 mM PMSF, 0.5 μM leupeptin and 0.5

μM pepstatin). The buffer was supplemented with 2% Triton X-100 and 0.6 M KCl and mixed with end-over-end rotation for 2 hours at 4°C.

The solubilized membranes were centrifugated at 190 000 x g for 1 hour at 4°C (42 000 rpm, Beckman 42.1 Ti rotor) to remove unsolubilized membranes. The supernatent consisting of solubilized membranes was kept and the pellet was discarded. A 250 μg sample of solubilized fraction F4 (as determined by BCA™ protein assay kit) was incubated overnight at 4°C with anti-Src rabbit polyclonal antibody conjugated to agarose (approximately 30 μl) (Santa Cruz Biotechnology Sc:19-AC), and anti-Grb2 rabbit polyclonal antibody conjugated to agarose (approximately 30 μl). Purified rabbit IgG conjugated to agarose (approximately 30 μl) was used as a negative control, which would detect non-specific interactions if present. Peptide neutralization (blocking) was performed for anti-Src agarose and anti-Grb2 agarose conjugate with blocking peptides Sc:19P and Sc255P (Santa Cruz Biotechnology). These peptides contain the immunogen used in the production of these antibodies and thus, effectively block the antigen recognition site of the antibodies. The antibody agarose conjugates were pre-incubated with their respective blocking peptide for 2 hours at room temperature prior to the addition of solubilized fraction 4 (described in skeletal muscle membrane fractionation). When un-conjugated antibodies were used, protein A/G agarose beads (60 μl of 50% slurry) were incubated for four hours at 4°C to collect/precipitate the antibody antigen complexes from solution. The agarose beads were centrifuged at 4000 rpm for ten seconds in a table-top centrifuge and the supernatent was removed. The beads were washed in this manner 4 x 5 min in PBS with 2% TritonX-100, 0.6 M KCL to remove non-specifically associated proteins, followed by a final wash in PBS with 2% TritonX-100 to remove KCl. The beads were resuspended in 30

µl of 2X SDS loading buffer and the proteins were boiled for 5 minutes. The immunoprecipitation samples along with a sample of the solubilized membranes (30 µg) were electrophoresed on a 10% discontinuous SDS polyacrylamide gel and the proteins were electroblotted on to PVDF membrane and Western Immunoblotting was performed as described above.

2.11 Site-directed Mutagenesis of the Proline-Rich Region of SOCK

Point mutations in the proline rich region of SOCK were performed via the QuickChange™ Site-Directed Mutagenesis method (Stratagene cat#200518). The basic procedure employs a supercoiled double-stranded DNA vector (protein expression plasmid) with an insert of interest and two complementary synthetic oligonucleotide primers containing the desired mutation. The mutant oligonucleotide primers are extended during temperature cycling by using 2 units of PfuTurbo™ DNA polymerase II, which replicates the entire template plasmid with high fidelity and incorporates the mutant oligonucleotide primers (Figure 2.2). After temperature cycling in a MiniCycler™ MJ Research (refer to table 2 for cycling parameters), the parental template plasmid is digested with the restriction enzyme Dpn I, an endonuclease which is specific for methylated DNA (target sequence is 5'-Gm6ATC-3'), leaving the newly synthesized mutated DNA intact, as it lacks methylation. The newly synthesized DNA remaining after Dpn I treatment, which contains the desired mutation was transformed into $RuCl_2$ competent XL-1 Blue *E. coli* and plated on LB-agar plates containing ampicillin.

The staggered nicks in the newly synthesized ds-DNA were repaired in the XL-1 Blue *E. coli* cells following transformation. The following day colonies were picked to

inoculate overnight cultures in LB media supplemented with ampicillin. Plasmid minipreps was performed with a Qiagen Plasmid DNA mini-prep isolation kit from the overnight cultures and sequencing was performed with the ABI PRISM™ Dye Terminator Cycle Sequencing Ready Reaction Kit (Perkin Elmer cat# 402078). Primers were designed so that point mutations altered specific codons encoding proline and arginine to alanine or valine. Primers were between 27-34 nucleotides (nt) long with the desired mutation in the middle. Melting temperatures (T_m) were estimated using the following formula, which accounts for the effect of mismatched base pairs in the target mutation site:

$$T_m\ (^{\circ}C) = 81.5 + 0.41(\%GC) - (675 / N) - \%\ \text{mismatch}$$

where N is the primer's length in base pairs.

Figure 2.2 Illustration of the Quick Change Site Directed Mutagenesis Technique

PCR amplification of the entire template DNA plasmid was accomplished with Pfu DNA polymerase using complementary primers with a point mutation of interest. The PCR product was separated from the template plasmid by incubating the PCR reaction with Dpn I, a restriction endonuclease that digests the methylated parental DNA plasmid and leaves the newly synthesized DNA intact. The synthesized plasmid with staggered nicks was transformed into XL-1 blue *E. coli* cells and plated on LB agar. Plasmid DNA was purified from cultures seeded with single colonies and was sequenced to check for the mutation.

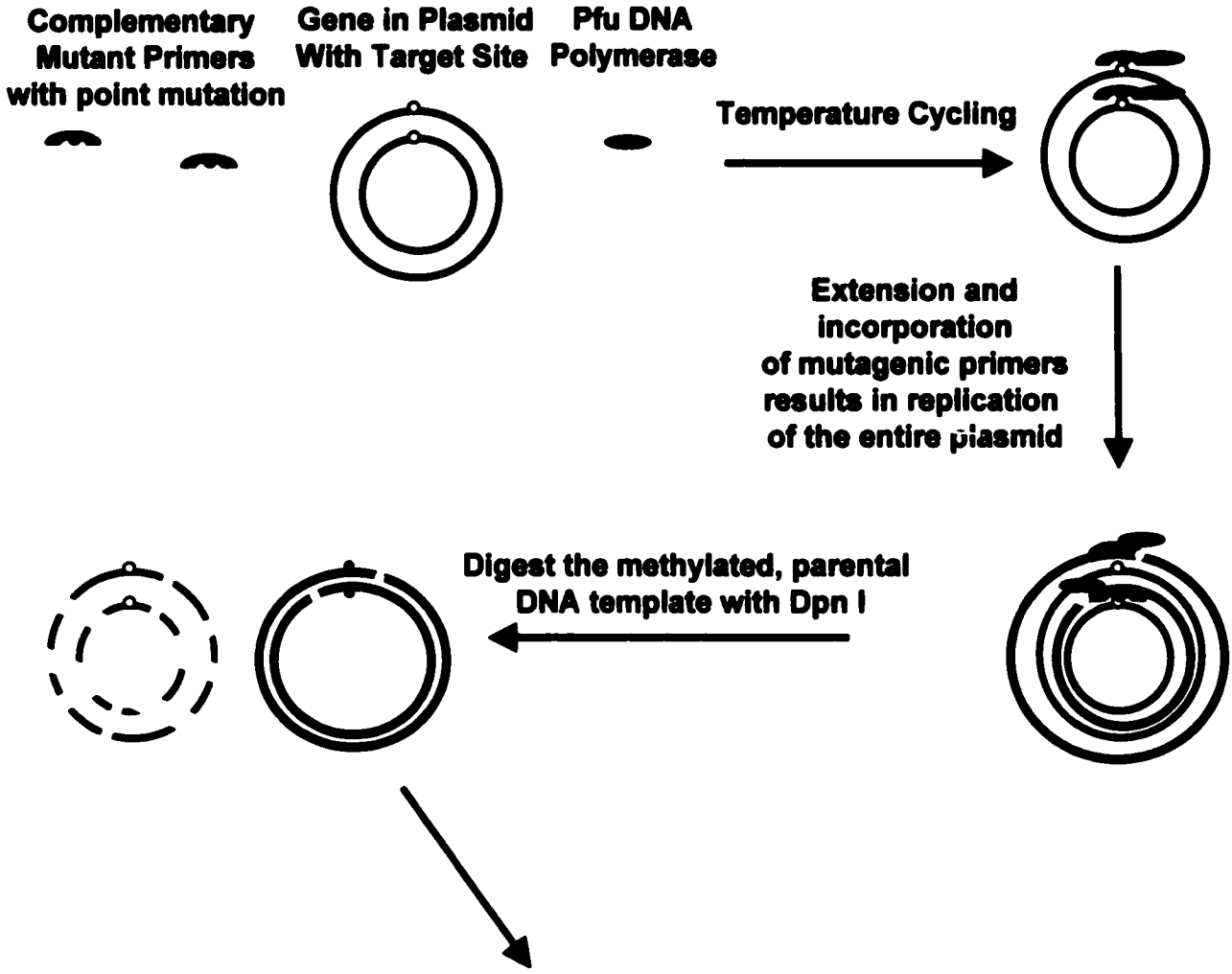

- Mutated dsDNA plasmid remains intact
- Transform into XL-1-Blue competent cells
- XL-1 Blue cells repair the staggered nicks
- Purify Plasmid DNA
- Sequence to check for mutation
- Perform SH3 domain binding assays

Table 2.2: Summary of targeted amino acids, predicted T_m and PCR parameters

Targeted Amino Acid/ (Codon)	Mutated Residue/ (Inserted Codon)	Corresponding Primer Sequence in nt from cDNA/ (Primer Length)	Predicted T_m	PCR* Cycling Parameters
R^{448} (AGG)	A^{448} (GCT)	1330-1356 (27nt)	71.3°C	Regular
R^{491} (AGG)	A^{491} (GCT)	1455-1488 (34nt)	79.4°C	High Temp
P^{516} (CCC)	V^{516} (GTT)	1533-1559 (27nt)	77.3°C	High Temp
P^{517} (CCG)	A^{517} (GCT)	1536-1562 (27nt)	78.5°C	High Temp
P^{520} (CCA)	A^{520} (GCT)	1546-1572 (27nt)	78.0°C	Regular
P^{522} (CCG)	V^{522} (GTT)	1552-1578 (27nt)	69.7°C	Regular
P^{525} (CCT)	A^{525} (GCT)	1559-1588 (29nt)	79.6°C	Regular
R^{533} (CGG)	A^{533} (GCT)	1585-1611 (27nt)	81.5°C	High Temp

* PCR cycling parameters are shown in Table 3.

Two different PCR cycling parameters were used as indicated in the PCR Cycling Parameters column in Table 3. Regular denotes the regular cycling parameters as outlined in the QuickChange™ instruction manual while high temperature denotes optimized conditions for GC rich primers.

Table 2.3: PCR Cycling Parameters for Mutagenic Primers

PCR STEP	Regular Temperature		High Temperature	
	Temperature	Time	Temperature	Time
1	95°C	1 min	95°C	1 min
2	95°C	30 sec	95°C	30 sec
3	58°C	1 min	66°C	1 min
4	68°C	14 min	72°C	10 min
5	To step 2: 18 times		To step 2: 18 times	
6	4°C	∞	4°C	∞
7	End		End	

2.12 Protein interaction assay with GST-fusion proteins

For the protein association assay, 500 µg aliquots of skeletal muscle cytosol (see section 2.1) was pre-cleared with 25 µl of GST-glutathione sepharose to reduce non-specific associations. The GST-beads were separated from the cytosol by a 10 second spin at 4000 rpm in a table top centrifuge (Eppendorf 5417C) and the supernatent was transferred to new 1.5 ml Eppendorf tubes. The supernatents were then incubated with 25 µl of GST-fusion protein (GST-Q2A, GST-Q2A with point mutations, GST-CaM Kinase II β, and GST-SOCK) or GST alone, on glutathione sepharose® beads, with rotation for 2 hours at 4°C. The fusion protein beads were washed four times with 1.5 mL of wash buffer (PBS, pH 7.4, 150 mM NaCl and 1 % Triton® X-100). The beads were sedimented by centrifugation at 4000 rpm for 10 seconds, the supernatent was aspirated and the beads were re-suspended in 25 µL of 2X SDS loading buffer, boiled for 5 minutes and electrophoresed on 10% polyacrylamide SDS gels. The proteins were electroblotted onto PVDF membranes and described above. The membranes were used in Western blot analysis and tested for the presence of Grb2 with an anti-Grb2 monoclonal mAb (Transduction Laboratories). The reaction was visualized with Horse Radish Peroxidase (HRP)-conjugated anti-mouse IgG (Jackson ImmunoResearch) and the addition of Enhanced Chemiluminescence (ECL) reagent (NEN), followed by exposure to Kodak BioMax® MR film and subsequent development in a Kodak X-ray film developer.

2.13 Biotinylation of GST-Fusion Protein Probes

Purified fusion proteins were biotinylated with Biotin XX-SE, an amine reactive succinimidyl-ester with a 14 atom spacer between Biotin and the reactive carboxylic acid

(Molecular Probes cat# B-1606). This reactive form of biotin was chosen over other forms of biotin due to its 14 atom spacer arm which ensures ease of interaction with avidin, streptavidin or neutravidin as utilized in overlay experiments in which the buffers are usually at or a near neutral pH of 7.2-7.4.

GST fusion constructs containing GST, GST-SH3 from Src, GST-SH3-C-terminus from Grb2, GST-SH3-N-terminus from Grb2 and GST-SH2 from Grb2 were expressed in BL21 Codon Plus® RP cells. The GST fusion proteins were purified from 1.5L cultures with glutathione sepharose 4B® (Pharmacia Biotech) as explained in section 2.5. The fusion proteins were eluted in 10 mL of elution buffer and were concentrated to 1 ml with Millipore Ultrafree BIOMAX-5K centrifugal filter devices with a molecular cut-off of 5 kDa (Millipore cat# UFV2BCC10).

The concentrated eluate was dialyzed using Slide-A-Lyzer® dialysis cassettes (PIERCE cat# 66380), which had a molecular weight cut-off of 10 kDa and a volume capacity of 0.5-3.0 mL. This dialysis procedure was performed in order to remove glutathione, which is not compatible with the BCA™ protein assay (PIERCE). Protein concentrations were determined with a BCA™ protein assay kit (PIERCE cat# 23225) using 100 µl of the dialyzed eluate with bovine serum albumen as standard.

The concentrated eluate was adjusted to a concentration of 0.15M Sodium-bicarbonate (pH 8.5) with a 1.5M stock of Sodium-bicarbonate (pH 8.5). 10 mg of Biotin XX-SE was dissolved in 1 ml of DMSO with a tabletop vortex. Biotinylation of the GST-fusion probes was accomplished via the addition of 200 µl of the dissolved Biotin to the GST-fusion proteins with end-over- end rotation at room temperature for 1.5 hours. The

reaction was terminated with the addition of 150 µl of Hydroxylamine (1.5 M, pH 8.5), followed by end-over-end rotation for 10 minutes at room temperature.

Unreacted labeling reagent was separated from the conjugate by gel filtration through a Sephadex G-25 (Pharmacia Biotech) column, consisting of 3.0 ml of pre-swollen Sephadex G-25, which was blocked with 1% BSA (Bovine serum albumen) in PBS and washed with PBS to remove unbound BSA. The conjugated proteins were diluted to 2.5 ml with PBS, added to the column and allowed to flow through. The first 1.0 ml of flow through was discarded (void volume) and the remaining 1.5 ml was kept for analysis. A further 2.5 ml of PBS was added to the column and the first 1.5 ml was also kept for analysis. An equal volume of glycerol was added to each of the 1.5 ml samples which were then frozen at -20°C. Protein concentrations of the biotinylated probes were determined with the BCA™ protein assay kit (PIERCE).

Analysis of biotinylation was performed by running 10 µg of each of the protein probes on an SDS PAGE gel, transferring to Hybond-P® PVDF membrane (Amersham Pharmacia), blocking with PBS-milk (5% Carnation skim milk powder) and treating the biotinylated probes with PBS-milk and neutravidin-HRP (1:10000). Neutravidin-HRP was used as it displays the least non-specific binding as compared to streptavidin and avidin. The neutravidin/biotin interaction was visualized by the addition of 4 ml of ECL® Plus reagent (NEN cat# Enhanced Chemiluminescence), followed by exposure to Kodak BioMax MR® film and subsequent development in a Kodak X-ray film developer.

2.14 PCR Amplification of Individual Exons P1, P2 and P3

In order to determine which of the three proline rich tandem repeats in SOCK can interact with SH3 domains of Src and Grb2, these exons had to be inserted individually into

the GST expression vector. Primers were designed and synthesized to amplify the individual exons via polymerase chain reaction (PCR)(Table 2.3). The PCR products of exon P1, P2 and P3 were prepared for ligation into the multiple cloning site of pGEX-Kg by digestion with the restriction endonucleases Eco RI and Bam HI. The restriction endonucleases were separated from the PCR products by means of electrophoresis through a 1% agarose DNA gel. The PCR products were excised and extracted from the agarose gel with a Qiagen DNA gel extraction kit. The PCR products were ligated into pGEX-Kg (also digested with Eco RI and Bam HI and separated from the endonucleases as explained above) by incubating the PCR products with the digested vector DNA with the addition of T4 DNA ligase in T4 DNA ligase buffer at 15°C overnight. The ligated constructs were transformed into $RuCl_2$ competent DH5α *E. coli* cells by a standard heat shock protocol (Maniatis and Maniatis, 1994). After this, the cells were plated onto LB agar plates supplemented with ampicillin (100 μg/ml) and placed into an Isotemp incubator (Fisher Scientific, Model 630D) overnight at 37°C. The next day, colonies were picked and inoculated into 5 ml of LB media supplemented with ampicillin (100 μg/ml). The plasmid DNA was purified with a Qiagen plasmid mini-prep kit based on the alkaline lysis DNA isolation method (Birnboim and Doly, 1979). To check for the insertion of the PCR product, the DNA vectors were digested with Bam HI and Eco RI and separated via electrophoresis on a 1% agarose gel. Vectors that contained the desired insert were sequenced to ensure for the correct orientation and reading frame. Positive vectors with the correct insert as determined with sequencing were tranformed into CodonPlus RP® BL21 cells and tested for protein expression as described above (section 2.5).

Table 2.4. Primers used to amplify individual exons of the proline rich region

Primer Name	Primer length	Primer Sequence 5'- 3'	Restriction Site
P1 Forward 5'	32 nt	cgggatccatagaggat gaagacgctaaagcc	Bam HI
P1 Reverse 3'	34 nt	ggaattcggatggggct ggcaggggctaaaggg	Eco RI
P2 Forward 5'	32 nt	cgggatccccctgcca gccccatcccccagg	Bam HI
P2 Reverse 3'	28 nt	ggaattcggacggggag gacaggggcc	Eco RI
P3 Forward 5'	30 nt	cgcggatcctgtcctcc cgtcccccagg	Bam HI
P3 Reverse 3'	28 nt	ggaattcgatctcctgctt ccgggatgg	Eco R1

2.15 Overlay with Biotinylated Probes Defining Exon Specific Associations

Overlay experiments were performed to test for the specific interactions between various domains in Grb2 and Src tyrosine kinase with the proline rich region of SOCK. The overlay technique was performed essentially as described by Schmeichel et al (Cell Biology: A Laboratory Handbook Vol 4).

Purified samples of GST, GST-Q2A (all three of the proline rich exons), GST-P1, GST-P2 and GST-P3 were subjected to electrophoresis using a 10% discontinuous SDS-PAGE gel (Laemmli, 1970). The resolved proteins were transferred to PVDF membranes electrophoretically in transfer buffer consisting of 50 mM Tris, 150 mM glycine and 20% methanol with a Bio Rad TransBlot™ electroblotting apparatus.

The PVDF membranes were blocked with blocking buffer (50 mM Tris-HCl, pH 7.6, 150 mM NaCl and 2% Carnation skim milk powder) at room temperature for one hour. The biotinylated probes (GST, GST-SH3 of Src, GST-SH3-N terminus of Grb2, GST-SH2 of

Grb2 and GST-SH3-C terminus of Grb2) were diluted 1:2000 (except for Src-SH3 which was diluted at 1:1000) separately in overlay solution (20 mM HEPES, pH 7.5, 100 mM NaCl, 2% Carnation skim milk powder, 0.25% gelatin, 1% Nonidet P-40 and 1 mM EGTA) and incubated with the PVDF membranes for 1.5 hours. Following this, the PVDF membranes were washed 3 x 10 min with Overlay Wash buffer (50 mM Tris-HCl, pH 7.6, 150 mM NaCl, 0.1% Tween 20 and 0.25% gelatin).

The neutravidin-HRP conjugate (PIERCE) was diluted 1:10 000 in overlay solution and incubated with the PVDF membranes for 1 hour at room temperature on a Lab-Line 3-D rotator. Neutravidin was used due to its increased specificity with biotin as compared with streptavidin and avidin. The membranes were washed 6 x 10 min with Overlay Wash buffer and treated with 4 ml of ECL® reagent for one minute at room temperature followed by exposure to Kodak BioMax MR® film for 10 minutes. The film was developed in a Kodak X-ray film developer.

2.16 Generation of Anti-peptide Antibodies and their Purification

Sigma Genosys injected two rabbits with an immunogenic peptide. The peptide composed of 13 residues, NSVRRGSGTPEAE, was selected with the assistance of Antigenicity Plot shareware, which predicts the hydrophobicity and antigenicity of a given peptide. Following an established boost regiment, the rabbits were immunized with 200μg of peptide in Complete Freund's Adjuvant (CFA) on day 1 followed by weekly immunizations of 100 μg of peptide in Incomplete Freund's Adjuvant (IFA) for three weeks. Bleed were collected one week after the previous immunization. The final bleed was performed 12 weeks after the primary injection. Western blots were performed with the

various bleeds on purified GST fusion proteins. The bleeds with the greatest specific immunoreactivity as determined from Western blots, were combined and diluted 1:1 in ImmunoPure® Gentle Binding Buffer (Sodium Borate, pH 8.0, Pierce cat# 21012) which is compatible with the ImmunoPure® Gentle Elution Buffer.

AminoLink® Plus Coupling Gel (PIERCE cat# 44894) was used to covalently couple an antigenic peptide/ fusion protein mix in order to purify anti-sera produced from rabbits injected with a synthetic peptide (NSVRRGSGTPEA synthesized by Sigma Genosys). The beaded agarose utilized aldehyde functional groups, which reacted with primary amines present in the peptide and purified GST-fusion proteins to form a covalent bond between the two. Because the peptide sequence occurs twice in SOCK, once in the second proline rich exon (P2) and once in the third proline rich exon (P3), purified proteins containing these exons were believed to be useful in purifying anti-sera when attached to an affinity support resin such as agarose. Synthesized peptides are also not as stable as fusion proteins and are more prone to degradation. GST-P2 and GST-P3 were purified from 1L cultures as explained in the fusion protein purification scheme (section 2.5). Coupling was accomplished with the enhanced coupling protocol at pH 10, which allows for maximal binding efficiency. Briefly, 5 mg of GST-P2, 5 mg of GST-P3 and 10 mg of the antigenic peptide were prepared in pH 10 Enhanced Coupling Buffer (0.1M sodium citrate, 0.05M sodium carbonate, pH 10). A total volume of 4 ml of this mixture was added to an AminoLink® Plus Column pre-equilibrated in pH 10 Enhanced Coupling Buffer.

The fusion proteins and peptides were bound to the amine reactive agarose by incubating the samples with gentle end over end rotation for 4 hours at room temperature. Following binding, the gel bed was drained and washed with 5 ml of pH 7.2 coupling buffer.

2 ml of pH 7 coupling buffer and 40 µl of Reducing Agent (5 M Sodium cyanoborohydride solution) was added and the samples were gently rotated end-over-end over night at room temperature. The gel bed was drained and washed with 4 ml of Quenching Buffer (1M Tris-HCl, pH7.4) and the remaining active sites were blocked by the addition of 2 ml of Quenching Buffer and 40 µl of Reducing Agent. This quenching reaction slurry was incubated for 30 minutes with end-over-end rocking at room temperature. The gel bed was drained and washed with 8 x 5 ml with AminoLink® Wash Solution (1M NaCl) to ensure the complete removal of uncoupled ligand from the affinity gel. A final wash with storage solution (PBS with 0.05% sodium azide) completed the ligand coupling procedure. Aliquots from each stage of the coupling procedure were taken, run on SDS-PAGE gel, electroblotted and analyzed via Western Blots (anti-GST) to determine the level of ligand coupling. The column was stored at 4°C until ready to be used in antibody purification from anti-sera.

A batch purification process was used which required the antigen-resin to be transferred to 50 ml conical tubes (Falcon). 50 ml of diluted serum was added to the antigen-resin and incubated at room temperature with gentle end-over-end rotation for 1 hour. The antibody/antigen-resin was separated from the mixture by centrifugation in a table-top centrifuge (Fisher Scientific, Centrific™ Centrifuge) for 1 min at 2500 rpm. The supernatent was poured off and a further 50 ml of diluted serum was added to the resin and incubated as above for 1 hour. This procedure was repeated until all of the serum was incubated with the antigen-resin for 1 hour.

The antibody/antigen-resin was transferred back to the column and washed with 15 column volumes of ImmunoPure® Gentle Binding Buffer. Bound antibodies were eluted with 5 column volumes of ImmunoPure® Gentle Elution Buffer (pH 6.55, ™PIERCE).

Under these near neutral pH elution conditions, the integrity of the antibody-antigen interaction in subsequent experiments is maintained to a higher degree when compared to traditional methods of elution with highly acidic elution buffer at pH 2.5-3.0. The purified antibodies were desalted with gel filtration through a Sephadex G-25 column which was pre-equilibrated with 50 mM Tris-HCl pH 7.2 supplemented with 1% BSA to reduce antibody binding to the matrix. The eluted antibodies were collected and glycerol was added to a final concentration of 25%. The purified antibodies were stored at -80°C until ready to be used in Western blot analysis and immunohistochemical experiments.

3. RESULTS

3.1 Distribution of SOCK in Skeletal Muscle Membrane Fractions

Previous studies in this laboratory led to the cloning of a cDNA from a human skeletal muscle cDNA library, encoding a novel CaM Kinase II β isoform called SOCK (Son Of CaM Kinase) (Leddy, 1999). The cDNA of the rat and mouse homologues of this novel CaM Kinase II β isoform have been cloned from rat and mouse skeletal muscle cDNA libraries (Bayer et al., 1998; 1999). This isoform differed from the neuronal CaM Kinase II-β isoform by the addition of three alternatively spliced exons in the variable domain that encoded a 13 kDa insert of three proline rich repeats. The cDNA of SOCK contained an open reading frame of 2.0 kb encoding for a polypeptide of 665 amino acids with a predicted molecular weight of 73 kDa as compared to the 60 kDa polypeptide of the neuronal CaM Kinase II β isoform. Studies have indicated that a 60 kDa CaM Kinase thought to be the brain-type CaM Kinase II β isoform is present in the sarcoplasmic reticulum SR of skeletal muscle (Campbell and Maclennan, 1982; Tuana and MacLennan, 1988; Shenolikar *et al.*, 1986).

In order to determine the subcellular distribution of CaM Kinase II in skeletal muscle as well as the isoform composition, cytosol and various membrane fractions were isolated and examined by Western blot analysis with CaM Kinase II specific antibodies. Rabbit fast twitch muscle was homogenized and subjected to differential and discontinuous sucrose density gradient centrifugation. As a result, five membrane subcellular fractions at the interface between sucrose cushions were collected and analysed. These fractions have been previously characterized on the basis of the enrichment of marker enzymes and other

proteins specific to each subcellular fraction (Saito et al., 1984; Chu et al., 1992). Enzymes such as adenylyl cyclase and the Na^+/K^+ ATPase pump in the plasmamembrane were enriched in fraction 1 and the Ca^{2+}-ATPase in the SR enriched in fraction 2-5. The different subcellular fractions obtained in this experiment were resolved by discontinuous SDS-PAGE and electroblotted onto PVDF membranes The membranes were stained with Ponceau S to visualize the proteins in each fraction. The light SR was distinguished from the heavy SR component in the fractions by monitoring the distribution of calsequestrin, a 55 kDa Ca^{2+} binding protein that associates with the terminal junctional cisternae and enriches in fractions 2-5 (absent in fraction 1) with maximal abundance in fractions 4 and 5 (figure 3.1 A). The Ca^{2+}-ATPase constitutes two thirds of the protein content of the SR and is abundantly present throughout the SR. It is not as abundant in the terminal cisternae, corresponding to a slight decrease in observed levels of this protein in fraction 5 (figure 3.1 A). Fraction 5 contains terminal cisternae of the SR but the contribution of these structures to the overall protein content in this fraction is decreased by the presence of aggregated contractile proteins (Saito et al., 1984).

Western blots were performed with antibodies specific to RyR1, CaM Kinase II β, CaM Kinase II α and a broad CaM Kinase II (α, β, γ, δ) antibody to determine the distribution of CaM Kinase II isoforms relative to the RyR1 in each fraction. The antigen antibody complexes were visualized with horse-radish peroxidase conjugated secondary antibodies incubated with chemiluminescent reagent.

Figure 3.1 shows the results of the Western blots with samples of the skeletal muscle membrane fractionation. The anti-RyR1 antibody displayed immunoreactivity with a polypeptide of approximately 560 kDa, corresponding to skeletal muscle RyR1 (Figure 3.1

panel B). RyR1 was weakly detected in the muscle homogenate (lane 1) and no immunoreactivity was observed in the cytosol (lane 2). RyR1 was detected in the membrane sample (lane 3), consisting of crude microsomes. Fraction one, thought to be enriched in plasmamembrane and some T-tubules, did not exhibit detectable levels of RyR1 (lane 4), while RyR1 was detected in fraction 2 (lane 5) and the immunoreactivity increased in fraction 3 (lane 6) with a further enrichment in fraction 4 (lane 7) where the RyR1 appeared to be the most abundant. A decrease in immunoreactivity with RyR1 was observed in fraction 5 (lane 8). The anti-ryanodine receptor antibody is specific for the RyR1 isoform and no immonoreactivity with the brain RyR3 isoform was observed in the brain homogenate (lane 10).

Western blot analysis with the anti-CaM Kinase II β-specific antibody, Cbβ-1, was performed to determine the distribution profile of the β isoform in skeletal muscle fractions as well as to determine which form of CaM Kinase II β is expressed in skeletal muscle (Figure 3.1 panel C). Cbβ-1 did not detect any CaM Kinase II β isoform in the muscle homogenate (lane 1) or the cytosol (lane 2) but did detect a 73 kDa polypeptide corresponding to the predicted size of SOCK in the membrane sample (lane 3). The lack of immunoreactivity with SOCK in the homogenate and cytosol samples indicates that the expression of this kinase is low and that SOCK is probably not a cytosolic protein, respectively. Fraction one is composed mainly of plasmamembrane and since Cbβ-1 did not detect SOCK in this sample, it is reasonable to assume that SOCK is not associated with the plasmamembrane (lane 4). Of the 5 membrane fractions, Cbβ-1 detected SOCK in fractions 2-5 (lanes 5-8) with a progressive enrichment from fraction 2 to fraction 4 followed by a decrease in fraction 5 (as compared to the immunoreactivity with fraction

4). Immunoreactivity with a 60/58 kDa doublet, corresponding to brain CaM Kinase II β was observed only in the brain homogenate (lane 10) and was not observed in any of the samples from skeletal muscle fractions (lanes 4-8). Cbβ-1 did not detect SOCK in the brain homogenate (lane 10), suggesting that SOCK is not expressed in brain. Since the CaM Kinase II β isoform specific antibody Cbβ-1 solely detected the 73 kDa band corresponding to SOCK in skeletal muscle membrane fractions, this indicates that SOCK is the only CaM Kinase II β isoform expressed in muscle. Furthermore, the distribution profile of SOCK as detected with Cbβ-1 was similar to that of RyR1, indicating that these proteins have the same subcellular distribution and suggests that SOCK may be localized to the terminal cisternae as is RyR1.

A polyclonal antibody RU16, which can detect all CaM Kinase II isoforms (α, β, γ and δ isoforms) was also used to detect the distribution profile of CaM Kinase II isoforms in skeletal muscle membrane fractions (Figure 3.1 panel D). The distribution of CaM Kinase II isoforms as detected with RU16 was similar to what was observed with anti-RyR1 and the anti-CaM Kinase II β specific antibody Cbβ-1. Western blot analysis with RU16 detected three proteins, a 73 kDa protein corresponding to SOCK as well as two bands with molecular weights of 58 kDa and 56 kDa. The 58 kDa and 56 kDa polypeptides in skeletal muscle membranes have been determined to correspond to CaM Kinase II δ_D and CaM Kinase II γ_B isoforms, respectively (Bayer et al., 1998).

To determine the distribution of CaM Kinase II α isoforms in skeletal muscle, a CaM Kinase II α-specific antibody was used in Western blot analysis of skeletal muscle fractions (Figure 3.1 panel E). This antibody immunoreacted solely with a 25 kDa

polypeptide in membrane fractions from skeletal muscle. The distribution of the immunoreactivity with a 25 kDa polypeptide observed when using anti-CaM Kinase II α antibody, was similar to that observed with Cbβ-1 and RU16 (progressive enrichment from fraction 2-4 with a decrease in fraction 5). Immunoreactivity with a 54 kDa polypeptide corresponding to the CaM Kinase II α isoform was observed only in the brain homogenate (lane 10) and was not detected in any of the skeletal muscle fractions. The 25 kDa polypeptide detected in the muscle fractions is most likely αKAP, which is comprised of the association domain of CaM Kinase II α with the addition of a hydrophobic domain at the N-terminus (Bayer et al., 1996). This indicates that αKAP has the same distribution as CaM Kinase II β, γ and δ isoforms in skeletal muscle membrane fractions. It has been suggested that αKAP acts as an anchoring protein for CaM Kinase II isoforms by associating with membranes and interacting with CaM Kinases via their association domains. Thus, the subcellular localization of CaM Kinase II isoforms in membrane systems of muscle may be a result of being targeted via association with αKAP, which is believed to be associated with the SR via its hydrophobic tail (Bayer et al., 1996 and 1998).

The RyR is believed to be associated with the terminal cisternae of the SR. Comparison of the CaM Kinase II components in skeletal muscle shows that these components followed the same distribution as the RyR, indicating that SOCK, CaM Kinase II δ_D, CaM Kinase II γ_B and the CaM Kinase II anchoring protein αKAP co-localize with the RyR in the terminal cisternae.

To demonstrate the distribution profile of proteins localized in T-tubules, Western blot analysis was performed on the skeletal muscle fractions with skeletal muscle DHPR α_{1S} and DHPR β_{1A} subunit specific antibodies. Anti-DHPR α_1 detected a 185 kDa polypeptide corresponding to skeletal muscle DHPR α_{1S} (Figure 3.1 F). DHPR α_{1S} was not detected in the crude muscle homogenate (lane 1) or in cytosol (lane 2) but was detected in the crude microsomes (lane 3). Fraction 1 (lane 4), thought to be enriched in plasma membrane and some T-tubules exhibited maximal levels of the DHPR α_{1S} subunit, followed by a progressive decrease in detection of DHPR α_{1S} in fractions 2-4 (lanes 5-7). The DHPR α_{1S} was not detected in fraction 5 (lane 8). The anti-DHPR α_{1S} antibody specific for the skeletal muscle isoform did not detect the DHPR α_{1C} brain isoform in the brain homogenate (lane 10). Anti-DHPR β_{1A} antibody detected a 56/52 kDa doublet in skeletal muscle fractions (figure 3.1 G). This doublet has also been observed in a study by Pichler et al., 1997 when immunoblotting with a DHPR β_{1A} specific antibody against triads. The DHPR β_{1A} subunit specific antibody had a similar distribution profile as the DHPR α_{1S} subunit with immunoreactivity detected in crude microsomes (lane 3) and in fractions 1-4 (lanes 4-7). Immunoreactivity was greatest in fraction 1 followed by a progressive decrease to fraction 4. At long exposure times the doublet was weakly observed in fraction 5 (Western blot not shown). The distribution profile of the DHPR subunits localized in the T-tubules were distinctly different than the distribution profile of RyR1 and the CaM Kinase II isoforms which co-localize in terminal cisternae of the SR.

3.2 Comparison of Affinity Purified Skeletal Muscle and Brain CaM Kinase II β Isoforms

When using the CaM Kinase II β specific antibody Cbβ-1 in Western blot analysis in skeletal muscle and brain samples, it was evident that immunoreactivity with a 73 kDa polypeptide was detected solely in skeletal muscle membranes and a 60/58 kDa doublet was detected solely in brain homogenate. The observed difference in apparent molecular weight as detected in Western blots may or may not be attributed to actual differences in molecular weight and can be due to altered migration/resolution through the gel resulting from differences in the sample composition (skeletal muscle membrane fraction versus brain homogenate), post-translational modification such as glycosylation or non-specific association with lipopolysaccharides. Non-specific interactions have been found to alter protein mobility on SDS polyacrylamide gels (Yuan et al., 1999). In order to rule out the possibility of these polypeptides being the same CaM Kinase II β isoform but running at different apparent molecular weights when electrophoresed in a crude homogenate versus a membrane sample, the CaM Kinases from brain and skeletal muscle were enriched by affinity purification on a calmodulin column. Although affinity purification with calmodulin should result in the co-purification of other calmodulin binding proteins in addition to CaM Kinase II, the differences between the affinity purified brain cytosol and skeletal muscle samples would not be as great as the differences between crude brain homogenate and skeletal muscle membranes. Also, the membrane bound CaM Kinase II from skeletal muscle was detergent extracted with 2% Triton X-100 and 0.6 M KCl and thus would be separated from association with membrane components. Affinity purification of brain cytosol and detergent solubilized skeletal muscle membranes with

calmodulin sepharose in the presence of $CaCl_2$ was performed and the CaM binding proteins were eluted with 5 mM EGTA and EDTA. SDS sample buffer was added to the eluted samples and were boiled for 5 minutes followed by electrophoreses on a 10% discontinuous polyacrylamide SDS gel. Samples of light SR (membrane fraction 2) and heavy SR (membrane fraction 4) were also included for comparison of migration of CaM Kinase II in membranes. The CaM binding proteins were electroblotted onto PVDF membrane and Western blot analysis was performed with a CaM Kinase II β specific antibody, Cbβ-1 to detect only the CaM Kinase II β isoforms. It is evident in figure 3.2 that a 60/58 kDa doublet was detected in the CaM affinity purified brain sample (lane 1) and a 73 kDa polypeptide was detected in the light SR (lane 2), heavy SR (lane 3) and affinity purified muscle sample (lane 4). The migration of the 73 kDa polypeptide was the same when comparing the affinity purified sample to that observed with the light and heavy SR membrane samples. These findings clearly demonstrate that the observed differences in detection of CaM Kinase II β isoforms in brain versus skeletal muscle membranes is most likely due to the differences in molecular weight between these two β isoforms and not due to other factors.

3.3 Immunohistochemical Localization of CaM Kinase II β Isoform in Rat Skeletal Muscle Sections

Immunohistochemical staining with antibodies specific for RyR1 and CaM Kinase II β was performed to assess whether SOCK colocalizes with RyR1 in skeletal muscle sections. These antibodies possessed specific reactivity with polypeptides of 560 and 73

kDa corresponding to RyR1 and SOCK in Western blots of skeletal muscle membrane fractions. Anti-RyR1 and anti-CaM Kinase II β were incubated with 12 μm sections of rat gastrocnemius muscle in single and double immunofluorescence labeling experiments, respectively. After incubating the primary antibodies with muscle sections for one hour, the sections were washed followed by incubation with immunoglobulin specific fluorochrome labeled secondary antibodies. The secondary antibodies used to detect anti-RyR1 and anti-CaM Kinase II-β were conjugated to Cy3™(red) and FITC (green), respectively.

The immunofluorescent staining of RyR1 was observed to have a striated pattern in both single (Figure 3.3 A) and double (Figure 3.3 A') immunohistochemically stained sections when observed through the red filter to visualize the Cy3™ fluorochrome. This banding pattern is attributed to the localization of RyR1 to terminal cisternae located at opposite ends of the sarcoplasmic reticulum that face the T-tubules. T-Tubules penetrate the muscle fiber perpendicularly to the length of the myofibrils and positive immunostaining of the junctional face (terminal cisternae) would demonstrate a striated pattern due to the close proximity and uniform association of these two distinct membrane systems.

Immunohistochemical staining with anti-CaM Kinase II β to detect SOCK was found to have a striated pattern of immunofluorescense in both single (Figure 3.3 B) and double (Figure 3.3 B') immunohistochemically stained skeletal muscle sections when observed through the green filter to visualize the FITC fluorochrome. This indicates that SOCK has a similar pattern of localization in skeletal muscle sections as compared to the localization of RyR1 and that SOCK may colocalize with RyR1 to the terminal cisternae. Merging the

captured images corresponding to anti-RyR1-Cy3 (Figure 3.3 A') and anti-CaM Kinase II β-FITC (Figure 3.3 B') maintained the striated pattern observed with the individual filters and appeared yellow indicating that the proteins detected are in close proximity to each other (Figure 3.3 C'). This finding suggests that SOCK and RyR both colocalize to the terminal cisternae of the SR membrane. A control was performed in order to ensure that the pattern of immunofluorescence observed with the green filter in the double labeled sections, is attributed to the FITC labeled secondary antibody interacting with SOCK. The control was simply observing the single immunohistochemical stained sections of anti-RyR1 and Cy3™ conjugated secondary antibodies, through the green filter instead of the red filter. The striated pattern was not observed and no immunofluorescence was detected in this control, demonstrating that there was no spectral overlap of the Cy3™ signal into the green spectrum (Figure 3.3 C). Cy3™ was used at the highest dilution (1:800) recommended by the manufacturer to ensure spectral overlap would not be observed. These data also support the cofractionation of RyR1 and SOCK observed in Western blot analysis of the skeletal muscle membrane fractions using anti-RyR1 and anti-CaM Kinase II,

Figure 3.1 Distribution of CaM Kinase II Isoforms in Skeletal Muscle

The subcellular distribution of CaM Kinase isoforms was carried out on isolated fractions from rabbit skeletal muscle. Ponceau staining of total protein content (A) shows the enrichment of the Ca^{2+}-ATPase pump (110 kDa) in fractions 2-5 (lanes 5-8) representing the SR, while the enrichment of calsequestrin (55 kDa) in membrane fractions 4 and 5 (lanes 7 and 8) distinguishes the heavy SR from the light SR (fractions 2 and 3). Western blot analysis performed with RyR1 specific (B), CaM Kinase II β specific (C), broad CaM Kinase II (α, β, γ and δ) (D), CaM Kinase II α specific (E). DHPR α_{1s}-specific (F) and muscle-specific DHPR β_{1A} (G) antibodies was visualized with horse radish peroxidase conjugated secondary antibodies in the presence of enhanced chemiluminescent reagent and subsequent exposure to Kodak BioMax® MR film. The anti-RyR1 antibody (B) detected a polypeptide of 560 kDa in the crude homogenate (lane 1) and crude microsomes (lane 3). A progressive enrichment of RyR1 was observed in membrane fractions 2-5 (lanes 5-8) with maximal detection of RyR1 in fraction 4 (lane 7). The anti-CaM Kinase II β-specific antibody (C) detected a polypeptide of 73 kDa corresponding to SOCK, in the crude microsomes (lane 3) with a progressive enrichment detected in membrane fractions 2-5 (lanes 5-8) with maximal detection of SOCK in fraction 4 (lane 7). The anti-CaM Kinase II β-specific antibody (C) detected a 60/58 kDa doublet in the brain homogenate sample (lane 10), corresponding to brain CaM Kinase II β and β' isoforms. The broad anti-CaM Kinase II antibody (D) that detects α, β, γ and δ CaM Kinase II isoforms detected three polypeptides of 73, 58 and 56 kDa in the crude microsomes (lane 3) with a progressive enrichment detected in membrane fractions 2-5 (lanes 5-8) with maximal detection of the three polypeptides in fraction 4 (lane 7). Two polypeptides of 60 and 58 kDa were detected in the brain homogenate (lane 10) with this antibody. The anti-CaM Kinase II α-specific antibody (E) detected a 25 kDa polypeptide corresponding to αKAP in the crude microsomes (lane 3) with a progressive enrichment detected in membrane fractions 2-5 (lanes 5-8) with maximal detection of the 25 kDa polypeptide in fraction 4 (lane 7). Anti-CaM Kinase II α detected a 54 kDa polypeptide in brain homogenate (lane 10), corresponding to CaM Kinase II α. The anti-DHPR α_{1S}-specific antibody (F) detected a 185 kDa polypeptide corresponding to DHPR α_{1S} in crude microsomes (lane 3) and in membrane fractions 1-4 (lanes 4-7). The 185 kDa polypeptide was maximally detected in fraction 1 followed by a decrease in fractions 2-4 (lanes 5-7). The anti-DHPR β_{1A}-specific antibody (G) detected a doublet comprised of 56 and 52 kDa polypeptides in crude microsomes (lane 3) and in membrane fractions 1-4 (lanes 4-7). The 56/52 kDa doublet was maximally detected in fraction 1 followed by a decrease in fractions 2-4 (lanes 5-7). The skeletal muscle fractionation experiment was replicated in muscle collected from different animals and all Western blots were performed at least three times for each antibody.

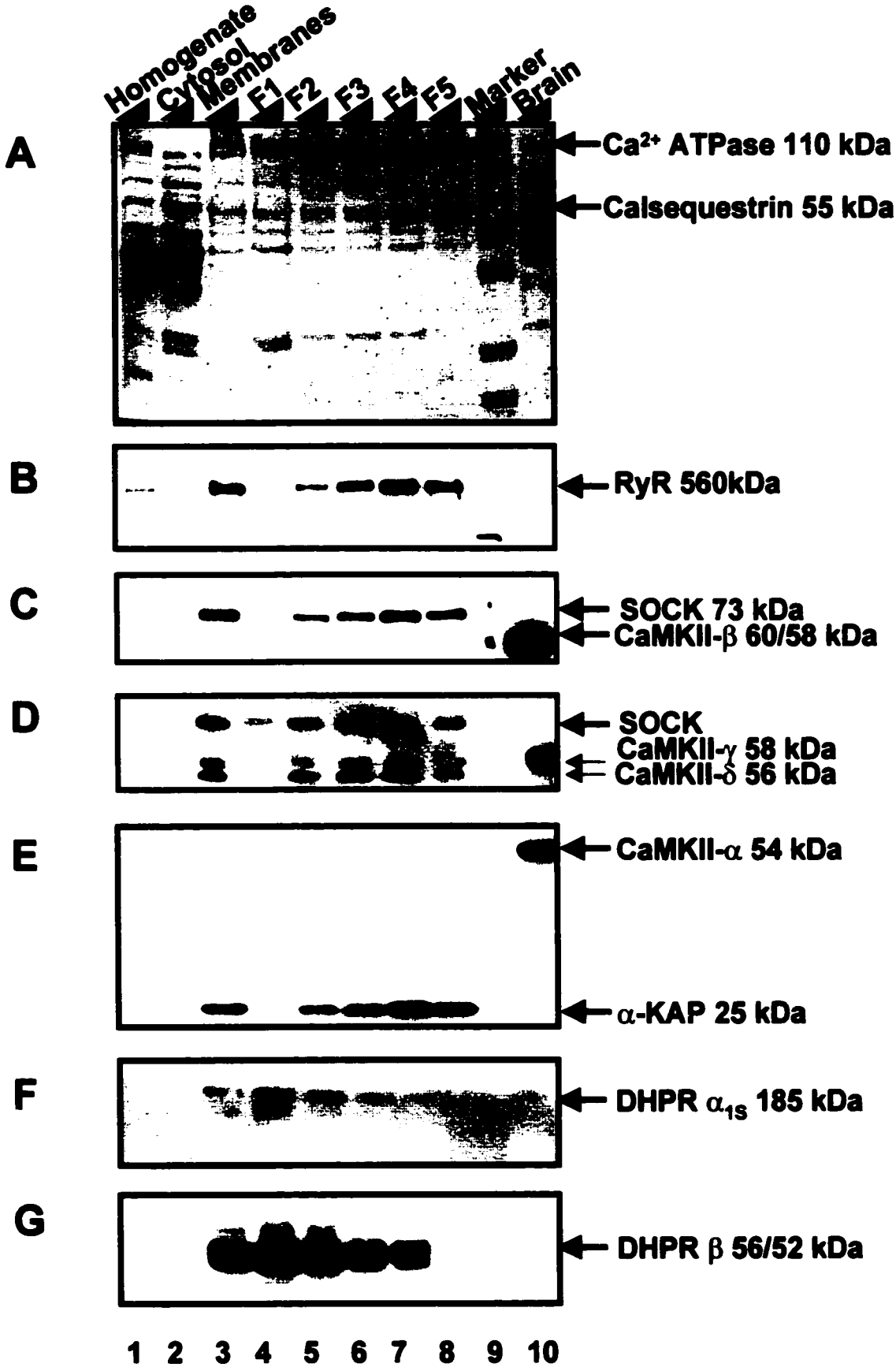
Homogenate
Cytosol
Membranes
F1
F2
F3
F4
F5
Marker
Brain
A
Ca2+ ATPase 110 kDa
Calsequestrin 55 kDa
B
RyR 560kDa
C
SOCK 73 kDa
CaMKII-β 60/58 kDa
D
SOCK
CaMKII-γ 58 kDa
CaMKII-δ 56 kDa
E
CaMKII-α 54 kDa
α-KAP 25 kDa
F
DHPR α1S 185 kDa
G
DHPR β 56/52 kDa
1 2 3 4 5 6 7 8 9 10

Figure 3.2 Isolation of Brain and Muscle CaM Kinase II β isoforms

The CaM Kinase II isoforms of brain and skeletal muscle were purified from brain cytosol and skeletal muscle solubilized SR membranes on a calmodulin sepharose 4B® column. The affinity purified CaM binding proteins were washed with a buffer containing 1% Triton-X 100 detergent and 10% sucrose to remove non-specifically associated proteins and were eluted with 5 mM EGTA and EDTA. Samples of eluted proteins from brain and skeletal muscle were separated by electrophoresis on 10% polyacrylamide SDS gels along with samples of membrane fractions corresponding to enriched longitudinal SR (membrane fraction 2) and terminal cisternae (membrane fraction 4). Western blot analysis with a CaM Kinase II β-specific antibody Cbβ-1, detected a 73 kDa polypeptide corresponding to SOCK solely in the muscle samples and a 60/58 kDa doublet corresponding to neuronal CaM Kinase II β and β' solely in the affinity purified brain sample.

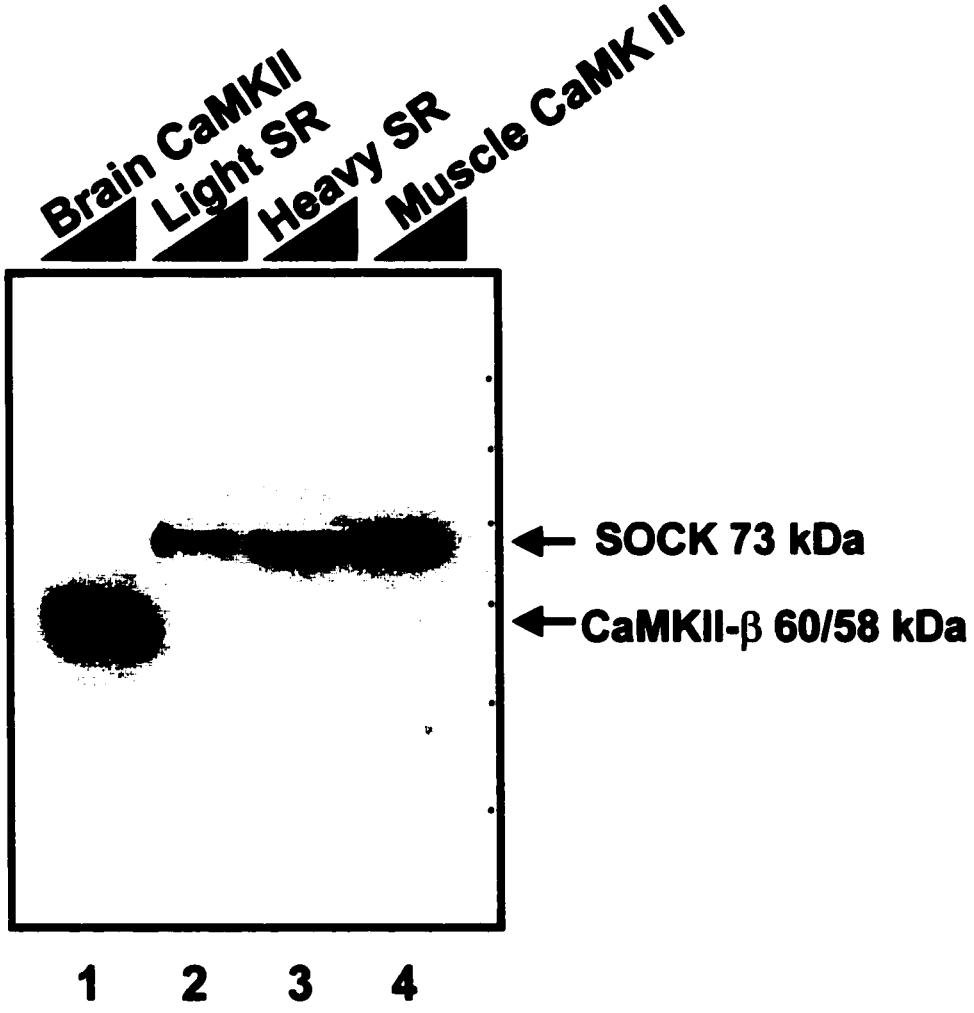
Brain CaMKII
Light SR
Heavy SR
Muscle CaMK II
SOCK 73 kDa
CaMKII-β 60/58 kDa
1
2
3
4

Figure 3.3 Immunohistochemical localization of CaM Kinase II β compared to RyR1 in skeletal muscle sections

Rat gastrocnemeus muscle was excised and sectioned longitudinally with a cryostat yielding 12 μm sections suitable for immunohistochemical analysis. The sections were mounted onto slides and blocked with 5% horse serum, 0.5% bovine serum albumen and 0.15% glycine in PBS pH 7.4 (Buffer A) for 20 minutes at room temperature. Anti-RyR1, anti-CaMKII β or a mixture of both were diluted in buffer A and incubated with the sections for one hour. After washing the sections with buffer A, secondary antibodies specific for detecting each primary antibody were incubated with the sections. The secondary antibodies were conjugated to the fluorochromes Cy3™ (red) and FITC (green) and specific for immunoreactivity with anti-RyR1 and anti-CaM Kinase II β, respectively. The immunofluorescent staining of RyR1 as observed in single (A) and double (A') immunohistochemically stained sections consisted of a striated pattern when observed through the red filter to visualize the Cy3™ fluorochrome. The immunofluorescent staining of muscle specific CaM Kinase II β as observed in single (B) and double (B') labeled sections consisted of a striated pattern when observed through the green filter to visualize the FITC fluorochrome. Merging the captured images corresponding to anti-RyR1/Cy3™ (A') and anti-CaM Kinase II β/FITC (B') is presented in panel C' in which shared regions of immunofluorscence appear yellow. Spectral overlap of Cy3™ fluorescence into the green filter was not observed when single labeled sections using anti-RyR1 and Cy3™ conjugated secondary antibody were viewed through the green filter (C). The scale bar represents 20 μm in panel A, B and C and 50 μm in panel A', B' and C'. Single and double labeling experiments were performed at least three times for each antibody on skeletal muscle sections collected from three animals.

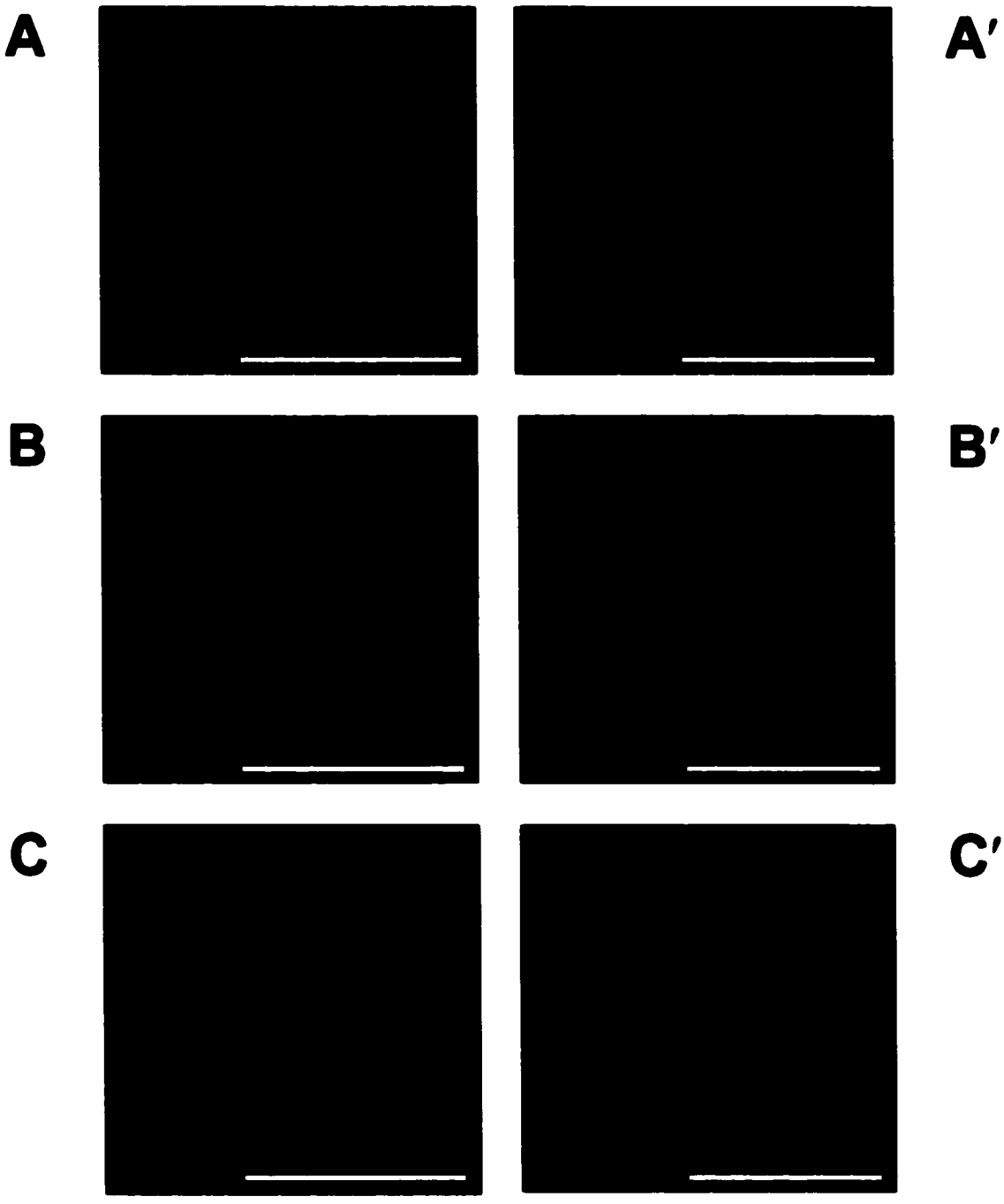
A
A′
B
B′
C
C′

3.4 Expression and Purification of SOCK and CaMKII-β Fusion Proteins

In view of the low abundance and membrane association of SOCK, we sought to generate recombinant SOCK to investigate its function. Purification of CaM Kinase II from solubilized heavy SR on a CaM column would not satisfy the requirement of a pure sample of SOCK as there are two other CaM Kinase II isoforms present in skeletal muscle as well as other CaM binding proteins. To generate sufficient quantities of SOCK protein, the cDNA sequences encoding full length SOCK and brain CaM Kinase II β isoform were sub-cloned into the multi-cloning site of the GST fusion protein expression vector pGEX-Kg such that the kinases would be expressed as C-terminal fusions to glutathione-S-transferase (GST) (Figure 3.4). Recombinant brain CaM Kinase II β isoform was used to determine if there are differences in enzyme activity between the brain and muscle specific CaM Kinase II β isoforms.

Initial expression and purification of the recombinant kinases in wild type BL21 protein expression bacteria resulted in low yields of truncated protein products of 75, 64, 62, 51, 30, 28, and 26 kDa that appeared to be the products generated by proteolytic degradation of the full length kinases of 99 and 86 kDa (Figure 4.5). The fusion proteins were only detected with long exposure times of Western blots performed with anti-GST antibody. The BL21 strain of bacteria which lack two of the major bacterial proteases would be expected to be able to produce substantial yields of the full-length kinases as the probability of proteolysis is decreased. Since this was not the case, investigation into other plausible reasons as to why the recombinant kinases were not expressed efficiently was pursued. Others have investigated the causes of problematic expression of mammalian genes in bacteria, which resulted in the identification of biased codon usage as a

significant problem encountered in the induced expression of foreign genes in *E. coli* (Rosenberg et al., 1993; Chen and Inouye, 1990; Wolin and Walter, 1988).

The researchers of Stratagene (California) recently addressed the aforementioned problem by creating CodonPlus® RP BL21 *E. coli,* that are engineered to express the argU and proL tRNA genes which rescues expression of genes restricted by either AGG/AGA codons or by CCC codons (Stratagene reference catalog, 1999). These cells were used to express the full-length kinases GST-SOCK and GST-CaM Kinase II β, which were purified from bacterial proteins by affinity purification with glutathione sepharose® 4B. The purified proteins were eluted from the beads with glutathione (25mM) and subjected to SDS-PAGE on 10% polyacrylamide gels followed by electroblotting onto PVDF membranes. The membranes were incubated with Ponceau S in order to visualize the transferred proteins. Western blots were performed with anti-GST. As depicted in Figure 3.5, the expression and purification of GST-SOCK and GST-CaM Kinase II β from CodonPlus® RP BL21 cells resulted in the efficient production of primarily full-length kinases as compared to expression obtained in regular BL21. The co-purification of four minor truncated products of 75, 65, 62 and 51 kDa were present in affinity purified recombinant SOCK and CaM Kinase II β when expressed in Codon Plus® RP BL21 cells

The immunoreactivity of GST-SOCK and GST-CaM Kinase II β with a monoclonal CaM Kinase II β specific antibody Cbβ-1 (Figure 3.6 A) and a polyclonal CaM Kinase II α, β, γ, δ antibody RU16 (Figure 3.6 B) as compared to CaM Kinase II in heavy SR samples, is shown in Figure 3.6. Both fusion proteins display specific reactivity with these antibodies, which indicates that these proteins express the appropriate sequences found in wild type CaM Kinase II and that the proteins were expressed properly.

Figure 3.4 Schematic of GST-SOCK Compared to GST-CaM Kinase II β

The complete cDNAs of SOCK and CaM Kinase II β were sub-cloned into the pGEX-Kg expression vector such that the recombinant kinases are expressed as glutathione-S-transferase fusion proteins in BL21 *E. coli*. GST is a 26 kDa polypeptide and expression of GST-SOCK and GST-CaM Kinase II β fusion proteins produces polypeptides of 99 kDa and 86 kDa respectively. The location of the 4 tandem arginine codons in SOCK and the single arginine codon pair in CaM Kinase II β is indicated. Three of the four tandem arginine codons are present in the proline rich sequence of SOCK corresponding to R_{420}-R_{421}, R_{457}-R_{458} and R_{500}-R_{501}, while the arginine codon pair R_{297}-R_{298} is present in the autoregulatory region in SOCK and CaM Kinase II β. The proline rich region of SOCK also contains numerous codons for proline that have also been found to be infrequently used in bacteria and thus, contribute to problematic protein expression of heterologous genes.

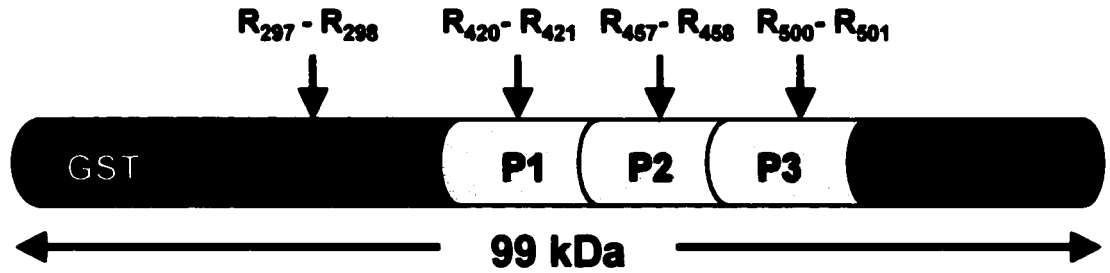

GST-SOCK

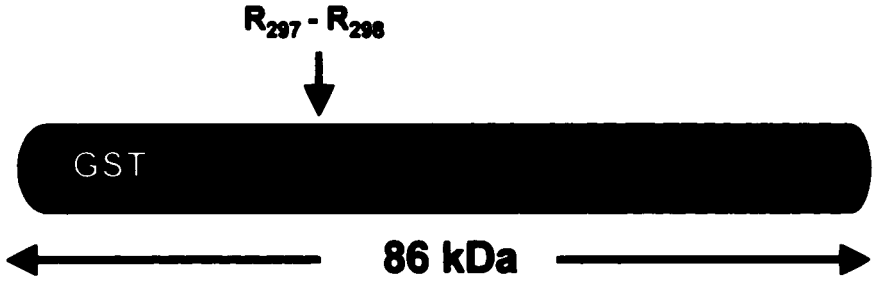

GST-CaM Kinase β

Figure 3.5 Expression and Purification of Recombinant SOCK and CaM Kinase II β

GST-SOCK and GST-CaM Kinase II β were expressed in cultures of CodonPlus® RP BL21 cells by the addition of IPTG (0.05 mM final) and were incubated at room temperature for four hours with shaking. The bacteria were separated from solution via centrifugation and lysed with lysozyme and 1% Triton X-100. The insoluble material was separated via centrifugation and the recombinant kinases were purified from the supernatent with glutathione sepharose. The purified kinases were eluted with glutathione (25 mM) and dialysed overnight and the protein concentration was determined with the BCA protein assay kit. Approximately 2 μg of the purified recombinant kinases was electrophoresed on 10% polyacrylamide SDS gels and electroblotted onto PVDF membranes. The membranes were stained with Ponceau red, which binds to proteins to visualize transferred proteins. Western blot analysis was performed with a monoclonal anti-GST antibody. The anti-GST antibody detected primarily full length fusion protein products corresponding to GST-SOCK (99 kDa) and GST-CaM Kinase II β (86 kDa) in affinity purified samples from Codon Plus RP BL21 cells. Truncated products of 75, 64, 62 and 51 kDa were weakly detected. Expression and purification of the recombinant kinases in wild type BL21 cells was very low and undetectable in the Ponceau stain but was detected with long exposure times of the Western blot. Anti-GST detected numerous truncated products of 75, 64, 62, 51, 30, 28, and 26 kDa when the proteins were purified from regular BL21 with only minimal contribution of full length recombinant kinases of 99 kDa and 86 kDa in these samples as observed.

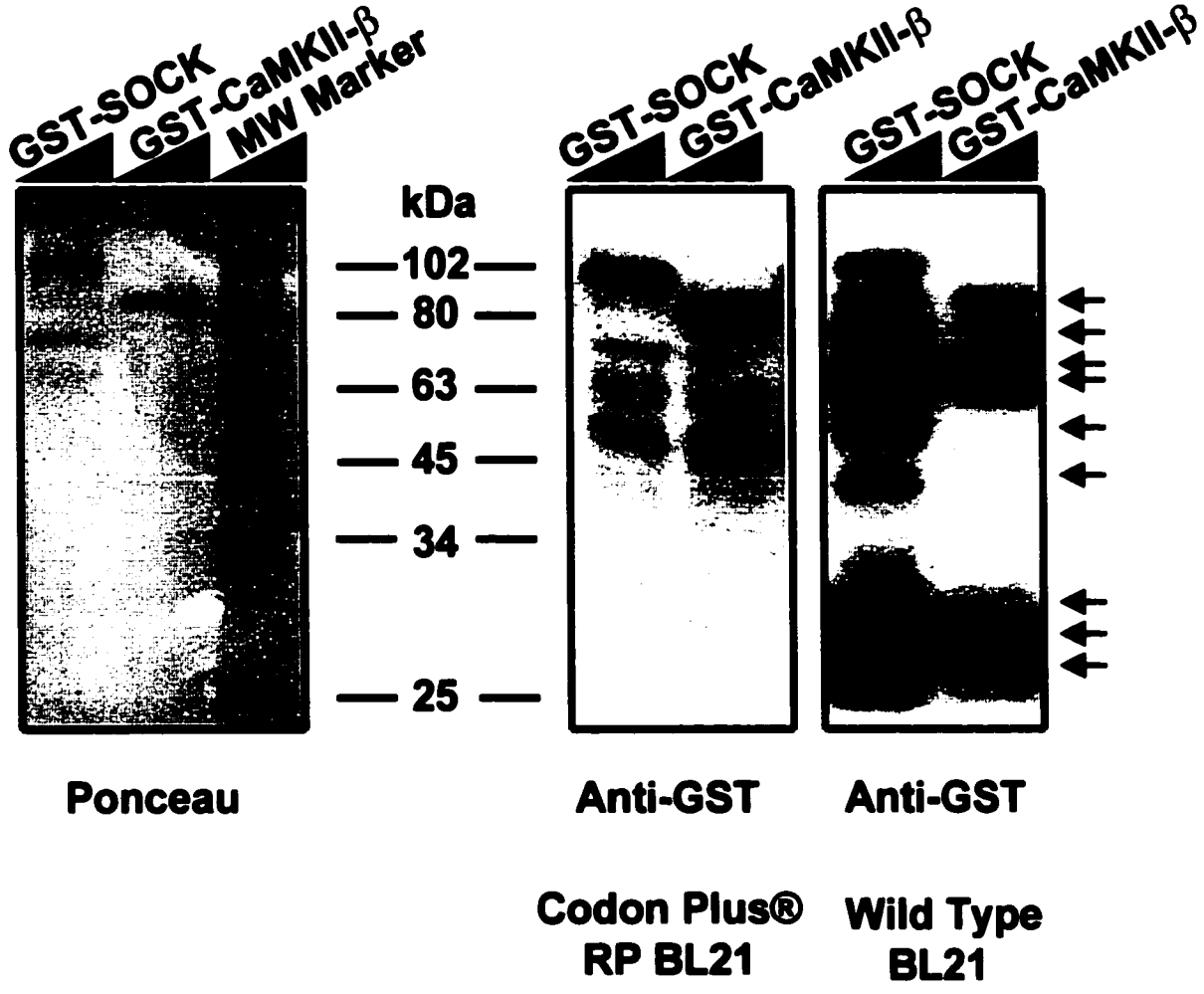
GST-SOCK
GST-CaMKII-β
MW Marker
kDa
102
80
63
45
34
25
GST-SOCK
GST-CaMKII-β
GST-SOCK
GST-CaMKII-β
Ponceau
Anti-GST
Anti-GST
Codon Plus®
RP BL21
Wild Type
BL21

Figure 3.6 **Immunoreactivity of Recombinant SOCK and CaM Kinase II β with CaM Kinase II antibodies**

Western blots were performed with a CaM Kinase II β specific mouse monoclonal antibody (Cbβ-1) (A) and a broad CaM Kinase II α, β, γ, and δ, rabbit polyclonal antibody (RU16) (B) to confirm the CaM Kinase II specific immunoreactivity of the recombinant kinases as compared to endogenous CaMKII in skeletal muscle SR. Cbβ-1 detected a 73 kDa polypeptide corresponding to SOCK in the membrane fraction of skeletal muscle and detected both full length GST-SOCK (99 kDa) and GST-CaM Kinase II β (86 kDa) (A). Cbβ-1 also detected some of the truncated products of the recombinant kinases. The polyclonal antibody RU16 detected polypeptides of 73 kDa, 58 kDa and 56 kDa in the skeletal muscle membrane fraction, corresponding to SOCK, CaM Kinase II γ and CaM Kinase II δ, respectively (B). RU16 displayed immunoreactivity with the recombinant kinases and detected the full length kinases of 99 and 86 kDa corresponding to GST-SOCK and GST-CaM Kinase II β, respectively. RU16 also detected two truncated products in each of the affinity-purified samples, which also represent truncated products of the recombinant kinases.

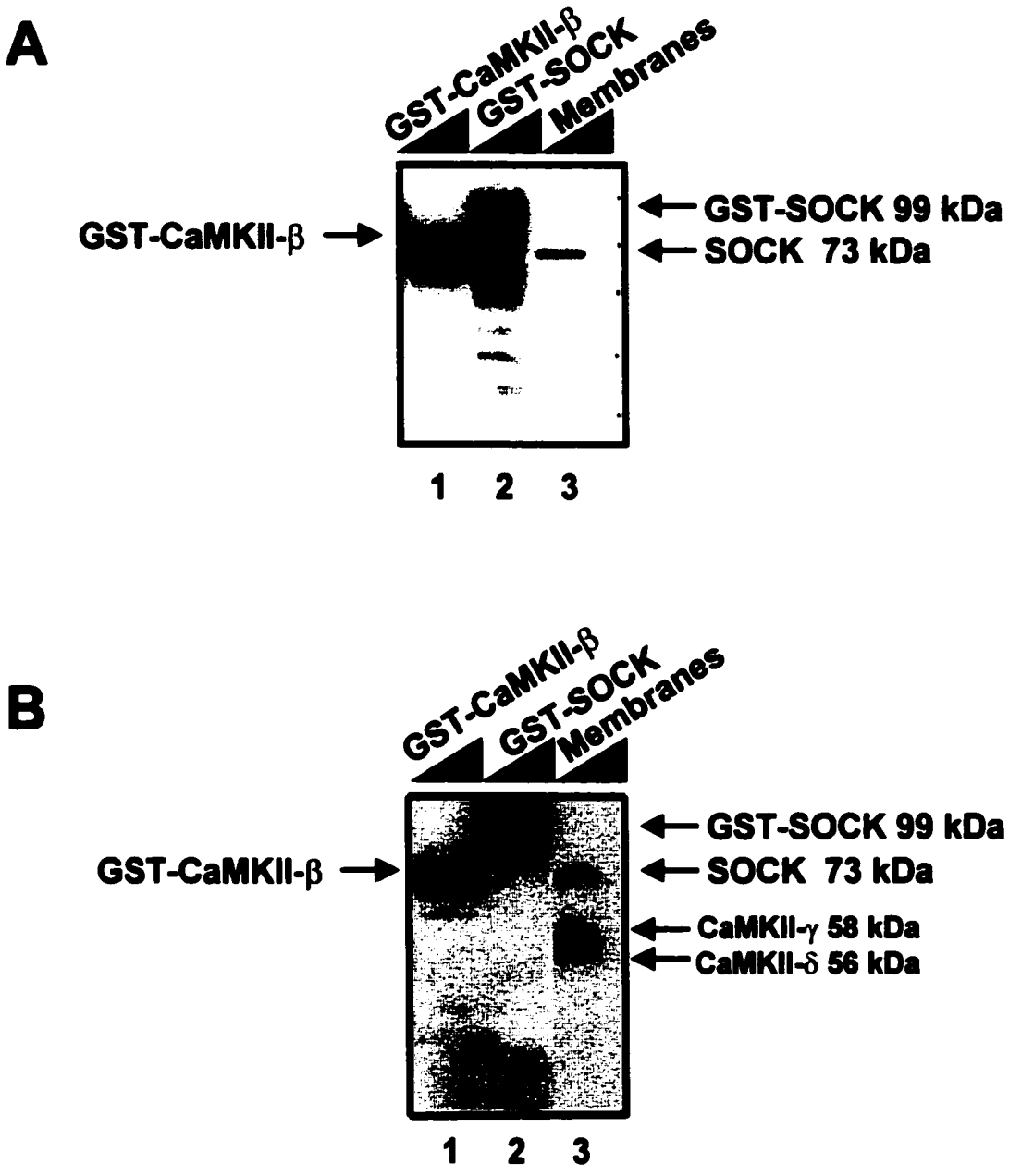
A
GST-CaMKII-β
GST-SOCK
Membranes
GST-CaMKII-β
GST-SOCK 99 kDa
SOCK 73 kDa
1 2 3
B
GST-CaMKII-β
GST-SOCK
Membranes
GST-CaMKII-β
GST-SOCK 99 kDa
SOCK 73 kDa
CaMKII-γ 58 kDa
CaMKII-δ 56 kDa
1 2 3

3.5 Activity of Recombinant SOCK and CaM Kinase II β

Both GST-SOCK and GST-CaM Kinase II β were tested for functional Ca^{2+}/CaM-dependent phosphotransferase activity in a CaM Kinase II phosphorylation assay using the CaM Kinase II specific substrate, Auto Camtide II.

Both kinases phosphorylated the substrate peptide in a Ca^{2+}/CaM-dependent manner with incorporation of over 150 times more [γ-^{32}P] in the peptide by both recombinant kinases as compared to assays performed in the absence of Ca^{2+} (Figure 3.7). The minimal activity observed for both kinases in the absence of Ca^{2+} is likely attributed to the Ca^{2+}-independent activity of CaM Kinases (Schulman, 1993).

Purified brain CaM Kinase II β (Upstate Biotech) used in this CaM kinase assay, was determined by the technicians of Upstate Biotech as having an activity of 7.1 pmoles [γ-^{32}P] incorporated into the substrate peptide/min/25 ng of enzyme. Recombinant SOCK and CaM Kinase II β used in this assay, were found to have activities of 6.1 and 5.9 pmoles [γ-^{32}P] incorporated into the substrate peptide/min/25 ng of enzyme. The specific activities of these kinases as compared to purified brain CaM Kinase II β were similar thus ensuring the catalytic activity of the recombinant proteins as functional CaM Kinases. These recombinant kinases appeared to be suitable for use in functional assays for examining the muscle specific substrates of CaM Kinase II.

Figure 3.7 CaM Kinase Activity of Recombinant SOCK and CaM Kinase II β

Affinity purified GST-SOCK (100 ng) and GST-CaM Kinase II β (100 ng) were incubated with the CaM Kinase II specific substrate, Auto Camtide II (100 μM) in kinase assay buffer with Mg^{2+} (15 mM) and [γ-^{32}P]-ATP (125 μM, 10 μCi/reaction) in the presence of Ca^{2+} (1mM) and CaM (0.4 μg) or CaM alone for ten minutes at 30°C. The reactions were terminated by the addition of 20 μL of cold trichloroacetic acid and 25 μl of the reaction sample was spotted onto numbered P81 phosphocellulose squares. The Squares were washed to remove unincorporated [γ-^{32}P]. Quantitation of [γ-^{32}P] incorporation into the substrate peptide was performed by liquid scintillation counting. Both recombinant SOCK and CaM Kinase II β phosphorylated Auto Camtide II as measured by the incorporation of 6.1 and 5.8 pmoles [γ-^{32}P] in the substrate peptide/min/25 ng of enzyme, respectively. The observed [γ-^{32}P] incorporated in the substrate peptide in the presence of CaM alone represents the basal level of enzyme activity, interpreted as the Ca^{2+}-independent activity of CaM Kinase II. The error bars represent the SDM of n=4 experiments and each measurement of [γ-^{32}P] incorporation was performed in duplicate.

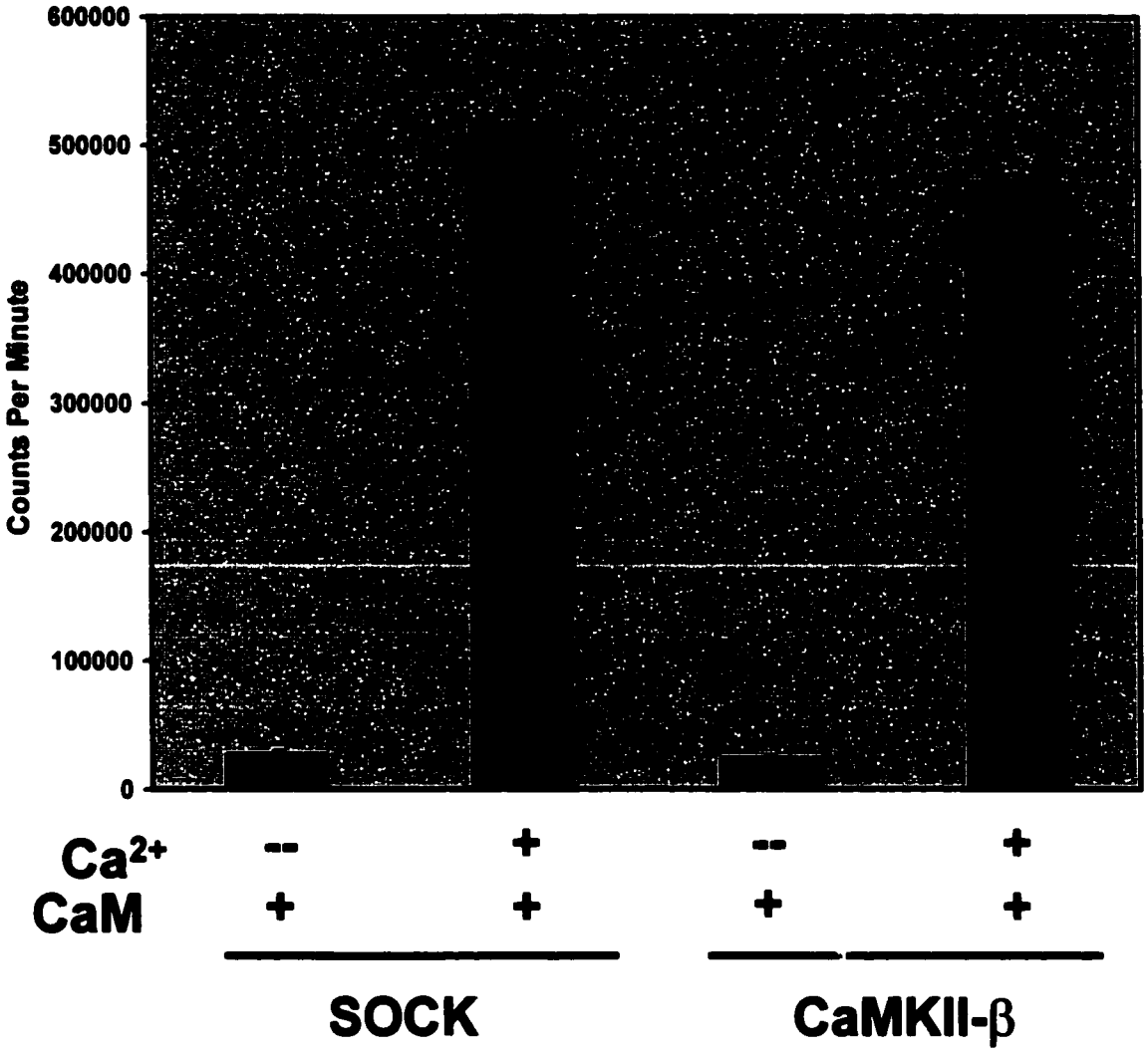
600000
500000
400000
300000
200000
100000
0
Counts Per Minute
Ca2+
CaM
--
+
--
+
+
+
+
+
SOCK
CaMKII-β

3.6 Substrate Specificity of Recombinant SOCK

A putative role for CaM Kinase II in Ca^{2+} entry, Ca^{2+} release and Ca^{2+} uptake from the L-type Ca^{2+} channel (DHPR), Ca^{2+} release channel (RyR) and the Ca^{2+}-ATPase pump, respectively, has been proposed by others and is thought to occur via direct phosphorylation of these proteins (Suko et al., 1993; Hawkin et al., 1994; Dzhura et al., 2000). The CaM Kinase II isoform in muscle responsible for these effects has not been clearly identified.

CaM Kinase II phosphorylates proteins on specific Ser and Thr residues with a minimum consensus sequence of R-X-X-S/T (Suko et al., 1993). A scan for putative CaM Kinase II phosphorylation sites indicates that the RyR1 has 11 and the DHPR α_{1S} subunit has three R-X-X-S/T sequences respectively, while the DHPR β_{1A} subunit has only one R-X-X-T site. To test if GST-SOCK can phosphorylate these proteins at these putative CaM KII phosphorylation sites, the RyR1 and DHPR α_{1S} and β_{1A} subunits were immunoprecipitated from detergent solubilized triads.

Triad vesicles consist of the terminal cisternae of the SR in junction with the T-tubule membrane system and thus would contain RyR1 and the L-type Ca^{2+} channel (DHPR).

The immunoprecipitated receptors were incubated with recombinant SOCK in kinase assay buffer in the presence of Ca^{2+} and CaM or CaM alone for ten minutes at 30°C (as described in Materials and Methods 2.9). Following this the beads were washed three times with a 1:1 mix of solubilization buffer and homogenization buffer to remove recombinant SOCK, which would be autophosphorylated and may interfere with the detection of phosphorylated substrates.

Immunoprecipitation of the receptors was done in the absence of [γ-^{32}P]-ATP and Western blot analysis was performed to check if the receptors immunoprecipitate in this procedure. A 560 kDa polypeptide was detected with anti-RyR1 in the input lane and the anti-RyR1 IP sample corresponding to RyR1 (Figure 3.8A). Products of 168 and 80 kDa, were also detected by anti-RyR1 and may represent proteolytic fragments of RyR1 (Figure 3.8A). The IgM heavy chain (55 kDa) was also detected in the anti-RyR1 IP. A 185 kDa polypeptide was detected with anti-DHPR α1 in both the input and anti-DHPR α1 immunoprecipitation samples (Figure 3.8A). A polypeptide of 200 kDa was also detected in addition to the 185 kDa polypeptide and may represent the full-length α1 subunit prior to post-translational cleavage of the C-terminus. The IgG heavy chain was also detected by anti-DHPR α1.

The autoradiogram in figure 3.8B clearly shows a 560 kDa phosphoprotein corresponding to RyR1 was phosphorylated in a Ca^{2+}/CaM-dependent manner by recombinant SOCK. A phosphopeptide of 560 kDa was also detected in the lane with only CaM and recombinant SOCK added but the incorporated γ-^{32}P in this polypeptide was much less than that observed when Ca^{2+} and CaM are present. The minimal level of γ-^{32}P incorporation in the absence of Ca^{2+} may represent the Ca^{2+}-independent activity of the recombinant kinase. It is evident from this result that immunoprecipitated RyR1 is a substrate of recombinant SOCK. Phosphoproteins of immunoprecipitated DHPR α_{1S} (185 kDa) and DHPR β_{1A} (56/52 kDa) subunits also incorporated γ-^{32}P when incubated with recombinant SOCK when Ca^{2+} and CaM is present, demonstrating that these subunits of the L-type Ca^{2+} channel are substrates of recombinant SOCK when immunoprecipitated from solubilized triads. The minimal levels of incorporated γ-^{32}P observed in the lanes

with only CaM and recombinant SOCK were present, are interpreted as the Ca^{2+} independent activity of the recombinant kinase. These results demonstrate for the first time that RyR1, DHPR α_{1S} sub-unit and the DHPR β_{1A} subunits of the L-type Ca^{2+} channel are substrates of the CaM Kinase II β isoform of skeletal muscle, SOCK.

Figure 3.8 **Immunoprecipitated RyR1 and DHPR α_{1S} and β_{1A} subunits serve as substrates for recombinant SOCK**

RyR1, DHPR α_{1S} and DHPR β_{1A} sub-units of the L-type Ca^{2+} channel were immunoprecipitated from detergent solubilized triads. The immunoprecipitated receptors were incubated with recombinant SOCK (100 ng) in kinase assay buffer (25 mM MOPS, pH 7.2, 10 mM β-glycerol phosphate, 1 mM sodium orthovanadate, 1 mM dithiothreitol, 1mM $CaCl_2$, 0.25 mM EGTA, 15 mM $MgCl_2$, 2 μM calmodulin, 0.4 mM ATP-cold/[γ-^{32}P]-ATP (200 μCi/mL), 0.3 M sucrose) in the presence of Ca^{2+} and CaM or CaM alone for 10 minutes at 30°C. Recombinant SOCK was separated from the immunoprecipitated protein/agarose complexes by a wash in homogenization-solubilization buffer. The remaining proteins were resolved by SDS PAGE and electroblotted to PVDF membrane. Western blot analysis with anti-RyR1 and anti-DHPR α1 were performed on immunoprecipitated receptors from samples of solubilized triads. Anti-RyR1 detected a 560 kDa polypeptide corresponding to RyR1 and a 168 kDa product corresponding to a truncated product of RyR1 was also detected in the input and IP samples (A) The IgM heavy chain was also detected in the IP. Anti-DHPR α1 detected a polypeptide of 185 kDa in the input and anti-DHPR α1 IP (A). Anti-DHPR α1 also detected polypeptides of 200 kDa and the IgG heavy chain in the Anti-DHPR α1 IP sample. The autoradiogram shows that anti-RyR1 immunoprecipitated a 560 kDa phosphoprotein while anti-DHPR α_{1S} and anti-DHPR β_{1A} immunoprecipitated phosphoproteins of 185 kDa and 56/52 kDa respectively (B). The incorporation of γ-^{32}P was greater in the samples incubated with Ca^{2+} and CaM as compared to the samples incubated in the absence of Ca^{2+}. The phosphorylation assays were performed at least three times for each immunoprecipitated protein.

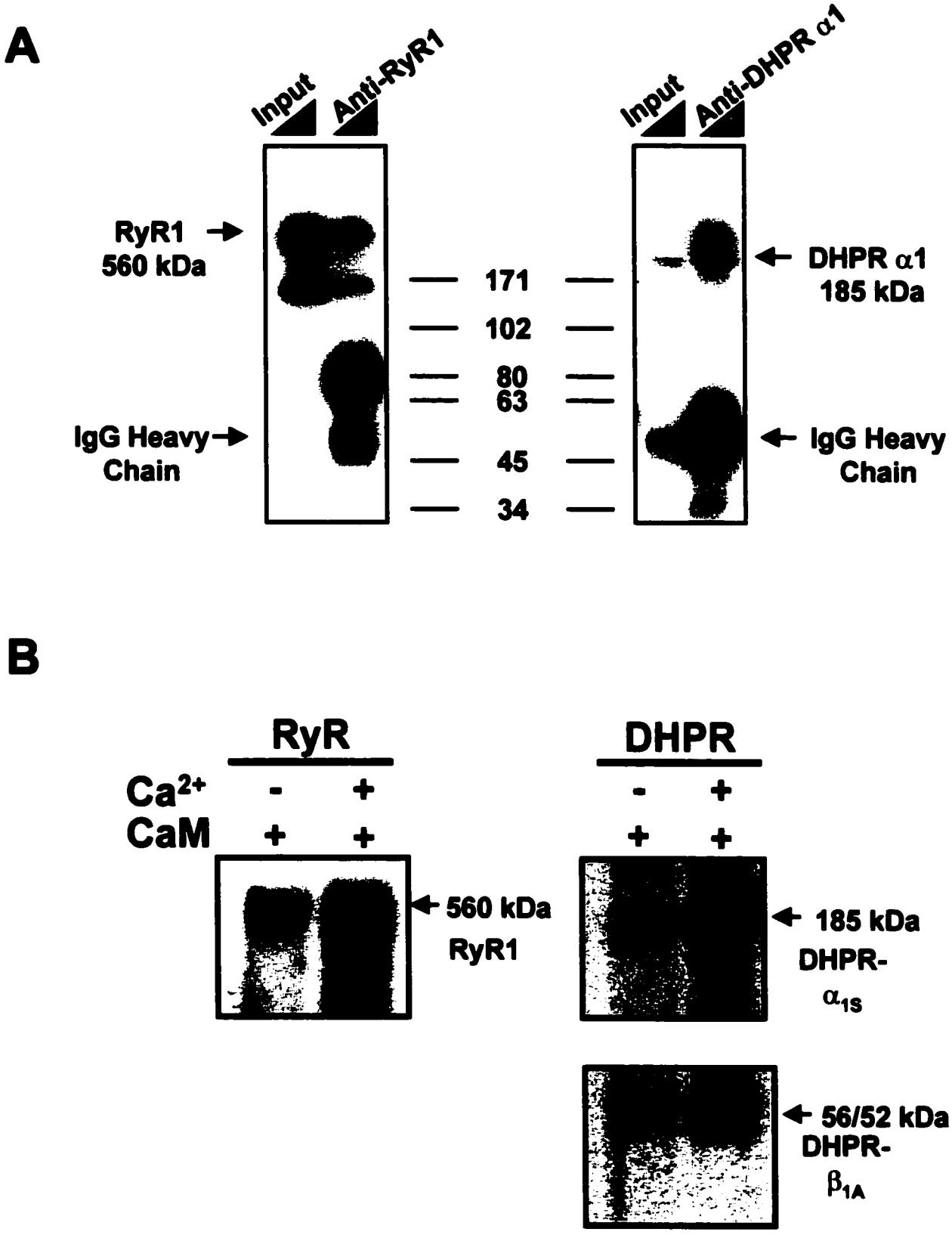
A
Input
Anti-RyR1
Input
Anti-DHPR α1
RyR1
560 kDa
IgG Heavy
Chain
171
102
80
63
45
34
DHPR α1
185 kDa
IgG Heavy
Chain
B
RyR
DHPR
Ca2+
CaM
560 kDa
RyR1
185 kDa
DHPR-
α1S
56/52 kDa
DHPR-
β1A

3.7 Substrate Specificity of Endogenous CaM Kinase II in Skeletal Muscle

The substrate specificity of endogenous CaM Kinase II in skeletal muscle has been shown to differ from that of exogenously added CaM Kinase II in *in vitro* phosphorylation assays (Hain et al., 1994,1995). The difference in substrate specificity based on the source of CaM Kinase II may be attributed to differences in accessibility to the substrate by the kinase. For example, phosphorylation of purified receptors by added CaM Kinase II may occur at sites that are not exposed under physiological conditions. Furthermore, the difference in substrate specificity may also be due to the fact that the exogenous CaM kinase added in previous experiments by Hain et al., 1995 and Suko et al., 1993 was not of the skeletal muscle specific CaM Kinase II β isoform (SOCK) that may or may not have a different substrate specificity. In light of these differences we examined the substrate specificity of endogenous CaM Kinase II isoforms in triads. Triads were incubated in kinase assay buffer in the presence of Ca^{2+} and CaM or CaM alone. PKA and PKC peptide inhibitors were added to all reactions to decrease the possibility of phosphorylation of the receptors by these kinases. The RyR1, DHPR α_{1S} and DHPR β_{1A} subunits were immunoprecipitated, subjected to SDS-PAGE and electroblotted onto PVDF membrane. The autoradiogram displayed in figure 3.9 contained phosphopeptides with apparent molecular weights of 56/52 kDa corresponding to the immunoprecipitated DHPR β_{1A} subunit. The DHPR β_{1A} subunit incorporated minimal amounts of γ-^{32}P in the absence of Ca^{2+} as compared to the Ca^{2+} and CaM lane. The low levels of γ-^{32}P incorporation in the DHPR β_{1A} subunit in the absence of Ca^{2+} may be due to the Ca^{2+}-independent activity of the endogenous CaM Kinases. This data indicates that the DHPR β_{1A} subunit is phosphorylated by endogenous CaM Kinases in a Ca^{2+} and CaM-dependent manner. A

phosphopeptide of 185 kDa, corresponding to immunoprecipitated DHPR α_{1S} was detected weakly on the autoradiogram in the sample containing Ca^{2+} and CaM and suggests that DHPR α_{1S} may be a substrate of endogenous CaM Kinase II (Figure 3.9). This phosphopeptide was not observed in the absence of Ca^{2+}. Immunoprecipitated RyR1 did not incorporate detectable levels of γ-^{32}P in either sample under these conditions. This result is in contrast to previous work by Hain et al., 1995 that demonstrated that RyR1 was phosphorylated by endogenous CaM Kinases in the SR. The lack of detectable γ-^{32}P incorporation in RyR1 (Figure 3.9) may be a result of the conditions used or may be attributable to the phosphorylation sequence not being accessible to the kinase when the RyR1 is in its normal homotetrameric form as opposed to the monomeric form in immunoprecipitated samples.

Figure 3.9 **Endogenous CaM Kinase II Activity in Skeletal Muscle Sarcoplasmic Reticulum**

Triads were incubated in kinase assay buffer in the presence of Ca^{2+} and CaM or CaM alone with PKA and PKC peptide inhibitors. The phosphorylation of RyR, DHPR α_{1S} and DHPR β_{1A} sub units was examined by immunoprecipitation from detergent solubilized triads. Immunoprecipitated RyR1, DHPR α_{1S} and DHPR β_{1A} subunits were subjected to SDS PAGE on 7% polyacrylamide gels. The proteins were electroblotted onto PVDF membranes and exposed overnight at -80°C. 56/52 kDa phosphoproteins corresponding to the immunoprecipitated DHPR β_{1A} subunit were detected on the autoradiogram. Substantially more γ-^{32}P was incorporated in the phosphoprotein corresponding to the DHPR β_{1A} subunit in the presence of Ca^{2+} and CaM than in the absence of Ca^{2+}. Minimal γ-^{32}P incorporation was detected in a phosphoprotein of 185 kDa, corresponding to the immunoprecipitated DHPR α_{1S} subunit in the presence of Ca^{2+} and CaM. This phosphoprotein was not detected in the absence of Ca^{2+}. Immunoprecipitated RyR1 did not incorporate detectable levels of γ-^{32}P when Ca^{2+} and CaM were present or in the absence of Ca^{+}. The phosphorylation assays were performed at least three times.

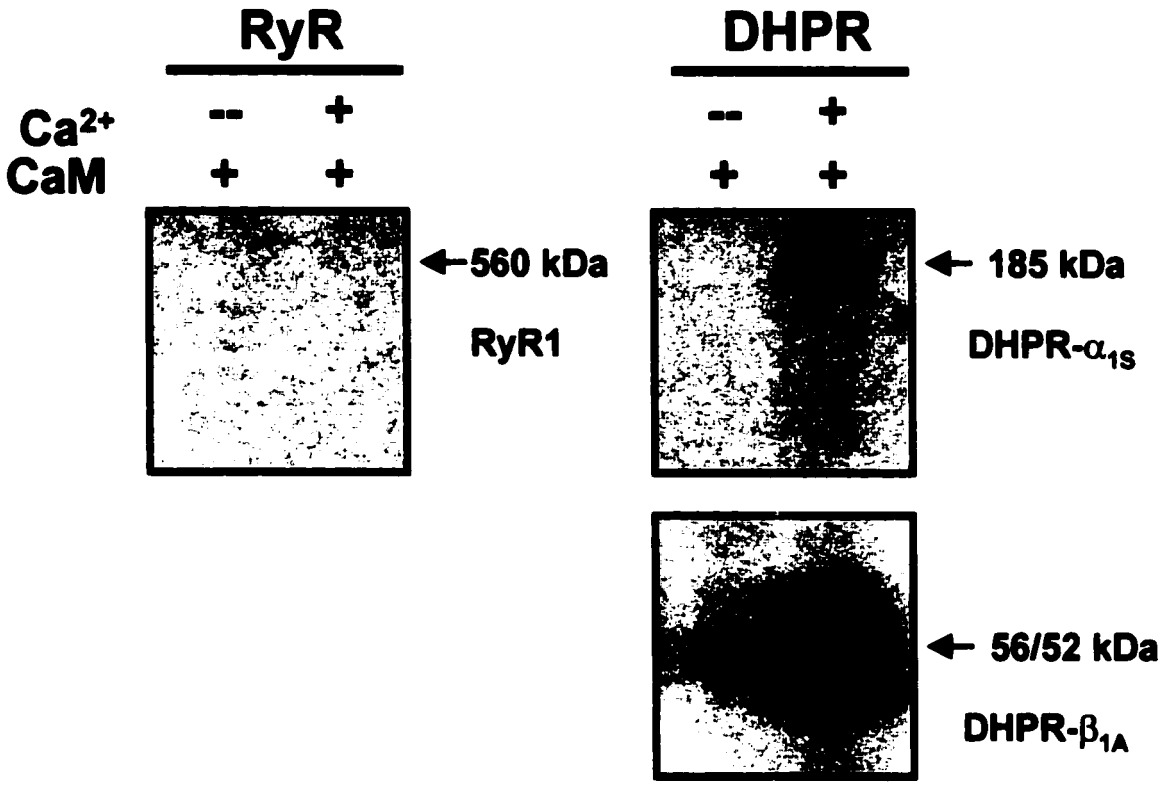
RyR
DHPR
Ca2+
CaM
--
+
--
+
+
+
+
+
560 kDa
RyR1
185 kDa
DHPR-α1S
56/52 kDa
DHPR-β1A

3.8 Endogenous Association of SOCK with Grb2 and Src in Skeletal Muscle

Previous studies in our laboratory have shown that the proline rich region of SOCK contains multiple P-X-X-P sequences. Proline rich sequences with a core P-X-X-P motif have been found to bind to Src Homology 3 Domains (SH3 domains) and serve in the targeting and activation of proteins involved in tyrosine kinase signaling cascades. The P-X-X-P sequences in SOCK were compared to consensus sequences shown to bind specific SH3 domains. The sequence PPVGPPPCPSP encoded in the third proline rich exon P3, appeared to mach the sequences of class II ligands that bind the SH3 domains of Src tyrosine kinase and the adapter protein Grb2 (Yu et al., 1994 and Vidal et al., 1998).

Previous studies indicated that the novel proline rich sequences in SOCK bind to Src SH3 domains (Leddy, 1999). This was determined by incubating the entire proline rich insert (fused to GST) with skeletal muscle cytosol in *in vitro* protein binding assays. However, whether this interaction occurs endogenously in the SR remained to be demonstrated.

Immunoprecipitations from detergent solubilized terminal cisternae with Grb2 and Src antibody-agarose conjugates were performed to test if indeed these proteins interact endogenously with SOCK. The antigen-antibody-agarose complexes were washed with PBS supplemented with 2% Triton-X 100 to remove non-specifically associated proteins. The washed beads (approximately 30 µl) were resuspended in 30 µl of 2X SDS loading buffer, boiled and subjected to SDS PAGE on 10% polyacrylamide gels. The proteins were electroblotted onto PVDF membranes. Western blot analysis was performed to test for the immunoprecipitation of Grb2 (lower panel in figure 3.10 A) and Src (lower panel

in figure 3.10B). Anti-Grb2 weakly reacted with a 25 kDa polypeptide (Figure 3.10A lane 2), corresponding to Grb2 in the input lane (30 μg of solubilized membrane fractions) and detected Grb2 to a greater extent in the IP sample (lane 3). The anti-Grb2-agarose pre-blocked with the blocking peptide Sc:255P, immunoprecipitated significantly less Grb2 as detected in the Western blot (lane 4). Rabbit IgG conjugated to agarose was used as a negative control to ensure that the immunoprecipitation of the proteins of interest was due to specific interactions with the anti-Grb2 and anti-Src antibodies. Grb2 was not immunoprecipitated by rabbit IgG-agarose control (lane 1).

Src was detected by anti-Src in the input sample (figure 3.10 B lane 1) and the IP sample (lane 3). Anti-Src-agarose pre-blocked with blocking peptide Sc:19P did not immunoprecipitate detectable amounts of Src (lane 4). Src was not immunoprecipitated by rabbit IgG-agarose control sample (lane 2).

When Western blot analysis was performed with the CaM Kinase II β specific antibody Cbβ-1, immunoreactivity with a 73 kDa polypeptide corresponding to SOCK was present in the input lane, as well as in the IP sample with both anti-Grb2 agarose (top panel in Figure 3.10 A) and anti-Src agarose samples (top panel in Figure 3.10 B). SOCK was not detected in the rabbit IgG agarose (negative control) sample and was not detected in the peptide blocked anti-Grb2 sample (Figure 3.10 A lane 3) and peptide blocked anti-Src samples (Figure 3.10 B lane 4), demonstrating that the detection of SOCK in the IP is the result of specific associations with Grb2 and Src and is not due to non-specific associations with agarose or the antibodies. The SOCK-Grb2 and SOCK-Src interactions are presumably due to proline motif/SH3 domain protein-protein interactions.

Immunoprecipitation experiments with unconjugated monoclonal anti-CaM Kinase II β (Cbβ-1) and anti-Grb2 antibodies were performed to determine if the soluble antibodies would be able to co-immunoprecipitate Grb2 and SOCK, respectively. (Figure 3.11 A and 3.11 B). To control for non-specific interactions, one sample of anti-Grb2 was pre-incubated with muscle cytosol which is rich in Grb2 and thus would saturate the antigen binding sites of the anti-Grb2 antibodies before being used in immunoprecipitation experiments. A sample of soluble membranes was incubated with purified mouse IgG as a control to test for non-specific interactions. Western blot analysis with anti-Grb2 detected a 25 kDa polypeptide corresponding to Grb2 in the anti-CaM Kinase II β immunoprecipitation sample (Figure 3.11A lane 5). For comparative purposes, immunoprecipitations with anti-Grb2 agarose were run alongside the anti-CaM Kinase II β and tested for the detection of Grb2. Immunoprecipitations with the soluble anti-Grb2 were probed for the presence of SOCK by Western blot analysis with Cbβ-1 (Figure 3.11B). SOCK was detected in the anti-Grb2 test sample (Figure 3.11B lane2) and was not detected in immunoprecipitations with protein A/G beads (lane 1), anti-Grb2 preblocked with skeletal muscle cytosol (lane 3) or mouse IgG (lane 4). This demonstrates that SOCK and Grb2 co-immunoprecipitate from solubilized terminal cisternae and also indicates that SOCK and Grb2 interact with each other endogenously. The detection of the IgG light chain of Cbβ-1 is indicated.

Figure 3.10 Immunoprecipitation of SOCK with Grb2 and Src in Skeletal Muscle Membranes

Immunoprecipitation with anti-Grb2 agarose conjugate and anti-Src agarose conjugate from solubilized heavy SR was performed to test for the co-immunoprecipitation of SOCK. The immunoprecipitated complexes were electrophoresed on 10% polyacrylamide SDS gels and electroblotted onto PVDF membranes. Western blot analysis with anti-Grb2 (A, lower panel) and anti-Src (B, lower panel) antibodies indicated that both of these proteins were present in the input sample and the IP sample. Pre-incubation of the antibodies with blocking peptides diminished the immunoprecipitation of Grb2 and Src. The presence of Grb2 (25 kDa) or Src (60 kDa) was not detected in the IgG-agarose control immunoprecipitation. Western blot analysis with anti-CaM Kinase II β (Cbβ-1) detected a 73 kDa polypeptide corresponding to SOCK in the input sample and the IP sample with anti-Grb2 agarose (A, top panel) and anti-Src agarose (B, top panel). SOCK was not detected in the lanes containing the anti-Grb2 and anti-Src pre-bound with blocking peptide or in the IgG control sample. The immunoprecipitation of SOCK, Src and Grb2 was performed at least three times and was performed in purified SR obtained from another animal.

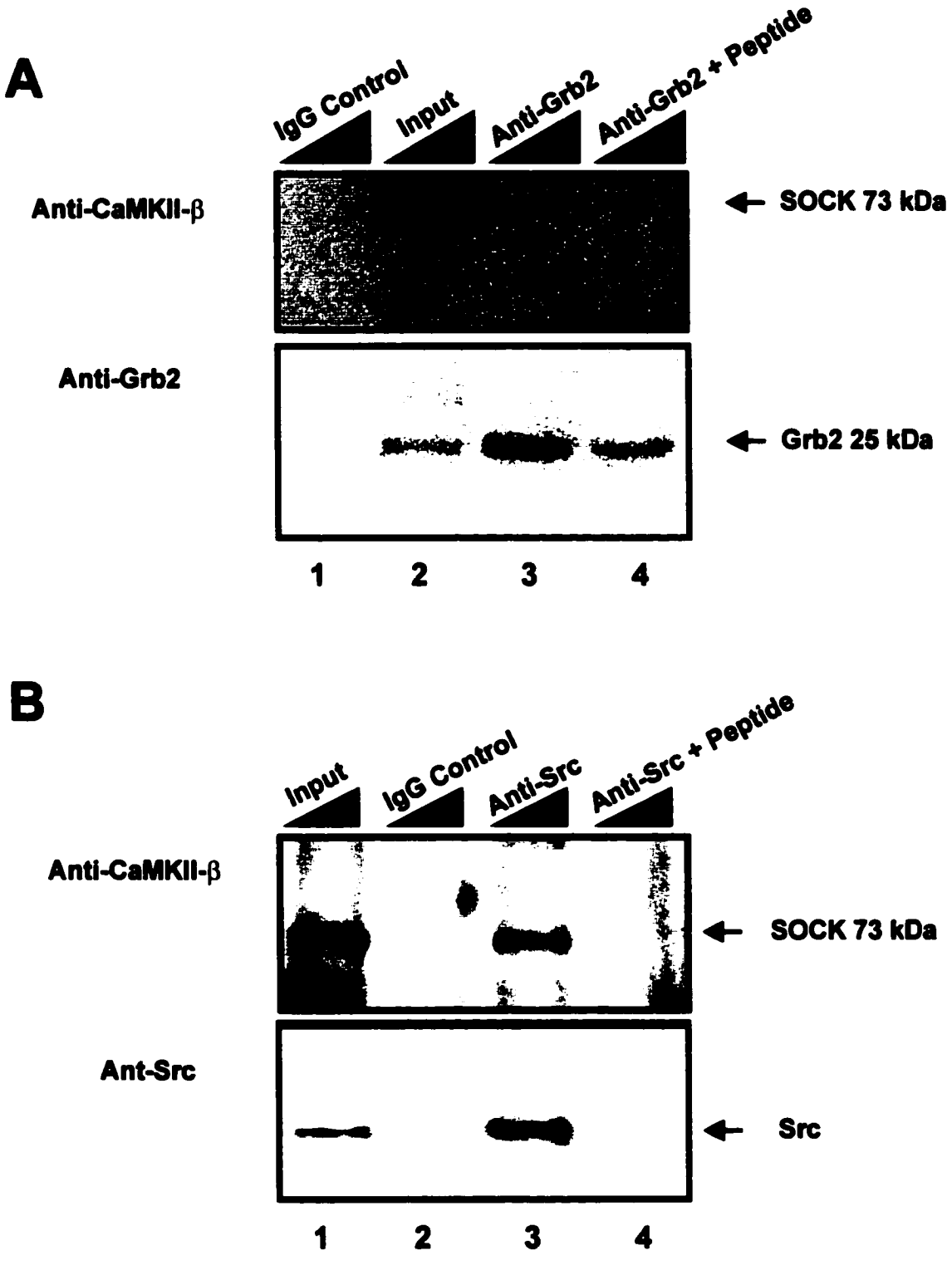
A
IgG Control
Input
Anti-Grb2
Anti-Grb2 + Peptide
Anti-CaMKII-β
SOCK 73 kDa
Anti-Grb2
Grb2 25 kDa
1
2
3
4
B
Input
IgG Control
Anti-Src
Anti-Src + Peptide
Anti-CaMKII-β
SOCK 73 kDa
Ant-Src
Src
1
2
3
4

Figure 3.11 Co-immunoprecipitation of Grb2 and SOCK from Skeletal Muscle SR

Co-Immunoprecipitation of Grb2 from solubilized heavy SR with anti-CaMKII β (Cbβ-1) or anti-Grb2 agarose immunoprecipitates Grb2 as detected in Western blots using a monoclonal anti-Grb2 antibody (A). A 25 kDa polypeptide corresponding to Grb2 was detected in the IP sample using Cbβ-1 (lane 5), the IgG light chain was also detected. A soluble anti-Grb2 mAb immunoprecipitated a 73 kDa protein corresponding to SOCK (lane 2) when Cbβ-1 was used to detect SOCK in Western blots (B). SOCK was not detected in the sample with anti-Grb2 that was pre-blocked with Grb2 from the cytosol (lane 3) or in the IgG control (lane 4) or protein A/G beads control (lane 1) samples. The co-immunoprecipitation of Grb2 and SOCK was replicated at least three times.

A

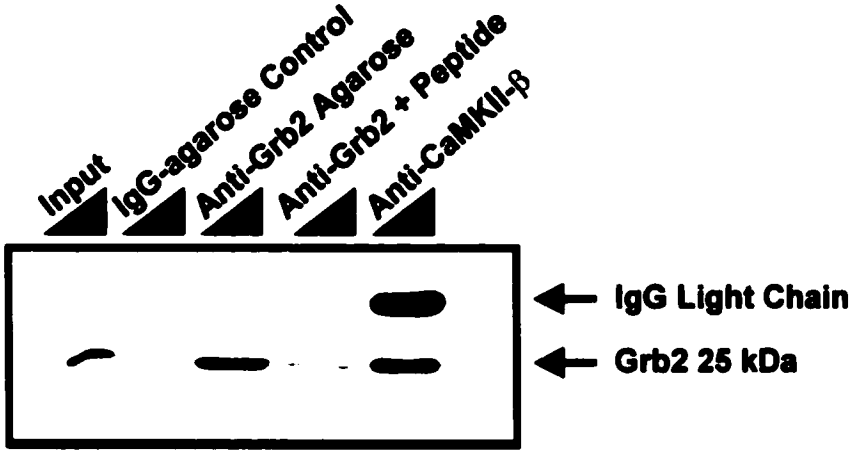
Input
IgG-agarose Control
Anti-Grb2 Agarose
Anti-Grb2 + Peptide
Anti-CaMKII-β
IgG Light Chain
Grb2 25 kDa

B

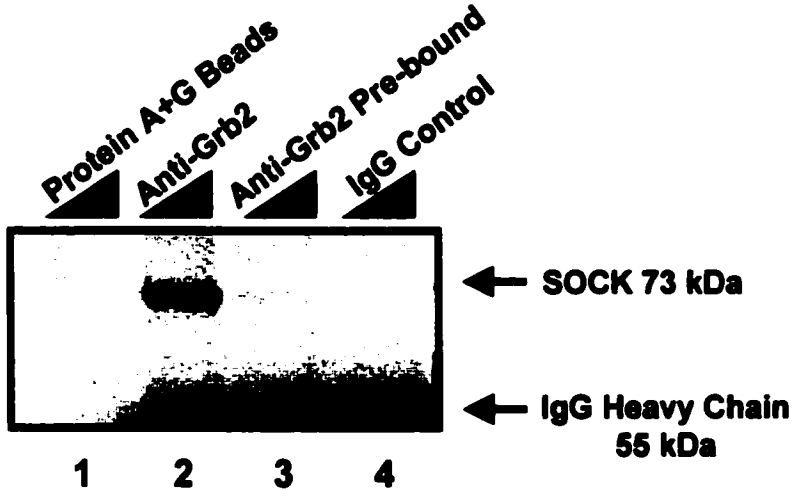
Protein A+G Beads
Anti-Grb2
Anti-Grb2 Pre-bound
IgG Control
SOCK 73 kDa
IgG Heavy Chain
55 kDa
1
2
3
4

3.9 Site-Directed Mutagenesis of the SH3 Binding Domain of SOCK

To identify the amino acids critical for the Src-SOCK and Grb2-SOCK interactions, point mutations in the putative SH3 binding domain of SOCK were engineered by site-directed mutagenesis to abrogate these associations in an *in vitro* binding assay. The specific residues targeted for mutation were chosen based on observations made by others who demonstrated that single amino acid substitutions of specific proline or arginine residues is sufficient for abrogating the SH3-proline rich interaction (Weng et al., 1995). Although, these studies used only small 12-15 a.a. sequences fused to GST, to test for the ablation of the test interaction.

Figure 3.12 shows the amino acids targeted for mutation as presented in the context of neighboring amino acids. The amino acids P_{516}, P_{517}, P_{520}, P_{522} and P_{525} were targeted for point mutations since each of these proline residues are found at the N or C terminal side of the P-X-X-P sequences. There are three tandem P-X-X-P sequences in the putative SH3 binding domain of SOCK but not all of these are expected to be critical for association with SH3 domains. However, they may be important for the tertiary structure consisting of a type II poly-proline helix that presents the critical P-X-X-P sequence to the SH3 domain. Three arginine residues were also targeted for point mutation (R_{448}, R_{491} and R_{533}) since arginine residues near the P-X-X-P motif are thought to form a salt bridge with sequences in the SH3 domain. The salt bridge is proposed to direct the orientation of the P-X-X-P motif interaction with SH3 domains and abrogation of this component of the P-X-X-P/SH3 interaction could inhibit their association.

Fusion proteins corresponding to GST-Q2A (proline rich exons P1, P2 and P3) and the various point mutants of GST-Q2A (DNA sequenced to confirm point mutation) as

well as GST alone, GST-CaM Kinase II β and GST-SOCK were expressed and affinity purified on glutathione sepharose® 4B (as described in materials and methods). The fusion protein/sepharose beads were incubated with pre-cleared skeletal muscle cytosol (500 μg) for 2 hours at 4°C and then washed three times in PBS containing 1% Triton X-100 detergent to remove non-specifically associated proteins. The beads were suspended in SDS loading buffer and were electrophoresed on 10% polyacrylamide SDS gels and electroblotted onto PVDF membranes. Western blot analysis with a monoclonal anti-Grb2 antibody was performed to test for the precipitation of Grb2 (Figure 3.13). The detection of a 25 kDa protein corresponding to Grb2 was not observed in the glutathione beads sample (lane 1), GST alone (lane2) or GST-CaM Kinase II β (lane 4) (Figure 3.13). Grb2 was detected in the GST-Q2A wild type sample (lane 3), GST-SOCK (lane5) and was also detected in all of the point mutants of GST-Q2A (lanes 6-13). In light of the observation that all of the point mutations maintained their interaction with Grb2, this indicates that the point mutations were insufficient to abrogate the Grb2-SOCK interaction.

Figure 3.12 Amino Acids of SOCK Targeted for Point Mutations

Schematic showing the proline rich regions in SOCK as compared to other proline rich domains known to bind to Grb2 and Src as well as the specific amino acids targeted for point mutation. The proline rich motif encoded by amino acids 511-533 in SOCK is similar to the proline rich motifs in SHC, SOS1, AFAP-110 and Dynamin1. Based on this similarity, prolines corresponding to amino acids P_{516}, P_{517}, P_{520}, P_{522} and P_{525} were deemed suitable targets for site directed mutagenesis. R_{533} was also targeted as it may be important in the formation of a salt bridge with SH3 domains. The proline rich motif encoded by amino acids 431-448 contains two P-X-X-P motifs, none of which appear to mach the consensus sequences present in the proteins indicated. R_{448} and R_{491} (not shown) was targeted for mutation to test if a point mutation here may alter the formation of the salt bridge.

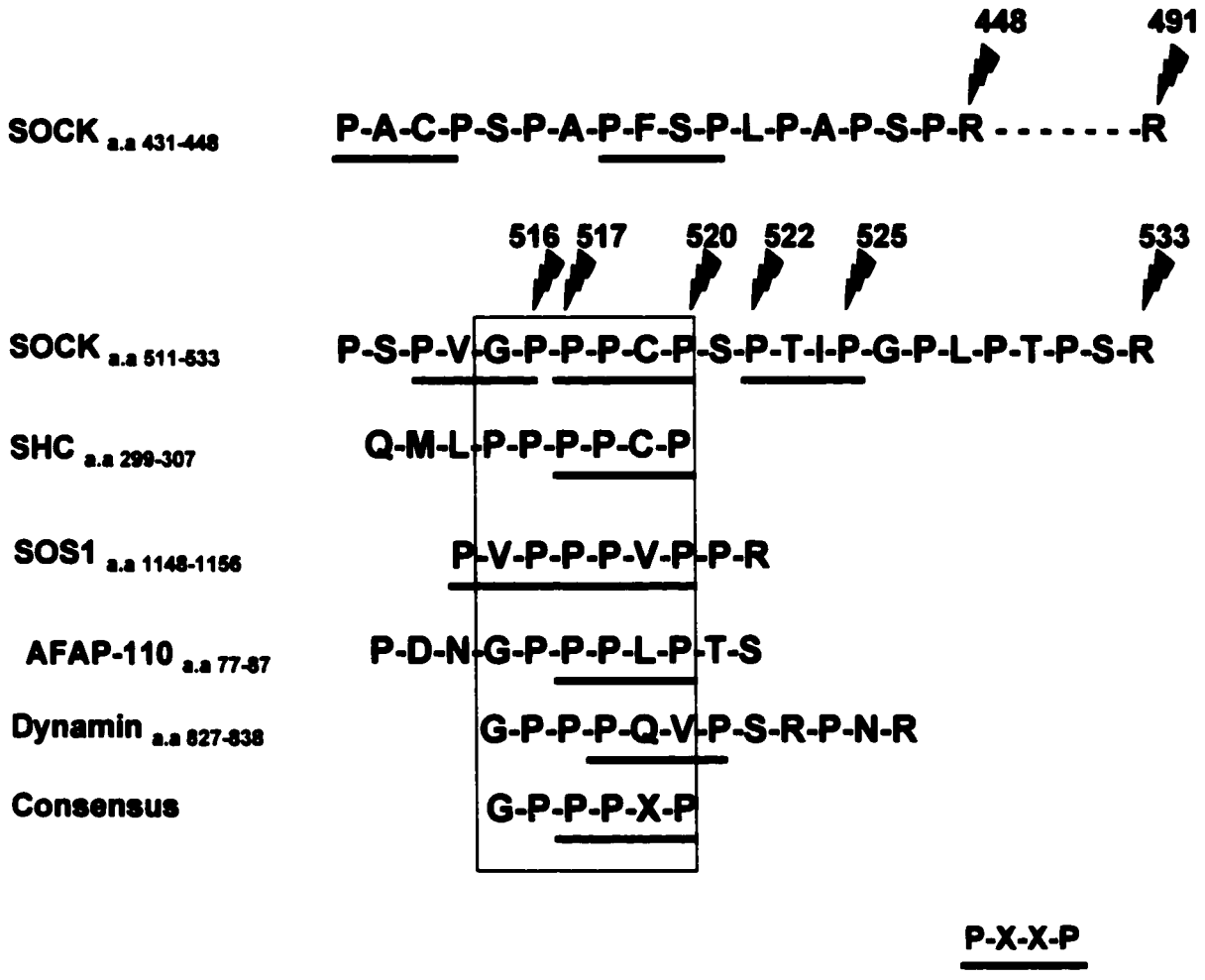
448
491
SOCK a.a 431-448
P-A-C-P-S-P-A-P-F-S-P-L-P-A-P-S-P-R - - - - - - -R
516 517
520
522
525
533
SOCK a.a 511-533
P-S-P-V-G-P-P-P-C-P-S-P-T-I-P-G-P-L-P-T-P-S-R
SHC a.a 299-307
Q-M-L-P-P-P-P-C-P
SOS1 a.a 1148-1156
P-V-P-P-P-V-P-P-R
AFAP-110 a.a 77-87
P-D-N-G-P-P-P-L-P-T-S
Dynamin a.a 827-838
G-P-P-P-Q-V-P-S-R-P-N-R
Consensus
G-P-P-P-X-P
P-X-X-P

Figure 3.13 Site Directed Mutagenesis of the Proline Rich Motif in SOCK and the Interaction with Grb2 and Src

Fusion proteins corresponding to GST-Q2A (containing all three proline rich tandem repeats) and the various point-mutated versions of GST-Q2A, as well as GST-CaM Kinase II β, GST-SOCK and GST alone were expressed in cultures of Codon Plus® RP BL21 and affinity purified on glutathione sepharose® 4B. The fusion protein/glutathione agarose beads (25 µl) were incubated with 500 µg of skeletal muscle cytosol for 2 hours at 4°C. The beads were washed with PBS containing 1% Triton X-100™, resuspended in SDS-loading buffer and were electrophoresed on 10% polyacrylamide SDS gels. Proteins were electroblotted onto PVDF membrane and probed for the presence of Grb2 and Src in Western blot analysis with monoclonal anti-Grb2 and anti-Src antibodies. 25 kDa or 60 kDa proteins corresponding to Grb2 (A) and Src (B), respectively were not detected in the glutathione beads control sample (lane 1), GST (lane 2) or with GST-CaM Kinase II β (lane 4). Grb2 and Src were detected in the GST-Q2A sample (lane 3), GST-SOCK (lane 5) as well as in the samples with the point mutants of GST-Q2A (lanes 6-13). The precipitation of Grb2 and Src was specific for association with sequences in the proline insert Q2A and SOCK, as is demonstrated by the absence of Grb2 or Src associations with GST and CaM Kinase II β.

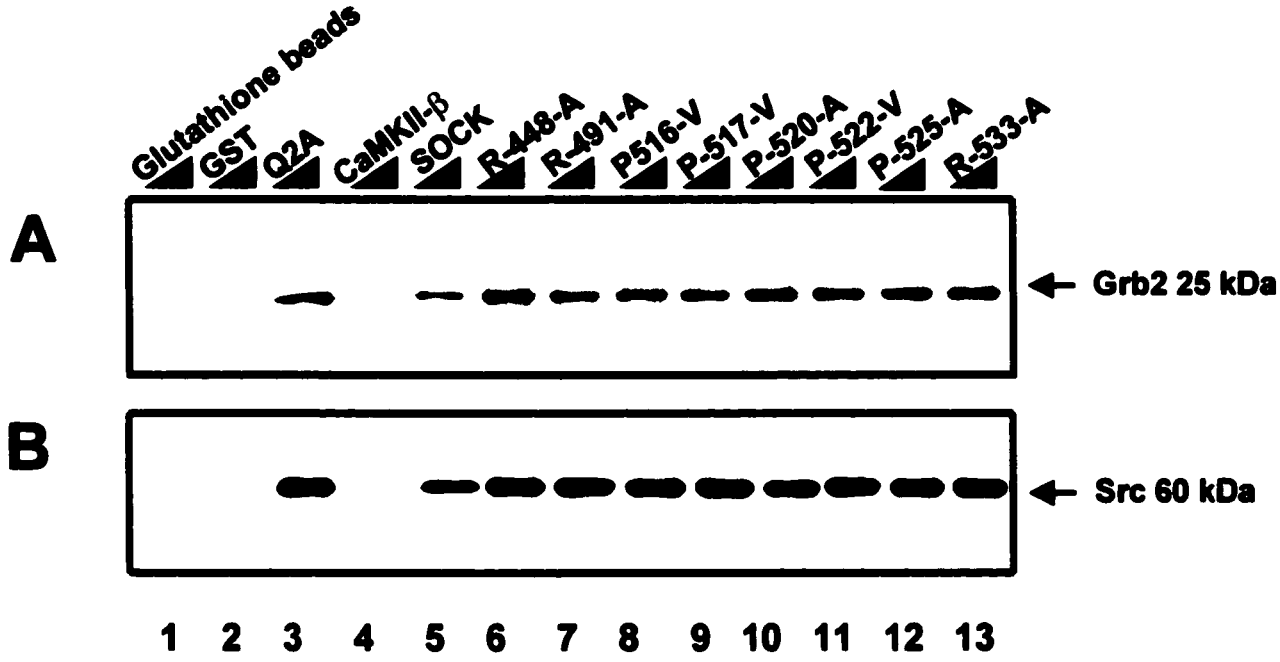
Glutathione beads
GST
Q2A
CaMKII-β
SOCK
R-448-A
R-491-A
P516-V
P-517-V
P-520-A
P-522-V
P-525-A
R-533-A
A
B
Grb2 25 kDa
Src 60 kDa
1 2 3 4 5 6 7 8 9 10 11 12 13

3.10 Exon Specific Binding of Biotinylated Grb2 and Src SH3 Domains

The 13-kDa insert in the variable domain of SOCK is comprised of three new exons that encode three proline rich tandem repeats. Point mutations in the proposed SH3 binding domain failed to abrogate the SH3-proline rich protein-protein interaction (possibly due to multiple P-X-X-P interactions with SH3 domains). To determine if the SH3 domains of Grb2 and Src bind to more than one region in SOCK, the individual exons were ligated into GST-fusion expression vectors and expressed and purified from *E. coli* (Figure 3.14 A). Purified fusion proteins consisting of GST-Q2A (all three proline rich sequences), GST-P1 (proline rich repeat 1), GST-P2 (proline rich repeat 2), GST-P3 (proline rich repeat 3) and GST alone were electrophoresed on 10% polyacrylamide SDS gels and electroblotted onto PVDF membranes. Biotinylated probes were generated by incubating purified GST fusion proteins (SH3 domain of Src, SH3 domain of Grb2 from N-terminus, SH3 domain of Grb2 from the C-terminus, SH2 domain of Grb2 and GST) with an amine reactive succinimidyl ester of biotin (Figure 3.14 B).

Proteins on the membrane were visualized with Ponceau S, demonstrating approximately equal amounts of fusion proteins in each lane (Figure 3.15). Overlay experiments were performed in which the biotinylated probes were incubated with fusion proteins attached to a PVDF membrane. The overlay using biotinylated GST alone did not demonstrate interaction with any of the fusion proteins. Biotinylated Grb2 N-terminus SH3 domain was observed to associate with GST-Q2A (lane 2), GST-P1 (lane 3) and GST-P3 (lane 5) as detected on the overlay blot (Figure 3.15). Association with GST (lane 1) or GST-P2 (lane 4) was not detected. This indicates that the P-X-X-P motif in the first proline rich repeat and the third proline rich repeat specifically interact with the N-

terminus SH3 domain of Grb2, while the second proline rich insert does not. The C-terminal SH3 domain of Grb2 and the SH2 domain of Grb2 were not observed to associate with any of the fusion proteins as determined by the absence of any detectable signal (Figure 3.15). The biotinylated SH3 domain of Src was observed (found) to interact with GST-Q2A (lane 2), GST-P1 (lane 3) and GST-P3 (lane 5) (Figure 3.15). This was the same pattern detected for the N-terminus SH3 domain of Grb2, indicating that the SH3 domain of Src can associate with the proline rich motifs in the first and the third proline rich repeat but not with the second proline rich repeat. The observed interaction of GST-P1 was greater than that observed with GST-P3, indicating that the SH3 domains of Src and Grb2 may prefer the P-X-X-P sequence in P1 to that in P3. The observed redundant binding of SH3 domains to two regions in SOCK may explain why the point mutations in the third proline rich repeat were not sufficient to abrogate the SH3-proline rich interaction. Other proteins such as Sam68 and DOCK 180 have multiple P-X-X-P sequences, which bind more than one SH3 domain (Tu et al., 2001).

Figure 3.14 **Generation of Fusion Proteins and Biotinylated Probes for Use in Overlay Experiments**

Schematic of fusion proteins corresponding to the individual proline rich exons GST-P1, P2 and P3, as well as GST-Q2A (P1-P2-P3) and GST for use in overlay assays (A). Schematic of biotinylated fusion proteins corresponding to the SH3 domain of Src (GST-Src-SH3), N-terminus SH3 domain of Grb2 (GST-NSH3-Grb2, SH2 domain of Grb2 (GST-SH2-Grb2), C-terminus SH3 domain of Grb2 (GST-CSH3-Grb2 and GST alone, for use as probes in overlay assays (B).

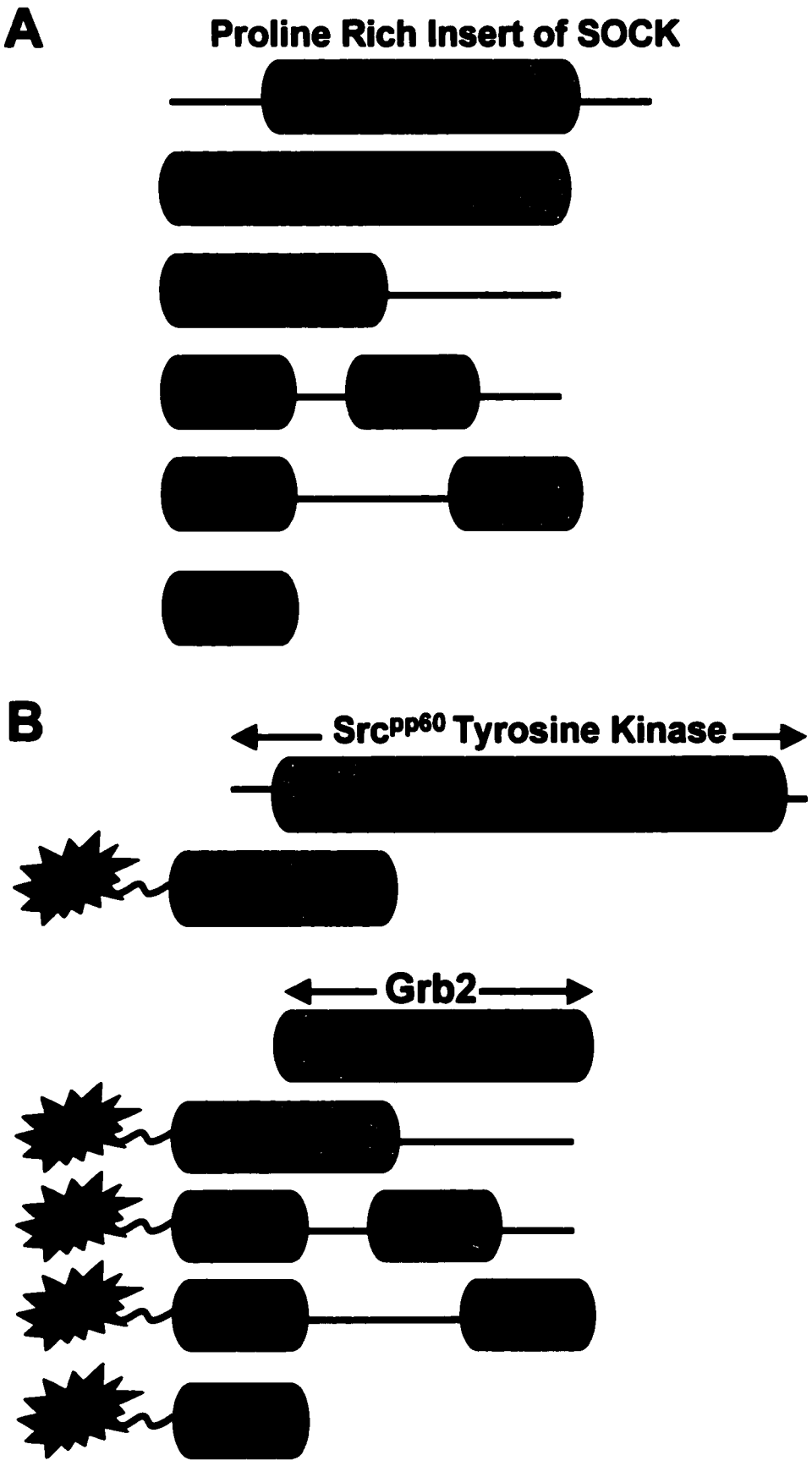
A
Proline Rich Insert of SOCK
B
Src^pp60 Tyrosine Kinase
Grb2

Figure 3.15 Interaction of Specific SH3 Domains with Specific Domains in SOCK

Overlay experiments were performed with biotinylated probes consisting of GST-Src-SH3, GST-NSH3-Grb2, GST-CSH3-Grb2, GST-SH2-Grb2 and GST. The biotinylated probes were incubated with membrane bound fusion proteins corresponding to GST, GST-Q2A (P1-P2-P3), GST-P1, GST-P2 and GST-P3. Staining with Ponceau red demonstrates the approximately equal amount of the test proteins on the PVDF membrane. Biotinylated Src-SH3 and Grb2-NSH3 domains interacted with GST-Q2A (lane 2), GST-P1 (lane 3) and GST-P3 (lane 5). Src-SH3 and Grb2-NSH3 domains did not interact with GST (lane 1) or GST-P2 (lane 4). Biotinylated GST, GST-SH2-Grb2 and GST-CSH3-Grb2 did not interact with any of the fusion proteins as demonstrated by the absence of a detectable signal. This data indicates that the SH3 domain of Src and the N-terminal SH3 domain of Grb2, specifically interact with the amino acids encoded by the proline rich exon 1 (P1) and proline rich exon 3 (P3) from the 13 kDa insert in SOCK. The overlay experiments were performed three times to confirm the observations.

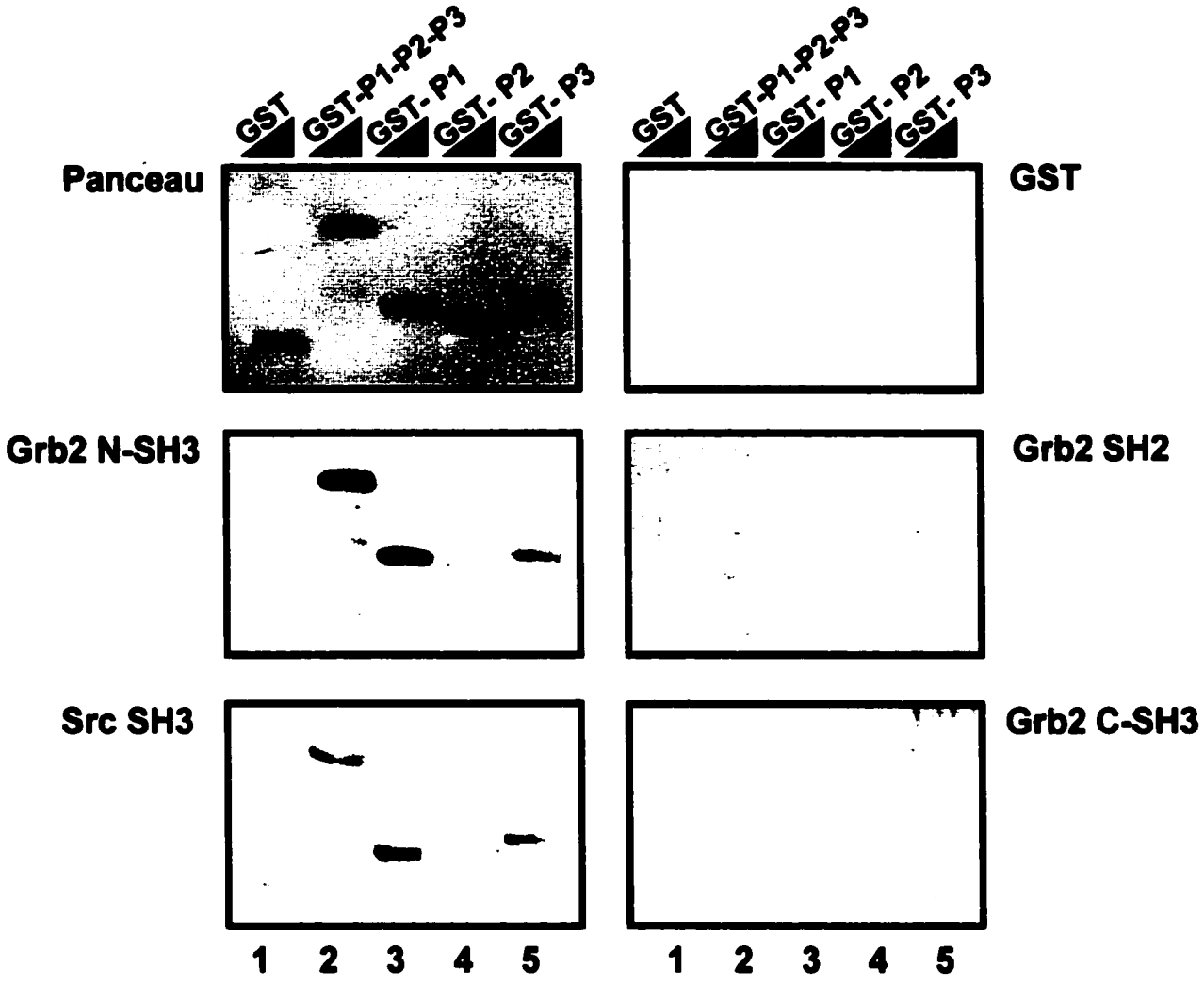
GST
GST-P1-P2-P3
GST- P1
GST- P2
GST- P3
GST
GST-P1-P2-P3
GST- P1
GST- P2
GST- P3
Panceau
GST
Grb2 N-SH3
Grb2 SH2
Src SH3
Grb2 C-SH3
1 2 3 4 5
1 2 3 4 5

3.11 SOCK-SH3 Domain Interaction and the Effect on Enzyme Activity

The function of SH3 domain interactions with proline sequences is not restricted to protein-protein interactions or sub-cellular targeting. It may also include the interactive regulation of enzyme activity. The effect of Src-SOCK and Grb2-SOCK associations on SOCK activity may also be a physiological mode of modulating enzyme activity. For example, the GTPase activity of Dynamin is stimulated upon interacting with SH3 domains (Gout *et al.*, 1993). In light of this, the interaction of SH3 domains with the proline rich region in SOCK might have a functional role by modifying the enzyme activity of SOCK. If true, this may be a physiological mode of modulating CaM Kinase II enzyme activity in response to the targeting of proteins involved in tyrosine kinase and MAP kinase signaling cascades such as Src and Grb2, respectively.

To determine if there is a functional consequence of SOCK-SH3 interactions on the enzyme activity of SOCK, enzyme assays were performed in the presence of different domains from Src and Grb2. GST-SOCK was incubated with 10 molar excess of Grb2 and Src domains since the abundance of these proteins in skeletal muscle is far greater than that of SOCK, which required isolation of membranes before detectable levels were observed in Western blots. A parallel set of reactions using GST-CaM Kinase II β instead of GST-SOCK served as a control. The data indicate that the binding of the SH3 domain of Src and the N-terminal SH3 domain of Grb2 to SOCK, results in a decrease of approximately 20% in the phosphorylation of the substrate peptide Auto Camtide II (Figure 3.16A). A one way Anova test was performed which indicated that the decrease in enzyme activity observed when SOCK was incubated with the SH3 domain of Src or the N-terminal SH3 domain of Grb2 as compared to the control, was statistically significant

($P<0.001$) with confidence intervals of 95% (ANOVA, n=4). SOCK activity when incubated with GST, Grb2-SH2, Grb2-C terminal SH3 or GST elution buffer alone was not significantly different than the control sample ($P>0.05$)(ANOVA). Phosphorylation of Auto Camtide II by GST-CaM Kinase II β in the presence of the different fusion proteins, was not significantly different than the control sample ($P>0.05$) (Figure 3.16 B). The decrease in substrate phosphorylation was not observed with GST-CaMKII β, indicating that the decrease in phosphorylation activity observed with GST-SOCK is a direct consequence of binding to SH3 domains. The decrease in substrate phosphorylation by SOCK may be interpreted as a modulation of phosphotransferase activity due to steric hindrance or conformational changes in SOCK as a result of binding to SH3 domains.

Figure 3.16 **The Effect of SOCK-SH3 Interactions on the Enzyme Activity of Recombinant SOCK**

Enzyme assays with Auto Camtide II as substrate peptide (P), were performed in the presence of purified GST fusion proteins consisting of Grb2-NSH3, Grb2-SH2, Grb2-CSH3, Src SH3 and GST alone to determine if there is a functional consequence of SOCK-SH3 interactions. The amount of phosphorylation of Auto Camtide II when SOCK was incubated with GST-Src-SH3 and GST-N-SH3 of Grb2 was significantly less than the control ($P<0.001$). SOCK activity was not affected by the other fusion proteins or the elution buffer (EB) of the GST fusion proteins ($P>0.05$). Phosphorylation of Auto Camtide II by GST-CaM Kinase II β in the presence of the different fusion proteins, was not significantly different than the control sample ($P>0.05$) (The error bars represent the SDM of n=4 experiments).

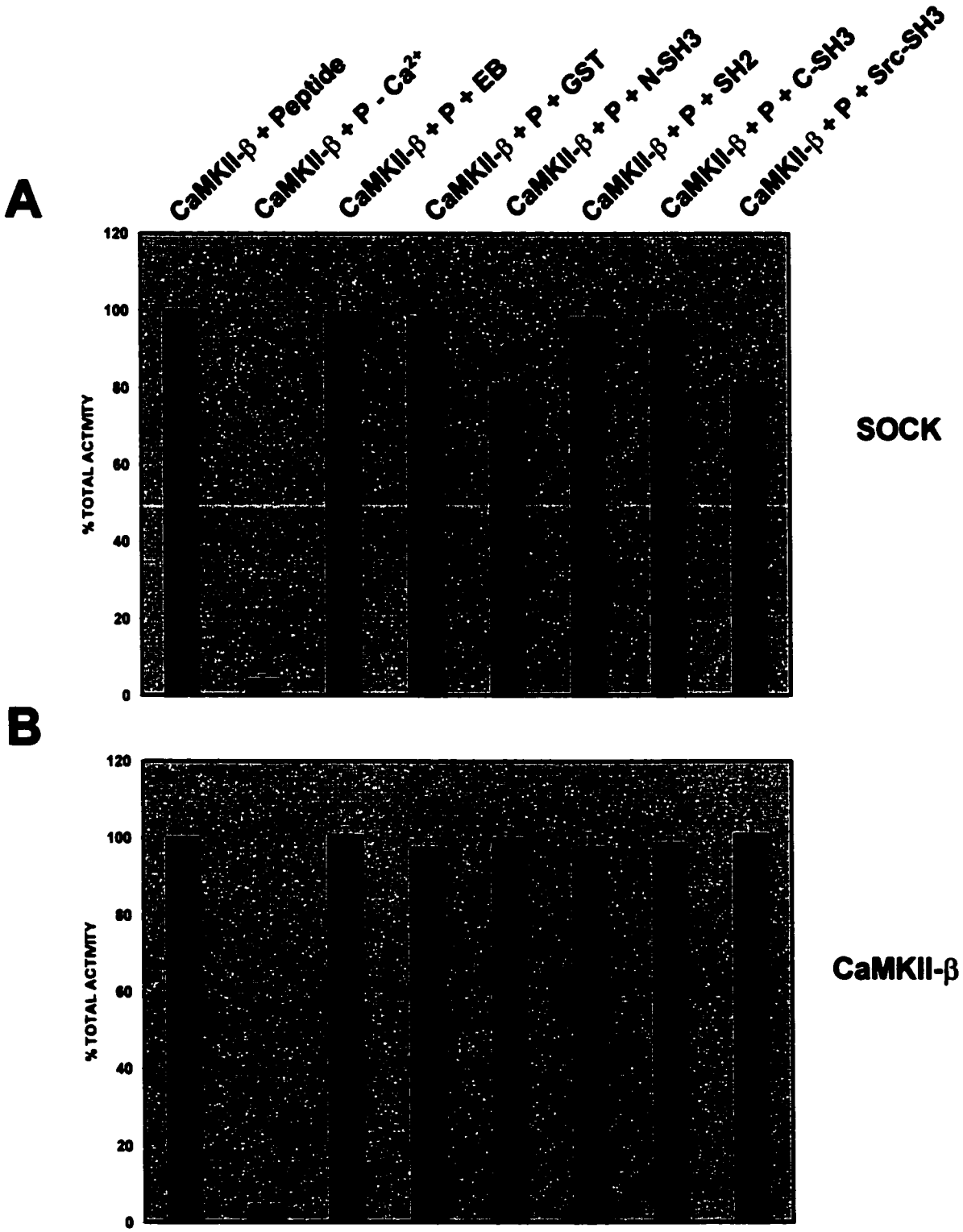
A
CaMKII-β + Peptide
CaMKII-β + P - Ca2+
CaMKII-β + P + EB
CaMKII-β + P + GST
CaMKII-β + P + N-SH3
CaMKII-β + P + SH2
CaMKII-β + P + C-SH3
CaMKII-β + P + Src-SH3
% TOTAL ACTIVITY
120
100
80
60
40
20
0
SOCK
B
% TOTAL ACTIVITY
120
100
80
60
40
20
0
CaMKII-β

3.12 Production and Purification of a SOCK Specific Antibody

The production of a SOCK specific antibody was undertaken in order to generate a useful molecular tool for Western blots, immunohistochemical staining, immunoprecipitations and immunopurification of SOCK. A synthetic peptide was used to immunize rabbits and generate anti-SOCK anti-sera. The sequence of the synthetic peptide immunogen NSVRRGSGTPEAE occurs twice in SOCK, once in the sequences encoded by exon P2 and once in exon P3.

Western blots with anti-sera collected at different times after initial immunization and booster immunizations were tested for immunoreactivity with affinity purified GST fusion proteins consisting of GST, GST-Q2A, GST-P1, GST-P2, GST-P3, GST-SOCK and GST-CaMKII-β and were compared to the reactivity of pre-immune serum (Figure 3.17). In all Western blots, the serum was used at a 1:500 dilution in TBS-Tween 20 with 5% skim milk powder. The pre-immune serum of both 1931 and 1932 detected a 65 kDa polypeptide in the GST-SOCK (lane 6) and GST-CaM Kinase II β (lane 7) samples and represents non-specific immunoreactivity. Anti-serum from the first bleed from rabbit 1931 primarily detected polypeptides of 39, 29 and 32 kDa corresponding to GST-Q2A (lane 2), GST-P2 (lane 4) and GST-P3 (lane 5) and weakly detected a 99 kDa polypeptide corresponding to GST-SOCK (lane 6). Anti-serum from the first bleed from rabbit 1932 did not detect any proteins in the Western blot. The second and third bleeds from rabbit 1931 displayed the same pattern of reactivity as in bleed one but bleed two possessed the greatest immunoreactivity of all the bleeds from 1931 tested. The second bleed from rabbit 1932 primarily detected polypeptides of 39, 29 and 32 kDa corresponding to GST-Q2A (lane 2), GST-P2 (lane 4) and GST-P3 (lane 5) and weakly detected a 99 kDa polypeptide

corresponding to GST-SOCK (lane 6). The third bleed from rabbit 1932 had the same pattern of immunoreactivity as the second bleed and possessed the greatest immonoreactivity of all the bleeds from 1932 tested. Immunoreactivity with GST, GST-P1 or GST-CaM Kinase II β was not detected with any of the bleeds.

Affinity purified anti-SOCK was tested for specific immunoreactivity with affinity purified fusion proteins consisting of GST, GST-Q2A, GST-P1, GST-P2, GST-P3, GST-SOCK and GST-CaMKII-β in Western blots (Figure 3.18). The affinity purified anti-SOCK antibody reacted specifically with GST-P2 (lane 4) and GST-P3 (lane 5) as well as with GST-SOCK (lane 6) and GST-Q2A (lane 2), with no observable reactivity with GST (lane 1), GST-P1 (lane 3) or GST-CaMKII β (lane 7).

The anti-SOCK antibody was tested in Western blots and immunohistochemistry to detect wild-type SOCK in skeletal muscle as compared to the reactivity of RU16. Anti-SOCK detected GST-SOCK (lane 7) but failed to detect a 73 kDa polypeptide in any of the membrane fractions (lane 1-3) or crude microsomes (lane 6) (Figure 3.19 A). Western blots performed with RU16 detected GST-SOCK (lane 7) and detected the three polypeptides of 73, 58 and 56 kDa corresponding to SOCK, CaM Kinase II γ and δ in the membrane fractions (lanes 1-3) and crude microsomes (lane 6) (Figure 3.19 B). In Western blots with GST-SOCK and SOCK from heavy SR, anti-SOCK detected recombinant SOCK (lane 1) and weakly immunoreacted with a 73 kDa polypeptide in the heavy SR sample (lane 2) at long exposure times (Figure 3.19 C).

Figure 3.17 **Testing of Pre-immunized and Immunized Anti-Serum from Rabbits Injected with a SOCK Specific Peptide Antigen**

Two rabbits designated 1931 and 1932 were injected with a peptide antigen corresponding to 13 amino acids (NSVRRGSGTPEAE) expressed within the second and third proline rich repeat in SOCK. Western blots were performed with the pre-immune serum and immunized serum collected at different time points after booster immunizations at a dilution of 1:500 in TBS-Tween 20 with 5% skim milk powder added. The anti-serum was tested for immunoreactivity with fusion proteins corresponding to GST (lane 1), GST-Q2A (lane 2), GST-P1 (lane 3), GST-P2 (lane 4), GST-P3 (lane 5), GST-SOCK (lane 6) and GST-CaMKII β (lane 7). The pre-immune serum from both rabbits detected a polypeptide of 65 kDa in lane 6 and 7 and represents non-specific immunoreactivity. The first bleed from rabbit 1931 detected GST-Q2A, GST-P2, GST-P3 and weakly detected SOCK. GST, GST-P1 and GST-CaMKII β were not detected by bleed 1 of 1931. Bleed one from rabbit 1932 did not detect any proteins. Bleed 2 of 1931 had the highest titer of all the bleeds from this rabbit and exhibited the same immunoreactivity as in bleed one. Bleed 2 of 1932 detected GST-Q2A, GST-P2, GST-P3 and GST-SOCK but did not detect GST, GST-P1 or GST-CaMKII β. Bleed 3 of 1931 detected the same proteins as Bleed 1 and Bleed 2 but the immunoreactivity was less than that observed in bleed 2. Bleed 3 of 1932 had the highest titer of anti-SOCK antibodies in this rabbit and detected the same proteins as in Bleed 2.

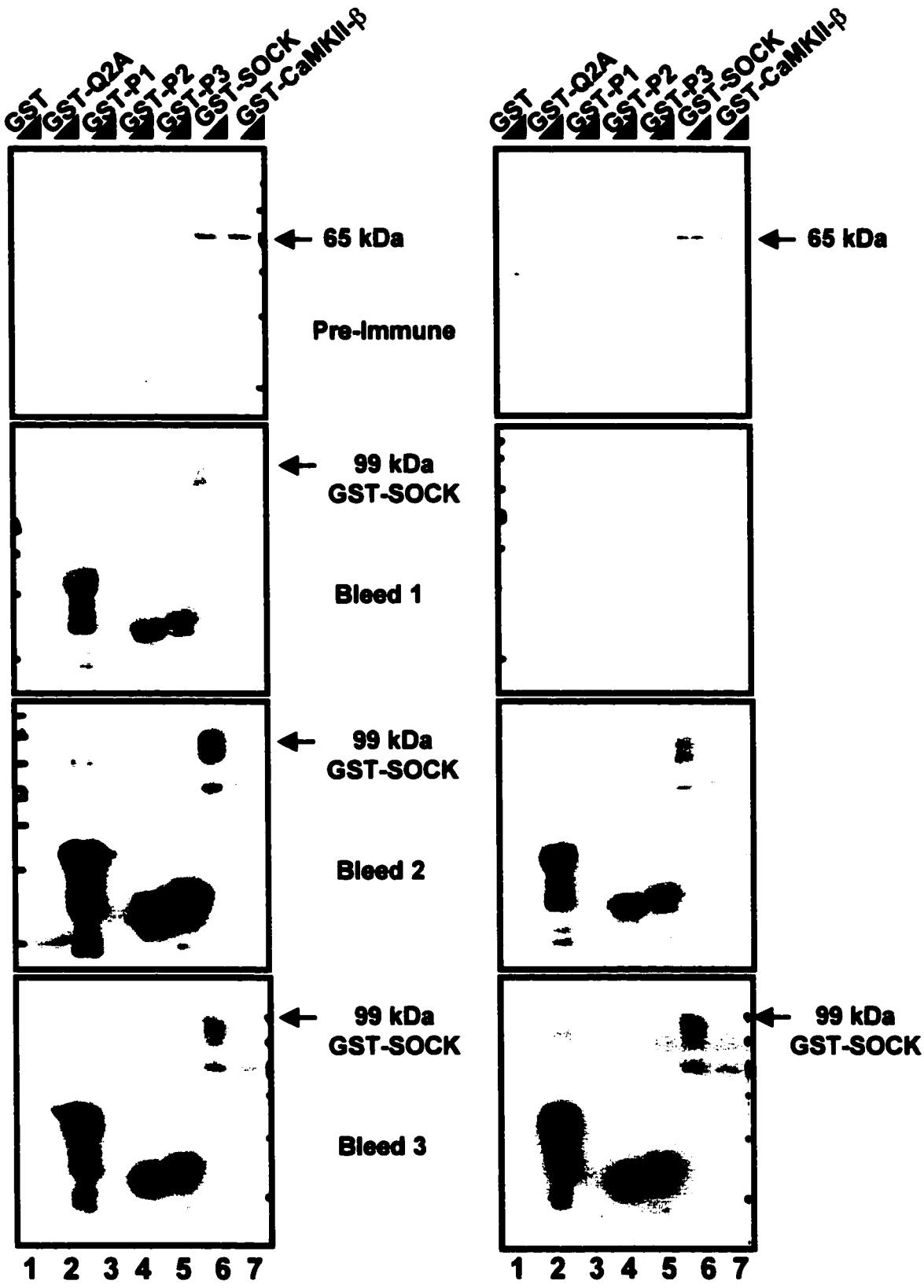
Rabbit 1931
Rabbit 1932
GST
GST-Q2A
GST-P1
GST-P2
GST-P3
GST-SOCK
GST-CaMKII-β
65 kDa
Pre-Immune
99 kDa
GST-SOCK
Bleed 1
99 kDa
GST-SOCK
Bleed 2
99 kDa
GST-SOCK
Bleed 3
1 2 3 4 5 6 7

Figure 3.18 **Testing the Immunoreactivity of Affinity Purified Anti-SOCK on Recombinant Proteins**

Anti-sera from rabbits designated 1931 and 1932 that were tested for specific immunoreactivity with sequences in the proline rich insert in SOCK were affinity purified on an agarose column coupled with GST-P2 and P3 as well as peptide corresponding to the immunogen. The immunoreactivity of the affinity purified anti-SOCK antibody was found to react specifically with the antigenic sequences in GST-P2 (lane 4) and GST-P3 (lane 5) (corresponding to exons P2 and P3 in SOCK) as well as with full length GST-SOCK (lane 6) and GST-Q2A (lane 2). No immunoreactivity was detected against GST (lane 1), GST-P1 (lane 3) corresponding to exon P1 in SOCK, and GST-CaMKII β (lane 7).

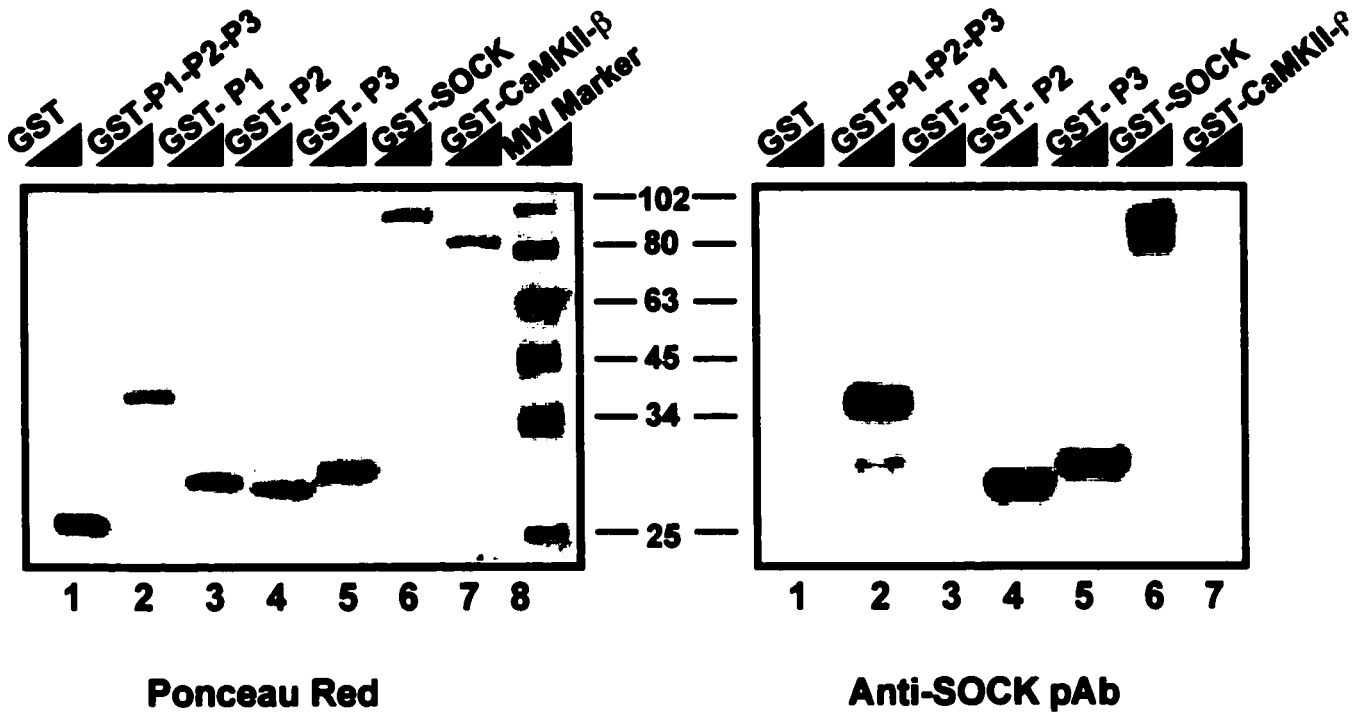
GST
GST-P1-P2-P3
GST- P1
GST- P2
GST- P3
GST-SOCK
GST-CaMKII-β
MW Marker
102
80
63
45
34
25
1 2 3 4 5 6 7 8
Ponceau Red
GST
GST-P1-P2-P3
GST- P1
GST- P2
GST- P3
GST-SOCK
GST-CaMKII-β
1 2 3 4 5 6 7
Anti-SOCK pAb

Figure 3.19 Immunoreactivity of Affinity Purified Anti-SOCK with SOCK from Skeletal Muscle in Western Blots and Immunohistochemistry

Anti-SOCK was tested in immunoblots with samples of skeletal muscle membrane fractions along with GST-SOCK (A). Western blot analysis was also performed for comparative purposes with the polyclonal anti-CaM Kinase II (detects α, β, γ and δ isoforms) RU16 (B). Anti-SOCK detected recombinant GST-SOCK but did not exhibit immunoreactivity with SOCK from skeletal muscle membrane fractions (lanes 1-4). RU16 immunoreacted with recombinant GST-SOCK and detected three proteins in the membrane fractions corresponding to SOCK (73 kDa), CaMKII γ (58 kDa) and CaMKII δ (56 kDa). When the exposure time on a Western blot with anti-SOCK was increased, detection of a 73 kDa protein corresponding to SOCK as well as a 96 kDa polypeptide was detected in skeletal muscle membrane fraction 4 (enriched terminal cisternae) (C). The affinity purified anti-SOCK antibody was tested in immunohistochemical staining of skeletal muscle sections. Anti-SOCK failed to produce a discernable signal when used in immunohistochemistry (D).

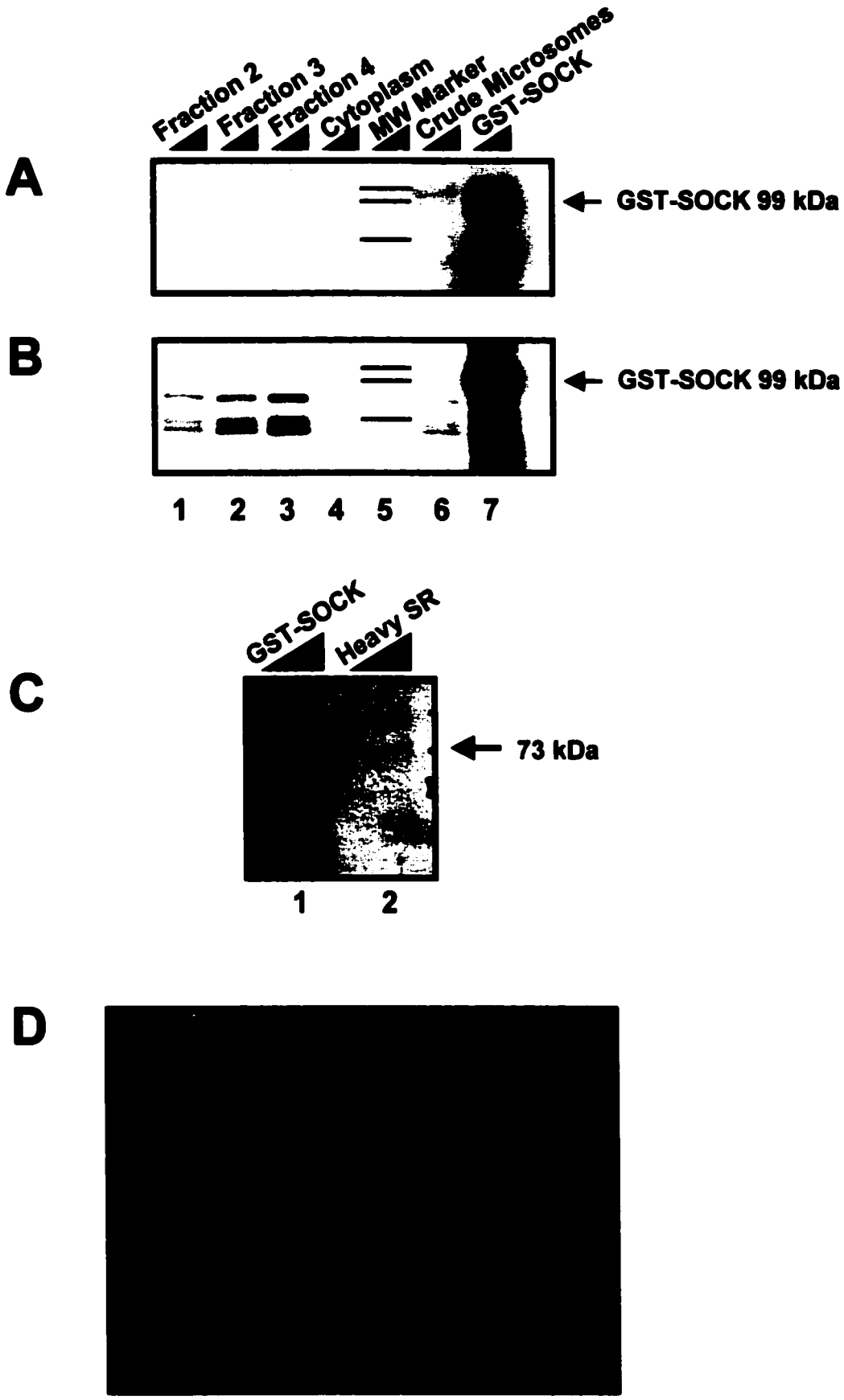
A
Fraction 2
Fraction 3
Fraction 4
Cytoplasm
MW Marker
Crude Microsomes
GST-SOCK
GST-SOCK 99 kDa
B
GST-SOCK 99 kDa
1 2 3 4 5 6 7
C
GST-SOCK
Heavy SR
73 kDa
1 2
D

4 Discussion

Calcium plays a crucial role in muscle contraction because it is the physiological regulator of this process. Both positive and negative feedback is observed in the DHPR and RyR in response to the initial increase in cytosolic Ca^{2+} that facilitates the release of more Ca^{2+}. This facilitation ensures that Ca^{2+} levels rise until contraction can occur, after which point, the channels are inhibited when cytosolic Ca^{2+} concentration is relatively high (0.15 mM) compared to that observed in resting muscle (0.1 μM). Ca^{2+} is also involved in other signaling cascades with a multitude of effects such as secretion, carbohydrate metabolism, cell cycle progression and gene expression (Means and Dedman, 1980). An intracellular protein important for Ca^{2+} signaling is calmodulin (CaM), which binds to and is activated by elevated cytoplasmic levels of Ca^{2+}. Ca^{2+} bound CaM can activate a number of downstream signaling effectors, including the Ca^{2+}/CaM-dependent protein kinase family, that are known to phosphorylate proteins on specific serine and/or threonine residues (Schulman, 1993).

The potential involvement of Ca^{2+}/CaM-dependent protein kinases in E-C coupling, mediated by a phosphorylation event, may be a mechanism for modifying the function of the DHPR and RyR in response to elevated cytosolic Ca^{2+} levels. We demonstrated that recombinant SOCK phosphorylated immunoprecipitated RyR1, DHPR α_{1S} and DHPR β_{1A} subunits and that endogenous CaM Kinase II was able to phosphorylate the DHPR β_{1A} subunit and DHPR α_{1S} to a lesser extent in kinase assays performed with purified triads. There is also evidence of Ca^{2+}/CaM-dependent phosphorylation of these receptors and/or accessory proteins that requires an ATP source

in addition to the presence of Ca^{2+}/CaM but the endogenously expressed CaM Kinase II isoform in muscle responsible for this remains to be defined (Dzhura et al., 1999; Wang and Best, 1992).

Previous studies have indicated that Ca^{2+}/CaM-dependent kinase activity was detected in isolated SR membranes of skeletal and cardiac muscle. In support of this, others have demonstrated that a polypeptide associated with the SR exhibits Ca^{2+}/CaM-dependent autophosphorylation in renaturation autophosphorylation assays, however, the exact isoform was not determined (Leddy et al., 1993). Work in this laboratory led to the cloning of a cDNA encoding for a CaM Kinase II isoform from human skeletal muscle cDNA libraries. This isoform exhibited high homology with CaM Kinase II β found in the brain but was found to contain three alternatively spliced exons in the variable domain, accounting for the differences between these two kinases (Leddy, 1999). On a functional level, the CaM Kinase in the SR has been implicated in the regulation of E-C coupling, presumably via phosphorylation of key regulators of intracellular Ca^{2+} levels such as the DHPR and RyR (Anderson et al., 1998, Dzhura et al., 2000, Hain et al., 1995, Wang and Best, 1992). Some have demonstrated phosphorylation of the RyR1 with exogenous sources of CaM Kinase II but this does not reflect the substrate specificity of the endogenously expressed isoform/s, as they were not used in these experiments (Hain et al., 1994 and 1995). CaM Kinase II is also thought to be involved in the facilitation of the inward Ca^{2+} current through the L-type Ca^{2+} channel. This effect was demonstrated with a recombinant CaM Kinase II α isoform engineered to be constitutively active and is thought to be mediated by a phosphorylation event, due to the requirement of ATP (Dzhura et al., 1999). The CaM Kinase II substrate that assists in

facilitation of the L-type Ca^{2+} channel was not determined. Further experiments designed to determine the identity of the CaM Kinase II isoform as well as the specific targets may provide new information into the regulation of E-C coupling through Ca^{2+}/CaM dependent activation of CaM Kinase II.

The initial characterization of the CaM Kinase II β in skeletal muscle involved the determination of its subcellular localization in relation to the RyR, a well-characterized marker of terminal cisternae of the sarcoplasmic reticulum (MacLennan et al., 1997). Skeletal muscle membrane fractionation experiments were performed, yielding five membrane fractions consisting of specific membrane systems such as sarcoplasmic reticulum, plasma membrane and mitochondrial membranes. The protein profile of each fraction were determined from the distribution profile of characteristic markers for each type of membrane, including the RyR of SR, DHPR of T-tubules, adenylate cyclase of sarcolemma, cytochrome c reductase in mitochondrial membranes (Chu et al., 1988; Saito et al., 1984).

Western blot analysis was performed on the subcellular membrane fractions of skeletal muscle to determine the distribution of CaM Kinase II isoforms as compared to that of RyR1. Similar distribution profiles were observed with the three different CaM Kinase II antibodies as well as with anti-RyR1, with maximal immunoreactivity in fractions enriched in terminal cisternae of the SR. The pattern of reactivity of anti-RyR is assumed to represent the distribution of proteins located solely in the terminal junctional cisternae of skeletal muscle. The CaM Kinase II β isoform in muscle was found to consist solely of a 73 kDa polypeptide corresponding to SOCK (Son Of CaM Kinase II) when using the CaM Kinase II β specific antibody, Cbβ-1. Identification of a

60 kDa polypeptide corresponding to brain CaM Kinase II-β isoform has been observed in purified SR vesicles (Campbell and MacLennan, 1982; Damiani et al., 1995; MacLennan and Tuana, 1984). The observation of a 60 kDa CaM Kinase II polypeptide may have been due to proteolytic degradation of the 73 kDa kinase into a 60 kDa degradation product, but the inclusion of a direct comparison of brain versus muscle CaMKII isoforms was not demonstrated in these studies. A 60 kDa polypeptide corresponding to the brain CaM Kinase II-β was not detected in Western blot analysis with Cbβ-1 in any of the skeletal muscle samples and was only observed in the brain homogenate. In order to further demonstrate the differences in apparent molecular weights of the CaM Kinase II β isoforms of brain and skeletal muscle, the kinases were affinity purified on calmodulin sepharose from brain cytosol and detergent solubilized skeletal muscle SR membranes. This purification and Western blot analysis was performed in order to enrich CaM Kinase II of skeletal muscle that is not as abundant as in the brain as well as to be certain that the observed differences in migration through the polyacrylamide SDS gel are due to actual differences in molecular weights and not due to aggregation of membranes or non-specific associations of the CaM Kinase complexes (as presented in the context of whole brain homogenate versus purified muscle membrane vesicles). Non-specific interactions have been found to alter protein mobility on SDS polyacrylamide gels (Yuan et al., 1999). Western blot analysis on the purified CaM complexes was performed to probe for the presence of CaM Kinase II β isoforms and it was found that a 60/58 kDa doublet corresponding to CaM Kinase II β and β' was present only in the brain sample and a 73 kDa polypeptide corresponding to SOCK was only observed in SR membrane samples and affinity purified sample from muscle.

My studies indicated that an anti-CaM Kinase II α specific antibody did not detect a 54 kDa band corresponding to CaM Kinase II α, suggesting that this isoform is not expressed in skeletal muscle. However, the presence of a 25 kDa band, most likely corresponding to the CaM Kinase II anchoring protein αKAP, was observed to cofractionate with the CaM Kinase II isoforms and RyR1. A 54 kDa polypeptide corresponding to CaM Kinase II α was only detected in brain homogenate. The truncated 25 kDa product arises from alternatively splicing of the association domain (from the cDNA encoding CaM Kinase II α) corresponding to αKAP and includes a unique 12 amino acid sequence at the N-terminus that is highly hydrophobic and thought to integrate this protein in the SR (Bayer et al., 1996). Since it contains an association domain of CaM Kinase II, it presumably interacts with CaM Kinase II isoforms much in the same way CaM Kinase II isoforms form a holoenzyme complex (protein-protein interaction with association domains of adjacent kinases). In support of this, Bayer et al. (1998) demonstrated that membrane association of CaM Kinase II isoforms can only occur if both αKAP and CaM Kinase II isoforms (α, β, γ, or δ) are co-expressed (co-transfected) in COS-7 cells. When CaM Kinase II isoforms were transfected without αKAP, Western blot analysis indicated that all CaM Kinase II isoforms were detected primarily in the cytosol (Bayer et al., 1998).

The detection of two other CaM Kinase II isoforms, CaMKII-γ (56 kDa) and δ (58 kDa), were observed along with SOCK (73 kDa) when using a broad CaM Kinase II antibody RU16 that immunoreacts with a conserved sequence found in all CaM Kinase II isoforms. These CaM Kinase II isoforms have been previously characterized in skeletal muscle and are ubiquitously expressed in all tissues (Bayer et al., 1998,

Schulman, 1993). All three CaM Kinase II isoforms detected with RU16 possessed the same distribution profile in the membrane fractions.

Colocalization of SOCK with RyR1 was also demonstrated in double immunohistochemical staining of skeletal muscle sections and these data suggest that they colocalize to the terminal cisternae of the SR. The immunohistochemical pattern of localization of SOCK and RyR1 in my study was similar to that observed for αKAP by Bayer et al., 1996 and suggests that SOCK may be targeted to the terminal cisternae by associating with αKAP.

These results are consistent with the observation of others that CaM Kinase II associates with the SR and is comprised of CaM Kinase II-β (SOCK), γ and δ. These data also support the notion of CaM Kinase II recruitment to the SR via associations with αKAP since the kinases and the anchoring protein had the same distribution profiles in Western blots. The co-localization of SOCK with RyR1 in double immunohistochemical staining of skeletal muscle sections indicates that these proteins co-localize to the terminal cisternae. Targeting of CaM Kinase II isoforms to the terminal cisternae via association with αKAP would be an important facilitator of substrate phosphorylation as it ensures that the targeted substrates are readily accessible for phosphorylation by CaM Kinase II. The kinase-targeting hypothesis is based on the premise that kinases can be targeted to specific membrane systems due to interactions with anchoring proteins (Pawson and Scott, 1997; Pawson, 1994). The targeting of kinases allows for a quick transition between the initial signaling event and effector response, namely phosphorylation of nearby substrates. This phenomenon is observed with PKA and PKC mediated regulation of E-C coupling via the targeting of these

kinases to the T-Tubules and/or SR by binding to membrane bound anchoring proteins AKAP and RACK, respectively (Johnson et al., 1994; Huang et al., 1997). Phosphorylation of the DHPR and RyR by PKA and PKC has been observed in both skeletal and cardiac muscle, which resulted in facilitation of Ca^{2+} entry and Ca^{2+} release, respectively and demonstrates phosphorylation-mediated regulation of E-C coupling (Suko et al, 1993 ; Bunemann et al., 1999; Puri et al.,1997. Phosphorylation of these receptors in the SR is facilitated by the accessibility of the kinases to the substrate. In light of this, the targeting of SOCK to the terminal cisternae of SR by binding to αKAP may serve a similar purpose, namely, the phosphorylation of proteins involved in the regulation of cytosolic Ca^{2+} such as DHPR and RyR or some accessory proteins. Phosphorylation of a target substrate in the SR or T-tubules may potentially result in either the facilitation or inhibition of E-C coupling.

The generation of a SOCK-specific antibody was pursued to provide a specific tool that would be useful in experiments such as Western blots, immunohistochemical staining as well as in affinity purification of SOCK from heavy SR membranes. The anti-SOCK polyclonal antibody was produced in rabbits in response to an antigenic peptide composed of a sequence that occurs twice in the proline rich sequences encoded by exon P2 and P3 of SOCK. Affinity purified anti-SOCK was effective in the specific detection of GST-SOCK compared to GST-CaM Kinase II β and specifically recognized amino acid sequences encoded by exon P2 and P3 as expected. No reactivity was observed when GST was expressed alone. However, the detection of wild-type SOCK in heavy SR samples was very weak and detected only with long exposure times. The weak level of detection may be due to; a) the conformation of the epitope not allowing for

antibody recognition when presented in the context of a mammalian protein modified post translationally, b) the peptide containing a consensus sequence for PKA phosphorylation that if phosphorylated would not allow for antibody recognition, and c) the peptide containing a consensus sequence for myrostylation.

In order to study the substrate specificity of SOCK with *in vitro* substrate phosphorylation assays, a suitable source of pure SOCK was required. Purification of SOCK from solubilized heavy SR on a CaM column would not satisfy this requirement, as there are two other CaM Kinase II isoforms present in skeletal muscle as well as other CaM binding proteins. Instead, the cDNA encoding SOCK was ligated into a GST fusion protein expression vector for use in the expression and purification of recombinant GST-SOCK from *E. coli.* Initial expression experiments using BL21 *E. coli* resulted in the purification of proteins of many sizes as detected in Western blots with anti-GST antibodies.

Expression and purification of GST-SOCK and GST-CaM Kinase II β in CodonPlus® RP bacteria resulted in the efficient purification of substantial yields of primarily full-length recombinant kinases. The expression and purification of full-length recombinant kinase is important to ensure the proper functioning of these polypeptides as enzymes. A premature translational stop in the autoregulatory domain may result in a polypeptide that may not exhibit proper autoregulation and may not activate in the presence of calcium and calmodulin, or may function independently of their presence.

Recombinant GST-SOCK and GST-CaM Kinase II β were found to exhibit Ca^{2+}/CaM-dependent kinase activity since they phosphorylated a CaM Kinase II specific substrate peptide, Auto Camtide II. Minimal levels of phosphorylation were observed in

the absence of Ca^{2+}. GST-SOCK activity was slightly higher than that of GST-CaM Kinase II β. A plausible explanation for this result may be due to increased accessibility of substrates to the catalytic domain in SOCK caused by a different three-dimensional structure attributable to the proline-rich insert.

Recombinant SOCK was found to phosphorylate immunoprecipitated RyR1, DHPR-α_1 and DHPR-β_1 subunits in a Ca^{2+}/CaM-dependent manner. A comparison of the substrate specificity of endogenous CaM Kinases to the substrate specificity of recombinant SOCK was assessed by incubating triads in conditions suitable for CaM Kinase phosphorylation, followed by immunoprecipitation of the RyR1, DHPR-α_1 and DHPR-β_1 subunits from solubilized samples. Phosphopeptides of 560 kDa, 185 kDa and 56/52 kDa corresponding to immunoprecipitated RyR1, DHPR-α_1 and DHPR-β_1 subunits, respectively, were phosphorylated in a Ca^{2+}/CaM dependent manner by recombinant SOCK. In comparison, phosphopeptides of 185 kDa and 56/52 kDa corresponding to DHPR-α_{1S} and DHPR-β_{1A} subunits, respectively, were phosphorylated in a Ca^{2+}/CaM-dependent manner presumably by the endogenous CaM Kinase II isoforms in the triads. The absence of detectable γ-^{32}P incorporation into RyR1 when probing for endogenous CaM Kinase II substrates indicates that the R-X-X-S/T phosphorylation site in RyR1 may not be a suitable substrate for CaM Kinase II associated with the SR. The immunoprecipitated proteins incorporated minimal amounts of γ-^{32}P in the absence of Ca^{2+}.

In support of our finding of RyR1 phosphorylation by an exogenous source of CaM Kinase II, RyR1 purified from detergent solubilized heavy SR was shown to be phosphorylated by exogenously added CaM Kinase II at Ser 2843 (Suko et al., 1993).

PKA was also shown to phosphorylate RyR1 in this study at the same serine residue. Our data suggests that RyR1 may be a potential substrate for SOCK in skeletal muscle but when comparing the substrate specificity of the endogenous kinases, RyR1 did not incorporate detectable levels of γ-^{32}P. A possible reason why RyR1 was not phosphorylated by the endogenous CaM Kinases may be that the RyR1 in triads are in the form of a homotetramer as compared to immunoprecipitated RyR1 monomers that may expose R-X-X-S/T sites that are not exposed under physiological conditions. Another reason may be due to the association of endogenous CaM Kinase II isoforms with αKAP, by not allowing the kinase to make contact with and phosphorylate the substrate sequence *in vivo*. When phosphorylation of RyR1 was observed with the addition of recombinant SOCK, it is important to note that the conformation of RyR1 may have been more extended (linear) due to the presence of detergent and sucrose, to prevent aggregation of the monomeric receptors. The accessibility of recombinant SOCK to the substrate sequences was also not inhibited due to fixed localization as a result of interactions with its anchoring protein αKAP. Taking these differences into account, the absence of detectable phosphorylation of RyR1 by endogenous CaM Kinases in triads, which maintain a greater level of natural protein conformation and kinase association suggests that the RyR is not likely to be an endogenous substrate of CaM Kinase *in vivo*.

In light of the evidence that demonstrates a dual mode of regulation of RyR1 channel activity by CaM Kinase II, the molecular basis of these effects may be more diverse then originally hypothesized. The effect of adding CaM Kinase II to purified RyR1 or heavy SR microsomes, leads to activation of Ca^{2+} release through the channel

as a direct result of phosphorylating RyR1 at Ser 2843 (Hain et al., 1995; Suko et al., 1993). A more physiological approach in investigating CaM Kinase II regulation of Ca^{2+} release through the RyR1 was focused on the effect of endogenous CaM Kinase II activity, which is tightly associated with the heavy SR. Studies by Wang and Best (1992) and Hain et al. (1994) demonstrated that activation of endogenous CaM Kinase II isoforms in SR resulted in a decrease in Ca^{2+} release which was ablated when incubating the skeletal muscle SR membranes with a CaM Kinase inhibitor (a.a 273-302 of CaM Kinase II, pseudosubstrate) or phosphatase. The phosphorylation of the RyR1 by the endogenous CaM Kinase II was never demonstrated. However, Witcher et al. (1991) and Damiani et al. (1995) investigated endogenous CaM activity and concluded that endogenous CaM Kinase II in skeletal muscle does not phosphorylate the RyR1. Taken together, these data indicate that endogenous CaM Kinase II activity may influence the release of Ca^{2+} through the RyR, possibly via phosphorylation of a nearby protein that inhibits RyR in some way. This may explain why the phosphorylation assays in our study of endogenous CaM Kinase II substrates did not result in phosphorylation of RyR1. In support of this notion, endogenous CaM Kinase II of skeletal muscle has been shown to phosphorylate triadin, presumably altering its association with the RyR1 and negatively regulating channel gating properties (Damiani et al., 1995).

Phosphorylation of the DHPR by CaM Kinase II is a recent observation based on evidence with an engineered recombinant CaM Kinase II α isoform. The kinase activity of CaM Kinase II α was made independent of Ca^{2+}/CaM by thiophosphorylation of Thr 286 (autophosphorylated under normal circumstances upon activation by Ca^{2+}/CaM), generating a constitutively active form of the kinase since phosphatases are unable to

remove thiophosphate from the kinase (Dzhura et al., 2000). The Ca^{2+}/CaM-independent activity of this kinase allowed the use Ba^{2+} instead of Ca^{2+} as the charge carrier since it improves the resolution of single channel recording. Since Ba^{2+} cannot form complexes with CaM, this also allowed determination of the facilitation of the I_{Ca} as modified by the presence of a constitutively active CaM Kinase alone and not due to Ca^{2+}/CaM mediated regulation. L-type Ca^{2+} channels treated with this kinase exhibited reconstitution of I_{Ca} facilitation presumably via phosphorylation since the presence of ATP was required and the addition of the non-hydrolysable ATP analogue AMP-PNP inhibited the facilitation (Dzhura et al., 2000). The direct phosphorylation and identification of the specific subunit of the DHPR in the study by Dzhura et al. was not clearly demonstrated. Although these experiments were performed in cardiac muscle the DHPR α_{1S} and β_{1a} sub-units in skeletal muscle have R-X-X-S/T consensus CaM Kinase II phosphorylation sites that if phosphorylated may alter the activity of the channel in a similar fashion. When considering this, it is reasonable to expect that SOCK can potentially phosphorylate the DHPR in skeletal muscle on the DHPR α_{1S} and β_{1A} sub-units. We demonstrated that recombinant SOCK phosphorylated both the DHPR α_{1S} and β_{1A} subunits in a Ca^{2+}/CaM-dependent manner and the phosphorylation of the DHPR α_{1S} was much less in the endogenous CaM Kinase assay as compared to that of the DHPR β_{1A}.

The Ca^{2+}/CaM dependent regulation of the DHPR as examined by Dzhura et al. (2000) has provided new insight into the mechanism of activation of the channel through facilitation of I_{Ca}. They demonstrated that a constitutively active CaM Kinase II α could activate I_{Ca} and that this effect was independent of the presence of Ca^{2+} and CaM. This

implies that facilitation of I_{Ca}, previously shown by others to be Ca^{2+}/CaM-dependent, may require the phosphorylation by endogenous CaM Kinase II of an unknown protein and it may not be due to the binding of Ca^{2+} and/or CaM on EF hand or IQ motifs of the DHPR α_1 subunit, respectively. They did not demonstrate the direct phosphorylation of the DHPR but demonstrated that ATP hydrolysis was required as determined by the abolishment of I_{Ca} when non-hydrolysable ATP analogue, AMP-PNP was used. Although this study focused on I_{Ca} in cardiac muscle (activated by CICR), the direct coupling mechanism in skeletal muscle DHPR and RyR responsible for E-C coupling exhibits similar Ca^{2+}/CaM-dependence, which may be the result of activating CaM Kinase II and subsequent phosphorylation of Ca^{2+} channel proteins. Our results demonstrate that recombinant SOCK is able to phosphorylate both the DHPR α_{1S} and β_{1A} sub-units and that endogenous CaM Kinase II phosphorylated the DHPR β_{1A} sub-unit primarily in purified skeletal muscle triads. It is also known that the presence of the β sub-unit is required for proper targeting and channel function of the DHPR in skeletal muscle. Phosphorylation of the cardiac DHPR β subunit by PKA has been found to facilitate the activation of the L-type Ca^{2+} channel current (Bunemann et al., 1999). Mutation of Ser_{459} abolished the PKA induced increase of L-type currents. Therefore, it is possible that CaM Kinase II would be able to regulate E-C coupling by a similar mechanism, via direct phosphorylation of the DHPR β subunit at the consensus CaM Kinase II phosphorylation site (Ser_{205}).

The three new alternatively spliced exons in the variable domain of SOCK encode for 123 amino acids, 25% of which are prolines indicating that this sequence is disproportionaly rich in proline compared to the rest of the polypeptide sequence (4%

proline). Proline-rich regions have been characterized and shown to interact with Src homology 3 (SH3) domains, an important modular domain involved in tyrosine kinase signaling cascades (Pawson, 1995). There are three P-X-X-P sequences encoded by each exon P1 and P3. Amino acids near the P-X-X-P region confer specificity of interaction with specific SH3 domains and contribute to the overall organization into polyproline type II helices. The P-X-X-P motif encoded by exon P3 of SOCK was found to share homology with Class II proline sequences that is found to bind to the SH3 domains of Src tyrosine kinase and the adapter protein Grb2. The Class II ligands of SH3 domains have an arginine residue C-terminally of the P-X-X-P sequence that dictates the orientation of the interacting proteins, as well as stabilizes the association by formation of a salt bridge (Pawson, 1995). The association of SOCK with SH3 domains via its proline-rich region was confirmed with endogenous immunoprecipitations and demonstrates that endogenous SOCK specifically interacts with Src and Grb2 in skeletal muscle. Furthermore, the SH3 domain of Src and N-terminal SH3 domain of Grb2 were found to bind to the proline rich regions encoded by exon P1 and exon P3 in *in vitro* overlay experiments.

The SH3-proline interaction can target tyrosine kinases like Src to specific membrane systems. This is demonstrated with the proline-rich sequences in FAK (focal adhesion kinase), shown to target Src to focal adhesions at the plasma membrane (Thomas et al., 1998). Activation of FAK at focal adhesions causes phosphorylation on Tyr, associating with the SH2 domain of Src (high affinity phosphotyrosine binding site), which activates the kinase and downstream signaling events. Mutation of the proline rich region of FAK inhibits this recruitment and does not result in the activation

of Src, indicating that the SH3-proline motif interaction is important for the initial targeting which is required before activation of the Src signaling cascade can ensue (Thomas et al., 1998). A similar mechanism of targeting and activating Src exists with another protein called AFAP-110 (actin filament associating protein) that also binds to the SH3 domain of Src via proline rich sequences and targets Src to actin filaments (Guappone and Flynn, 1997). They determined that abrogation of the Src-AFAP 110 interaction *in vivo* (in transfected Cos-1 cells) via point mutations in the proline rich motif in AFAP, decreased tyrosine phosphorylation on the SH2 binding sites of AFAP and inhibited activation of Src. It is possible that SOCK may target Src to the terminal cisternae via the proline rich-SH3 interaction, at which point, Src is activated by some other protein. There is a putative consensus Y-E-E-I tyrosine kinase phosphorylation site at the N-terminus of SOCK, which if phosphorylated may serve in activating Src in the SR. This putative tyrosine kinase phosphorylation site is present in brain CaM Kinase II β isoform but this site has not been found to be phosphorylated on tyrosine as of yet.

Investigation into the specific sequence in SOCK responsible for the interaction with SH3 domains was not resolved with point mutations in the P-X-X-P motif encoded by exon P3. The possibility that more than one interaction of Src and Grb2 can occur by binding to more than one of the P-X-X-P sites of SOCK was demonstrated in overlay experiments. The SH3 domain of Src and the N terminus SH3 domain of Grb2 were found to bind to the sequences encoded by exon P1 and exon P3 when expressed individually and probed for interaction with biotinylated SH3 domains in overlay assays. There is evidence in the literature of proteins having more than one SH3 binding domain. A signaling protein implicated in the regulation of membrane ruffling and

migration, DOCK180, has multiple P-X-X-P sequences. Tu et al. (2001) demonstrated that the adapter protein Nck2 could bind to two different P-X-X-P sequences in the C-terminal region of DOCK180.

Inclusion of the SH3 domains of Grb2 (N-terminal) and Src in phosphorylation assays were found to significantly decrease the activity of recombinant SOCK by approximately 20% as measured by the phosphorylation of a CaM Kinase II specific substrate Auto Camtide II. The same inhibition was not observed with recombinant CaM Kinase II β, indicating that the observed effect is a consequence of the specific interaction of SOCK and the SH3 domains of Src and Grb2. This level of inhibition suggests that SOCK's activity may be modulated by way of interaction with SH3 domains in Src or Grb2 that have been recruited to the SR membrane system via this interaction. Considering the nature of this *in vitro* phosphorylation assay, it is important to note that recombinant SOCK was not anchored to a membrane system by its anchoring protein αKAP (occurring naturally in the SR of skeletal muscle). As a result of this, the recombinant kinase may be more sensitive to conformational changes occurring due to interaction with SH3 domains, possibly causing steric hinderence of the catalytic domain and moderate inhibition of phosphotransferase activity.

The localization of SOCK in close proximity to the RyR1 in skeletal muscle sarcoplasmic reticulum, as a result of its association with the anchoring protein αKAP may serve to modulate E-C coupling. The mechanism of action may involve the direct phosphorylation of the DHPR on the α_{1S} or β_{1A} subunits or possibly the RyR1 under certain conditions. It is also possible that SOCK may phosphorylate near by proteins like triadin and histadine-rich Ca^{2+} binding protein, which have been implicated in the

regulation of Ca^{2+} release from RyR1 (Damiani et al., 1995). The interaction of SOCK with SH3 domains implicates CaM Kinase II as an integrator of Ca^{2+} and tyrosine kinase signaling cascades. SOCK may serve to target proteins with SH3 domains like Src and Grb2 to terminal cisternae of the SR. This may result in activation of kinases like Src or may serve to dock adapter proteins like Grb2 to the terminal junctional cisternae of the SR. The schematic in figure 4.1 outlines some of the putative roles SOCK may have in the SR.

Tyrosine kinases have also been implicated in the regulation of the L-type Ca^{2+} channel function in smooth, skeletal and cardiac muscle as well as in the brain. Treatment of rat cardiac myocytes with insulin stimulated the L-type Ca^{2+} channel (Aulbach et al., 1999). Insulin and insulin like growth factor (IGF-1) activate Src tyrosine kinase, which is an important mediator of intracellular signaling caused by insulin or IGF-1 treatment. Experiments with IGF-1 in neuronal cells demonstrated that active Src is required for stimulation, which phosphorylates the L-type Ca^{2+} channel on Tyr_{2122} of the DHPR-α_{1C} subunit (Bence-Hanulec et al., 2000). In skeletal muscle IGF-1 treatment also enhances the L-type Ca^{2+} channel function but they did not determine if the channel was directly phosphorylated (Wang et al., 1999). DHPR α_{1S} contains a putative tyrosine kinase phosphorylation site Tyr_{1543} that may also serve as a target of Src phosphorylation. When considering these findings, the targeting of Src to the SR by binding to the proline rich region of SOCK, may serve to facilitate the regulation of E-C coupling by Src possibly mediated by phosphorylation of the DHPR α_{1S} subunit.

A putative role for the targeting of Grb2 to the SR by SH3/proline rich interactions with SOCK may involve the Ras pathway, that has been found to be stimulated in

response to the L-type calcium channel current (Misra et al., 1994) . Maranti et al., 1995 showed that increases in cytosolic Ca^{2+} levels were found to activate serum response element (SRE)-dependent transcription and that overexpression of constitutively active CaM Kinase stimulated SRF-dependent transcription. Thus the recruitment of Grb2 to the terminal cisternae via associating with SOCK may serve to localize the signaling event in response to activation of the L-type Ca^{2+} channel.

Figure 4.1 Potential Roles of SOCK in Skeletal Muscle

Recruitment of SOCK to terminal cisternae of heavy SR may facilitate the phosphorylation of nearby receptors such as the RyR1, DHPR β_1 subunit as well as proteins that associate with receptors such as triadin. This may be a potential mode of regulating E-C coupling in response to elevated cytosolic Ca^{2+} levels. The interaction of SOCK with SH3 domains of Src and Grb2 may serve in targeting these proteins to the terminal cisternae and facilitate the propagation of tyrosine kinase or Ras mediated signaling pathways. SOCK could therefore integrate these pathways at the level of SH3-proline rich interactions in the terminal cisternae and mediate cross-talk between these signaling cascades and Ca^{2+}/CaM-dependent signaling in skeletal muscle. This may result in short term changes via the regulation of Ca^{2+} channels during contraction or in long term changes via the regulation of gene expression.

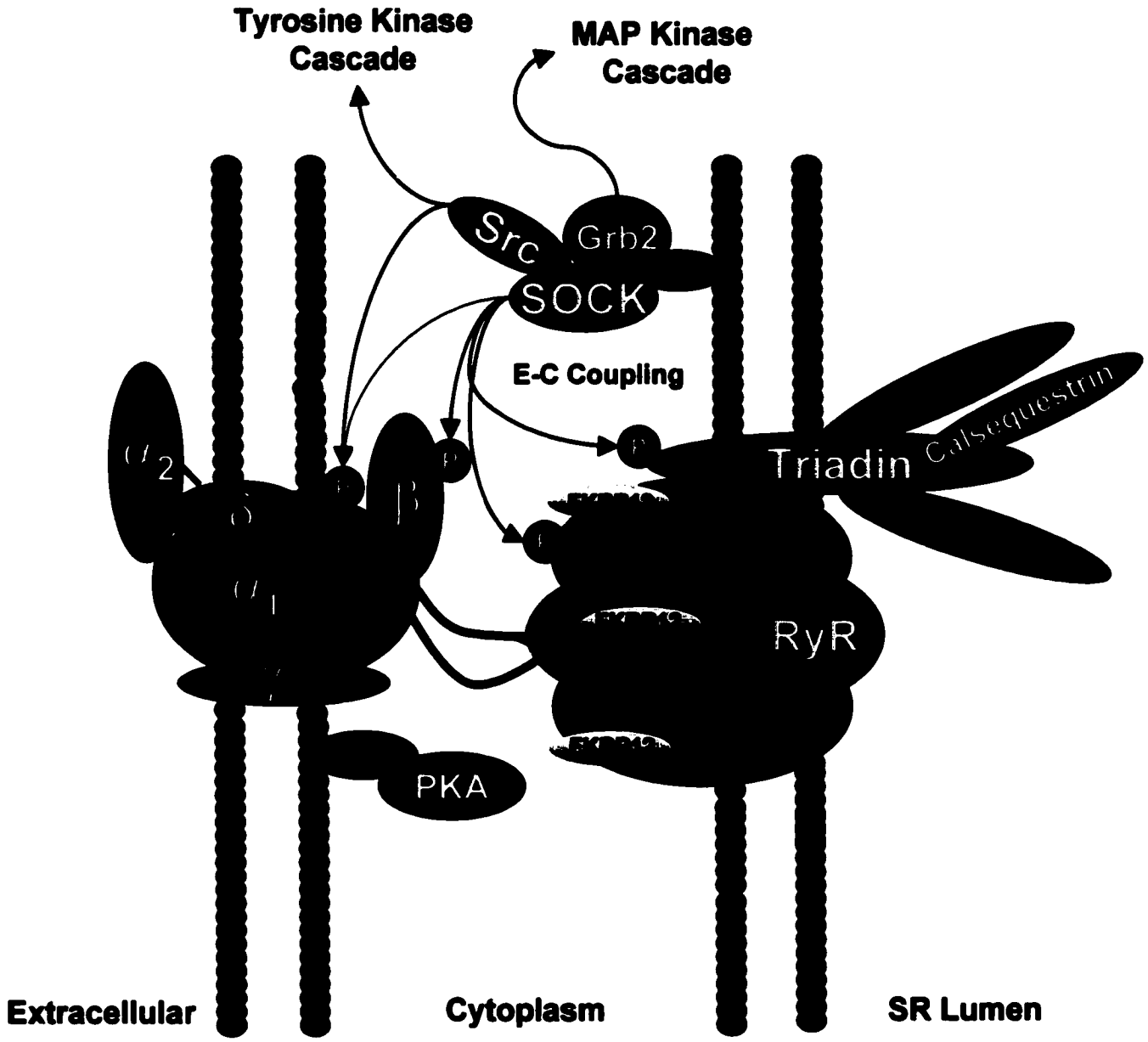
Tyrosine Kinase Cascade
MAP Kinase Cascade
Src
Grb2
SOCK
E-C Coupling
Triadin
Calsequestrin
RyR
PKA
Extracellular
Cytoplasm
SR Lumen

Future Experiments:

Further characterization of SOCK activity in the SR aimed at elucidating the molecular basis of Ca^{2+}/CaM-dependent regulation of E-C coupling may help to explain in greater detail, the regulation of muscle contraction.

The role of SOCK's interaction with SH3 domains may yield knowledge about the ways in which two separate signaling pathways, namely the Ca^{2+}/CaM-dependent and tyrosine kinase cascades, may influence one another at discrete points in their signaling cascades. Often, cross talk between cascades serve as redundant mechanisms that protect the integrity of a cell's ability to regulate its intracellular environment or respond to changes in its external environment (Pawson, 1995). This may serve as a safety mechanism that ensures the proper functioning of both pathways. For example, if the function of a signaling intermediate in one of the signaling cascades is altered due to a mutation, cross-talk between signaling cascades may serve as a redundant mechanism that protects the cell from an overactive cascade. This could be achieved by providing another mode of negative feedback to maintain homeostasis. Experiments designed to gauge the consequence of SH3 domains binding to SOCK would need to define the downstream signaling partners and events, involving either the activation of transcription of genes or possibly regulation of E-C coupling via tyrosine kinases. Also, the generation of a SOCK homozygous knockout mouse line would assist in the characterization of SOCK function. The ultimate goal would be to characterize in detail the function of SOCK, resulting in the possible implication of SOCK in a specific disease and with this knowledge, design a specific tool aimed at the treatment and restoration of a disease state back to normal health.

REFERENCES

Adams, B.A. Tanabe, T. Mikami, A. Numa, S. and Beam, K.G.: Intramembrane charge movement restored in dysgenic skeletal muscle by injection of dihydropyridine receptor cDNAs. Nature. 346: 569-572, 1990.

Anderson, M.E. Braun, A.P. Schulman, H. and Premack, B.A.: Multifunctional Ca^{2+}/calmodulin dependent protein kinase mediates Ca(2+) –induced enhancement of the L-type Ca^{2+} current in rabbit ventricular myocytes. Circ. Res. 75:854-861, 1994.

Anderson, M.E. Braun, A.P. Wu, Y. Lu, T. Wu, Y. and Schulman, H.: KN-93, an Inhibitor of Multifunctional Ca^{2+}/Calmodulin-Dependent Protein Kinase, Decreases Early Afterdepolarizations in Rabbit Heart. J. Pharm. and Exp. Thera. 287: 996-1006, 1998.

Aulbach, F. Simm, A. Maier, S. Langenfeld, H. Walter, U. Kersting, U. and Kirstein, M.: Insulin stimulates the L-type Ca2+ current in rat cardiac myocytes. Cardiovasc. Res. 42: 113-120, 1999.

Bangalore, R. Mehrke, G. Gingrich, K. Hofmann, F. and Kass, R.S.: Influence of L-type Ca channel α_2/δ subunit on ionic and gating current in transiently transfected HEK293 cells. Am. J. Physiol. 39: H1521-H1528, 1996.

Bayer, K.U. Lohler, J. and Harbers, K.: An Alternative, Nonkinase Product of the Brain-Specifically Expressed Ca^{2+}/Calmodulin-Dependent Kinase II α Isoform Gene in Skeletal Muscle. Mol. Cell. Biol. 16: 29-36, 1996.

Bayer, K.U. Harbers, K. and Schulman, H.: αKAP is an anchoring protein for a novel CaM kinase II isoform in skeletal muscle. EMBO J. 17: 5598-5605, 1998.

Bayer KU, Lohler J, Schulman H, Harbers K.: Developmental expression of the CaM kinase II isoforms: ubiquitous gamma-and delta-CaM kinase II are the early isoforms and most abundant in the developing nervous system. Brain Res. Mol. Brain Res. 7: 147-154, 1999.

Bence-Hanulec, K.K. Marshall, J. and Blair, L.A.: Potentiation of neuronal L calcium channels by IGF-1 requires phosphorylation of the alpha1 subunit on a specific tyrosine residue. Neuron 27: 121-131, 2000.

Bennet, M.K. and Kennedy, M.B.: Deduced primary structure of the beta subunit of brain type II Ca2+/calmodulin-dependent protein kinase determined by molecular cloning. Proc. Natl. Acad. Sci. U.S.A. 84: 1794-1798, 1987.

Benson, D.L. Isackson, P.J. Hendry, S.H. and Jones, E.G.: Differential gene expression for glutamic acid decarboxylase and type II calcium-calmodulin-dependent protein kinase in basal ganglia, thalamus, and hypothalamus of the monkey. J. Neurosci. 11: 1540-1564, 1991.

Berridge, M.J.: Elementary and global aspects of calcium signaling. J. Physiol. 499: 291-306, 1997.

Bers, D.M., and Stiffel, V.M.: Ratio of ryanodine to digydropyridine receptors in cardiac and skeletal muscle and implications for E-C coupling. Am. J. Physiol. 264: C1587-1593, 1993.

Bhardwaj, S.K. and Kaur, G.: Effect of diabetes on calcium/calmodulin dependent protein kinase-II from rat brain. Neurochem. Int. 35: 329-335, 1999.

Birnboim, H.C. and Doly, J.: A rapid alkaline extraction procedure for screening recombinant plasmid DNA. Nucleic Acids Res. 7: 1513-1523, 1979.

Braun, A.P. and Schulman, H.: The multifunctional calcium/calmodulin-dependent protein kinase: from form to function. Annu. Rev. Physiol. 57: 417-445, 1995.

Brilliantes, A. Ondrias, K. Scott, A. Kobrinsky, E. Ondriasova, E. Moschella, M. Jayaraman, T. Landers, M. Ehrlich, B and Marks, A.: Stabilization of Calcium Release Channel by FK506-binding protein. Cell 77: 513-523,1994

Brozinich, J.T. Reynolds, T.H. Dean, D. Cartee, G. and Cushman, S.W.: 1-[N,O-Bis-(5-isoquinolinesulphonyl)-N-methyl-L-tyrosyl]-4-phen (KN-62), an inhibitor of calcium-dependent calmodulin protein kinase II, inhibits both insulin- and hypoxia-stimulated glucose transport in skeletal muscle. Biochem. J. 339: 533-540, 1999.

Brushia, R.J. and Walsh, D.A.: Phosphorylase kinase: the complexity of its regulation is reflected in the complexity of its structure. Front Biosci. 4: D618-641, 1999.

Buck, E.D. Nguyen, H.T. Pessah, I.N. and Allen, P.D.: Dyspedic Mouse Skeletal Muscle Express Major Elements of the Triadic Junction but Lacks Detectable Ryanodine Receptor Protein and Function. J. Biol. Chem. 272:7360-7367, 1997.

Bunemann, M. Gerhardstein, B.L. Gao, T. and Hosey, M.M.: Functional regulation of L-type calcium channels via protein kinase A mediated phophorylation of the β_2 subunit. J. Biol. Chem. 274: 33851-33854, 1999.

Caswell, A.H. and Brandt, N.R.: Does muscle activation occur by direct mechanical coupling of transverse tubules to sarcoplasmic reticulum? TIBS. 14: 161-165, 1989.

Catterall, W.A.: Functional subunit structure of voltage-gated calcium channels. Science 253: 1499-1500, 1991.

Campbell, K.P. and MacLennan, D.H.: A Calmodulin-dependent Protein Kinase System from Skeletal Muscle Sarcoplasmic Reticulum. J. Biol. Chem. 257: 1238-1246, 1982.

Campbell, K.P. Sharp, A. Strom, M. and Kahl, S.D.: High-affinity antibodies to the 1,4-dihydropyridine Ca2+-channel blockers. Proc. Natl. Acad. Sci. USA. 83: 2792-2796, 1986.

Chamberlain, B.K., Volpe, P., and Fleischer, S.: Calcium-induced calcium release from purified cardiac sarcoplasmic reticulum vesicles: general characteristics. J. Biol. Chem. 259: 7540-7546, 1984.

Chatzis, G.J. and Tuana, B.S.: Biochemical characteristics and subcellular localization of CaMKII-β_4: Molecular Biology of the Cell. Abstracts, v10: 334a Abstract # 1931, 1999.

Chen, G.F. and Inouye, M.: Suppression of the negative effect of minor arginine codons on gene expression; preferential usage of minor codons within the first 25 codons of the *Escherichia coli* genes. Nucleic Acids Res. 18: 1465-1473, 1990.

Chen, G.T. and Inouye, M.: Role of AGA/AGG codons, the rarest codons in global gene expression in *Escherichia coli*. Genes Dev. 8: 2641-2652, 1994.

Chien, A.J. Zhao, X. Shirokov, R.E. Puri, T.S. Chang, C.F. Sun, D. Rios, E. and Hosey, M.M.: Roles of a membrane-localized β-subunit in the formation and targeting of functional L-type Ca^{2+} channels. J. Bio. Chem. 270: 30036-30044, 1995.

Chu, A. Sumbilla, C. Inesi, G. Jay, S.D. and Campbell, K.P.: Specific association of calmodulin-dependent protein kinase and related substrates with the junctional sarcoplasmic reticulum of skeletal muscle. Biochemistry. 29: 5899-5905, 1990.

Colbran, R. J. and Soderling, T. R.: Calcium/calmodulin-independent autophosphorylation sites of calcium/calmodulin-dependent protein kinase II. Studies on the effect of phosphorylation of threonine 305/306 and serine 314 on calmodulin binding using synthetic peptides. J Biol. Chem. 265: 11213-11219, 1990.

Colbran, R.J. Schworer, C.M. Hashimoto, Y. Fong, Y.L. Rich, D.P. Smith, M.K. and Soderling, T.R.: Calcium/calmodulin-dependent protein kinase II. Biochem. J. 258: 313-325, 1989.

Coronado, R., Morrissette, J., Sukhareva, M., and Vaughan, D.M.: Structure and function of ryanodine recptors. Am. J. Physiol. 266: C1485-1504, 1994.

Currie, S. and Smith, G.L.: Calcium/calmodulin-dependent protein kinase II activity is increased in sarcoplasmic reticulum from coronary artery ligated rabbit hearts. FEBS Lett. 459: 244-248, 1999.

Damiani, E. Picello, E. Saggin, L. and Margteth, A.: Identification of triadin and of histidine-rich Ca -binding protein as substrates of 60 kDa calmodulin-dependent protein kinase in junctional terminal cisternae of sarcoplasmic reticulum of rabbit fast muscle. Piochem Biophys Res Commun. 209: 457-465, 1995.

De Jonge, M. and Racine, R.J.: The effects of repeated induction of long-term potentiation in the dentate gyrus. Brain Res. 328: 181-185, 1985.

De Jongh, K.S. Warner, C. and Catterall, W.A.: Subunits of purified calcium channels. Alpha 2 and delta are encoded by the same gene. J. Biol. Chem. 265: 14738-14741, 1990.

De Jongh, K.S. Murphy, B.J. Colvin, A.A. Hell, J.W. Takahashi, M. and Catterall, W.A.: Specific phosphorylation of a site in the full-length form of the alpha 1 subunit of the cardiac L-type calcium channel by adenosine 3',5'-cyclic monophosphate-dependent protein kinase. Biochemistry. 35: 10392-10402, 1996.

Delbono, O.: Regulation of Excitation Contraction Coupling by Insulin-Like Growth Factor-1 in Aging Skeletal Muscle. J. Nutr. Health Aging. 4: 162-164, 2000.

De Leong, M. Wang, Y. Jones, L. Perez-Reyes, E. Wei, X. Soong, T.W. Snutch, T.P. and Yue, D.T.: Essential Ca(2+)-binding motif for Ca(2+)-sensitive inactivation of L-type Ca2+ channel. Science. 270: 1502-1506, 1995.

Dzhura, I. Wu, Y. Colbran, R.J. Balser, J.R. and Anderson, M.E.: Calmodulin kinase determines calcium-dependent facilitation of L-type calcium channels. Nature Cell Biology. Vol 2, 173-177, 2000.

Ebashi, S.: Excitation-contraction coupling and the mechanism of muscle contraction. Annu. Rev. of Biochem. 53: 1-16, 1991.

Edman,C.F. and Schulman, H: Identification and characterization of delta B-CaM kinase and delta C-CaM kinase from rat heart, two new multifunctional Ca2+/calmodulin-dependent protein kinase isoforms. Biochim. Biophys. Acta. 1221: 89-101, 1994.

Enslen, H and Soderling, T.R.: Roles of calmodulin-dependent protein kinases and phosphatase in calcium-dependent transcription of immediate early genes. J. Biol. Chem. 269: 20872-20877, 1994.

Erondu, N.E. and Kennedy, M.B.: Regional distribution of type II Ca2+/calmodulin-dependent protein kinase in rat brain. J. Neurosci. 5: 3270-3277, 1985.

Fabiato, A.: Calcium-induced release of calcium from the cardiac sarcoplasmic reticulum. Am. J. Physiol. 245: C1-14, 1983.

Fen, G. Chen, T. and Inouye, M.: Suppression of the negative effect of minor arginine codons on gene expression; preferential usage of minor codons within the first 25 codons of the *Escherichia coli* genes. Nucl. Acid. Res. 18: 1465-1473, 1990.

Field, A.C., Hill, C., and Lamb, G.D.: Asymmetric charge movement and calcium currents in ventricular myocytes of neonatal rat. J. Physiol. 406: 277-297, 1988.

Fischer, L.J. Wagner, M.A. and Madhukar, B.V.: Potential involvement of calcium, CaM kinase II and MAP kinases in PCB-stimulated insulin release from RINm5F cells. Toxicol. Appl. Pharmacol. 159: 194-203, 1999.

Flucher, B.E. Conti, A. Takeshima, H. and Sorrentino, V.: Type 3 and Type 1 Ryanodine Receptors are Localized in Triads of the Same Mammalian Skeletal muscle Fibers. J. Cell. Biol. 146: 621-629, 1999.

Fluck, M. Waxham, M.N. Hamilton, M.T. and Booth, F.W.: Skeletal muscle Ca(2+)-independent kinase activity increases during either hypertrophy or running. J. Appl. Physiol. 88: 352-358, 2000.

Franzini-Armstrong, C., and Jorgensen, A.O.: Structure and development of E-C coupling units in skeletal muscle. Annu. Rev. Physiol. 56: 509-534, 1994.

Fuentes, O. Valdivia, C. Vaughan, D Coronado, R. and Valdivia, H.H.: Calcium-dependent block of ryanodine receptor channel of swine skeletal muscle by direct binding of calmodulin. Cell Calcium. 15: 305-316, 1994.

Gao, T. Yatani, A. dell'Acqua, M.L. Sako, H. Green, S.A. Drascal, A. Scott, S.D. and Hosey, M.M.: cAMP-dependent regulation of cardiac L-type Ca2+ channels requires membrane targeting of PKA and phosphorylation of channel subunits. Neuron. 19: 185-196, 1997.

Garcia, J. Nakai, J. Imoto, K. and Beam, K.G.: Role of S4 segments and the leucine heptad motif in the activation of an L-type calcium channel. Biophys. J. 72: 2515-2523, 1997.

Guappone, A.C. and Flynn, D.C.: The integrity of the SH3 binding motif of AFAP-110 is required to facilitate tyrosine phosphorylation by, and stable complex formation with, Src. Mol. Cell. Biochem. 175: 243-252, 1997.

Guo, W. and Campbell, K.P.: Association of triadin with the ryanodine receptor and calsequestrin in the lumen of the sarcoplasmic reticulum. J. Biol. Chem. 270: 9027-9030, 1995.

Gurnett, C.A. Felix, R. and Campbell, K.P.: Extracellular interaction of the voltage-dependent calcium channel alpha 2 delta and alpha 1 subunits. J. Biol. Chem. 272: 18508-18512,1997.

Groh, S. Marty, I. Ottolia, M. Prestipino, G. Chapel, A. Villaz, M. and Ronjat, M.: Functional interaction of the cytoplasmic domain of triadin with the skeletal ryanodine receptor. J. Biol. Chem. 274: 12278-12283, 1999.

Hain, J., Onoue, H., Mayrleitner, M., Fleischer, S., and Schindler, H.: Phosphorylation modulates the function of the calcium release channel of sarcoplasmic reticulum from cardiac muscle. J. Biol. Chem. 270: 2074-2081, 1995.

Hain, J. Nath, S. Mayrleitner, M. Fleischer, S. and Schindler, H.: Phosphorylation modulates the function of the calcium release channel of sarcoplasmic reticulum from skeletal muscle. Biophys. J. 67: 1823-1833, 1994.

Hakamata, Y. Nakai, J. Takeshima, H. and Imoto, K.: Primary structure and distribution of a novel ryanodine receptor/calcium release channel from rabbit brain. FEBS Lett. 312: 229—235, 1992.

Haase, H. Bartel, S. Karczewski, P. Morano, I. and Krause E.G.: In-vivo phosphorylation of the cardiac L-type calcium channel β subunit in response to catecholamines. Mol. Cell. Biochem. 163-164: 99-106, 1996.

Hawkins, C. Xu, A. and Narayanan, N.: Sarcoplasmic Reticulum Calcium Pump in Cardiac and Slow Twitch Skeletal Muscle but Not Fast Twitch Skeletal Muscle Undergoes Phosphorylation by Endogenous and Exogenous Ca /Calmodulin-dependent Protein Kinase. J. Biol Chem. 269: 31198-31206, 1994.

Hanks, S.D. Quinn, A.M. and Hunter, T.: The protein kinase family: conserved features and deduces phylogeny of the catalytic domains. Science 241: 42-52, 1988.

Hanson, P.I. and Schulman, H.: Neuronal Ca2+/calmodulin-dependent protein kinases. Ann. Rev. Biochem. 61: 559-601, 1992.

Haribabu, B. Hook, S.S. Selbert, M.A. Goldstein, E.G. Tomhave, E.D. Edelman, A.M. Snyderman, R. and Means, A.R.: Human calcium-calmodulin dependent protein kinase I: cDNA cloning, domains structure and activation by phosphorylation at threonine-177 by calcium-calmodulin dependent protein kinase I kinase. EMBO J. 14: 3679-3686, 1995.

Herrmann-Frank, A. and Varsanyi, M.: Enhancement of Ca2+ release channel activity by phosphorylation of the skeletal muscle ryanodine receptor. FEBS Lett. 332: 237-242, 1993.

Hohenegger, M. and Suko, J.: Phosphorylation of the purified cardiac ryanodine receptor by exogenous and endogenous protein kinases. Biochem. J. 296: 303-308, 1993.

Huang, X.P. Pi, Y. Lokuta, A.J. Greaser, M.L. and Walker, J.W.: Arachidonic acid stimulates protein kinase C-ε redistribution in heart cells. J. Cell. Sci. 110: 1625-1634, 1997.

Inui, M., Saito, A., and Fleischer, S.: Isolation of the ryanodine receptor from cardiac sarcoplasmic reticulum and identity with the feet structures. J. Biol. Chem. 262: 15637-15642, 1987.

January, C.T. and Moscucci, A.: Cellular mechanisms of early afterdepolarizations. Ann. N Y Acad. Sci. 644: 23-32, 1992.

James, P., Inui, M., Tada, M., Chiesi, M., and Carafoli, E.: Nature and site of phospholamban regulation of the Ca^{2+} pump of sarcoplasmic reticulum. Nature 342: 90-92, 1989.

Jayaraman, T. Brillantes, A.M. Timerman, A.P. Fleischer, S. Erdjument-Bromage, H. Tempst, P. and Marks, A.R.: FK506 binding protein associated with the calcium release channel (ryanodine receptor). J. Biol. Chem. 267: 9474-9477, 1992.

Johnson, B.D. Scheuer, T. and Catterall, W.A.: Voltage-dependent potentiation of L-type Ca^{2+} channels in skeletal muscle cells requires anchored cAMP-dependent protein kinase. Proc. Natl. Acad. Sci. USA. 91: 11492-11496, 1994.

Kane, J.F.: Effects of rare codon clusters on high-level expression of heterologous proteins in *Escherichia coli*. Curr. Opin. Biotechnol. 6: 494-500, 1995.

Kamp, T.J. Perez-Garcia, M.T. and Marban, E.: Enhancement of ionic current and charge movement by coexpression of calcium channel β_{1a} with α_{1c} in human embryonic kidney cell line. J. Physiol. 492: 89-96, 1996.

Kim, D.H. Ohnishi, S.T. and Ikemoto, N.: Kinetic studies of calcium release from sarcoplasmic reticulum in vitro. J. Biol. Chem. 258: 9662-9668, 1983.

Kim, D.H. and Ikemoto, N.: Involvement of 60 kilodalton phosphoprotein in the regulation of calcium release from skeletal muscle sarcoplasmic reticulum. J. Biol. Chem. 261, 11674-11679, 1986.

Kim, H.W. Kim, D.H. Ikemoto, N. and Kranias, E.G.: Lack of effects of calcium X calmodulin-dependent phosphorylation on Ca2+ release from cardiac sarcoplasmic reticulum. Biochim. Biophys. Acta. 903: 333-340, 1987.

Lamb, G.:Excitation-Contraction Coupling in Skeletal Muscle: Comparisons with Cardiac Muscle. Clin and Exper Pharm and Phys. 27: 216-224, 2000.

Lamb, G.D., and Walsh, T.: Calcium currents, charge movement and digydropyridine binding in fast- and slow-twitch muscles of rat and rabbit. J. Physio. 393: 595-617, 1987.

Laemmli, U.K.: Cleavage of structural proteins during the assembly of the head of bacteriophage T4. Nature. 227: 680-685, 1970.

Laver, D.R., Baynes, T.M., and Dulhunty, A.F.: Magnesium inhibition of ryanodine-receptor calcium channels: Evidence for two independent mechanisms. J. Membr. Biol. 156: 213-229, 1997.

Ledbetter, M.W., Preiner, J.K., Louis, C.F. and Mickelson, J.R.: Tissue distribution of ryanodine receptor isoforms and alleles determined by reverse transcription polymerase chain reaction. J. Biol. Chem. **269:** 13544-13551, 1994.

Leddy, J.J. Murphy, B.J. Yi, Q. Doucet, J-P. Pratt, C and Tuana, B.S.: A 60 kDa polypeptide of skeletal-muscle sarcoplasmic reticulum is a calmodulin-dependent protein kinase that associates with and phosphorylates several membrane proteins. Biochem. J. 295: 849-856, 1993.

Leddy, J.J.: Molecular Characterization of Muscle-Specific Calmodulin-Dependent Protein Kinases. University of Ottawa, 1999.

Lee, J.C. and Edelman, A.M.: A protein activator of Ca(2+)-calmodulin-dependent protein kinase Ia. J. Biol. Chem. 269: 2158-2164, 1994.

Leong, P., and MacLennan, D.H.: Complex interactions between skeletal muscle ryanodine receptor and dihydropyridine receptor proteins. Biochem. Cell. Biol. 76: 681-694, 1998a.

Leong, P., and MacLennan, D.H.: A 37-Amino acid sequence in the skeletal muscle ryanodine receptor interacts with the cytoplasmic loop between domains II and III in the skeletal muscle dihydropyridine receptor. J. Biol. Chem. 273: 7791-7794, 1998b.

Lindemann, J.P. and Watanabe, A.M.: Phosphorylation of Phospholamban in Intact Myocardium. J. Biol. Chem. 260: 4516-4525, 1985.

Lisman, J.: The CaM Kinase II hypothesis for the storage of synaptic memory. Trends Neurosci. 17: 304-412, 1994.

Lokuta, A.J. Rogers, T.B. Lederer, W.J. and Valdivia, H.H.: Modulation of cardiac ryanodine receptors of swine and rabbit by a phosphorylation-dephosphorylation mechanism. J. Physiol. 487: 609-622, 1995.

Lu, X., Xu, L., and Meissner, G.: Activation of the skeletal muscle calcium release channel by a cytoplasmic loop of the dihydropyridine receptor. J. Biol. Chem. 269: 6511-6516, 1994.

MacLennan, D.H., Rice, W.J. and Green, N.M.: The mechanism of Ca2+ transport by sarco (endo) plasmic reticulum Ca2+ ATPases.: J. Biol. Chem. 272: 28815-28818, 1997.

MacLennan, D. H., Brandl, C.J., Korczak, B., and Green, N.M.: Amino-acid sequence of a Ca2+ and Mg2+ dependent ATPase from rabbit muscle sarcoplasmic reticulum, deduced from its complementary DNA sequence. Nature. (Lond) 316: 696-700, 1985.

MacLennan, D.H. Campbell, K.P.: A calmodulin-dependent protein kinase system from skeletal muscle sarcoplasmic reticulum. Adv. Cyclic Nucleotide Protein Phosphorylation Res. 17: 393-401, 1984.

Marks, A. R., Tempst, P., Kwang, K. S., Taubman, M. B., Inui, M., Chadwick, C. C., Fleischer, S., and Nadal-Ginard, B.: Molecular cloning and characterization of the ryanodine receptor/junctional channel complex cDNA from skeletal muscle sarcoplasmic reticulum. Proc. Natl. Acad. Sci. USA 86: 8683-8687, 1989.

Marty, E. Robert, M. Villaz, M. De Jongh, K.S. Lai, Y. Catterall, W.A. and Ronjat, M.: Biochemical evidence for a complex involving digydropyridine receptor and ryanodine receptor in triad junctions of skeletal muscle. Proc. Natl. Acad. Sci. USA. 91: 2270-2274, 1994.

Matsushita, M. and Nairn, A.C.: Inhibition of the Ca2+/calmodulin-dependent protein kinase I cascade by cAMP-dependent protein kinase. J. Biol. Chem. 274: 10086-10093, 1999.

Mayrleitner, M. Chandler, R. Schindler, H. and Fleischer, S.: Phosphorylation with protein kinases modulates calcium loading of terminal cisternae of sarcoplasmic reticulum from skeletal muscle. Cell Calcium. 18: 197-206, 1995.

McGlade-McCulloh, E. Yamamoto, H. Tan, S.E. Brickey, D.A. and Soderling, T.R. Phosphorylation and regulation of glutamate receptors by calcium/calmodulin-dependent protein kinase II. Nature 362: 640-642, 1993.

Means, A.R.: Calcium, calmodulin and cell cycle regulation. FEBS lett. 347: 1-4, 1994.

Means, A.R. and Dedman, J.R.: Calmodulin-an intracellular calcium receptor. Nature. 285: 73-77, 1980.

Meissner, G., Darling, E., and Eveleth, J.: Kinetics of rapid Ca2+ release by sarcoplasmic reticulum. Effects of Ca2+, Mg2+ and adenine nucleotides. Biochemistry 25: 236-244, 1986.

Meissner, G. and Henderson, J. Rapid calcium release from cardiac sarcoplasmic reticulum vesicles is dependent on Ca2+ and is modulated by Mg2+, adenine nucleotide, and calmodulin. J. Biol. Chem. 262: 3065-3073, 1987.

Melzer, W., Herrmann-Frank, A., and Luttgau, H.C.: The role of Ca2+ ions in excitation-contraction coupling of skeletal muscle fibers. Biochim. Biophys. Acta. 1241: 59-116, 1995.

Meszaros, L.G. Minarovic, I. and Zahradnikova, A.: Inhibition of the skeletal muscle ryanodine receptor calcium release channel by nitric oxide. FEBS. Lett. 380: 49-52, 1996.

Michalak, M. Fu, S.Y. Milner, R.E. Busaan, J.L. and Hance, J.E.: Phosphorylation of the carboxyl-terminal region of dystrophin. Biochem. Cell. Biol. 74: 431-437, 1996.

Mikami, A. Imoto, K. Tanabe, T. Niidome, T. Mori, Y. Takeshima, H. Narumiya, S. and Numa, S.: Primary structure and functional expression of the cardiac dihydropyridine-sensitive calcium channel. Nature 340: 230-233, 1989.

Miranti, C.K. Ginty, D.D. Huang, G. Chatila, T. and Greenberg, M.E.: Calcium activates serum response factor-dependent transcription by a Ras- and Elk-1 independent mechanism that involves a Ca2+/calmodulin-dependent kinase. Mol. Cell. Biol. 15: 3672-3684, 1995.

Misra, R.P. Bonni, A. Miranti, C.K. Rivera, V.M. Sheng, M. and Greenberg, M.E.: L-type voltage-sensitive calcium channel activation stimulates gene expression by a serum response factor-dependent pathway. J. Biol. Chem. 269: 25483-25493, 1994.

Mitchell, R.D. Skimmermann, H.K.B. and Jones, L.R. Ca^{2+} binding effects on protein conformation and protein interactions of canine cardiac calsequestrin. J. Biol. Chem. 263: 1376-1381, 1988.

Mochly-Rosen, D. and Gordon, A.S.: Anchoring proteins for protein kinase C: a means for isozyme selectivity. FASEB J. 12: 35-42, 1998.

Moore, R.L. Musch, T.I. and Cheung, J.Y. Modulation of cardiac contractility by mysosin light chain phosphorylation. Med. Sci. Sports Exerc. 23: 1163-1169, 1991.

Nakai, J., Imagawa, T., Hakamat, Y., Shigekawa, M., Takeshima, H., and Numa, S.: Primary structure and functional expression from cDNA of the cardiac ryanodine receptor/calcium release channel. FEBS Lett. 271: 169-177, 1990.

Nairn, A.C. and Picciotto, M.R.: Calcium/calmodulin-dependent kinases. Semin. Cancer. Biol. 5: 295-303, 1994.

Narayanan, N. and Xu, A.: Phosphorylation and regulation of the Ca^{2+}-ATPase in cardiac sarcoplasmic reticulum by calcium/calmodulin-dependent protein kinase. Basic Res. Cardiol. 92: 25-35, 1997.

Netticadan, T. Xu, A. and Narayanan, N.: Divergent Effects of Ruthenium Red and Ryanodine on Ca / Calmodulin-Dependent Phosphorylation of the Ca2+ Release Channel (Ryanodine Receptor) in Cardiac Sarcoplasmic Reticulum. Arche of Biochem and Biophys. 333: 368-376, 1996.

Netticadan, T. Temsah, R.M. Kawabata, K. and Dhalla, N.S.: Sarcoplasmic reticulum Ca(2+)/Calmodulin-dependent protein kinase is altered in heart failure. Circ. Res. 86: 596-605, 2000.

Nghiem, P. Saati, S.M. Martens, C.L. Gardner, P. and Schulman, H.: Cloning and analysis of two new isoforms of multifunctional Ca2+/calmodulin-dependent protein kinase. Expression in multiple human tissues. J. Biol. Chem. 268: 5471-5479, 1993.

Niki, I. Yokokura, H. Sudo, T. Kato, M. and Hidaka, H. Ca2+ signaling and intracelular Ca2+ binding proteins. J. Biochem. 120: 685-698, 1996.

Ontell, M. and Kozeka, K.: The organogenesis of murine striated muscle: a cytoarchitectural study. Am. J. Anat. 171: 133-148, 1984.

O'Neil, K.T. and Degrado, W.F. How calmodulin binds its targets: sequence independent recognition of amphiphilic alpha-helices. Trends Biochem. Sci. 12:59-64. 1990

Opie, L.H.: The Heart Physiology and Metabolism. (New York: Raven Press), 1991.

Otsu, K. Willard, H.F. Khanna, V.K. Zorzato, F. Green, N.M. and MacLennan, D.H.: Molecular cloning of cDNA encoding the Ca release channel (ryanodine receptor) of rabbit cardiac muscle sarcoplasmic reticulum. J. Biol. Chem. 265: 13472-13483, 1990.

Patel. R. Holt, M. Philipova, R. Moss, S. Schulman, H. Hidaka, H. and Whitaker, M.: Calcium/calmodulin-dependent phosphorylation and activation of human Cdc25-C at the G2/M phase transition in HeLa cells. J. Biol. Chem. 274: 7958-7968, 1999.

Patton, B.L. Miller, S.G. and Kennedy, M.B.: Activation of type II calcium/calmodulin-dependent protein kinase by Ca2+/calmodulin is inhibited by autophosphorylation of threonine within the calmodulin-binding domain. J. Biol. Chem. 265: 11204-11212, 1990.

Pavur, K.S. Petrov, A.N. and Ryazanov, A.G.: Mapping the functional domains of elongation factor-2-kinase. Biochemistry. 40: 12216-12224, 2000.

Pawson, T.: Tyrosine kinase signaling pathways. Princess Takamatsu Symposia 24: 303-322, 1994.

Pawson, T.: Protein modules and signaling networks. Nature 373, 573-580, 1995.

Pawson, T. and Scott, J.D.: Signaling through scaffold, anchoring and adaptor proteins. Science 278: 2075-2080, 1997.

Pelosi, M. and Donella-Deana, A.: Localization, Purification, and Characterization of the Rabbit Sarcoplasmic Reticulum Associated Calmodulin-Dependent Protein Kinase. Biochemistry (Mosc). 65: 259-268, 2000.

Pessah, I.N., Waterhouse, A.L., and Casida, J.E.: The calcium-ryanodine receptor complex of skeletal and cardiac muscle. Biochem. Biophys. Res. Commun. 128: 449-456, 1985.

Pichler, M. Cassidy, T.N. Reimer, D. Haase, H. Kraus, R. Ostler, D. and Striessnig, J.: β Subunit Heterogeneity in Neuronal L-type Ca^{2+} Channels. J. Biol. Chem. 272: 13877-13882, 1997.

Polishchuk, S.V. Brandt, N.R. Meyer, H.E. Varsanyi, M. and Heilmeyer, L.M.: Does phosphorylase kinase control glycogen biosynthesis in skeletal muscle? FEBS Lett. 362: 271-275, 1994.

Pragnell, M. De Waard, M. Tanabe, T. Mori, Y. Snutch, T.P. and Campbell, K.P.: Calcium channel β-subunit binds to a conserved motif in the I-II cytoplasmic linker of the α1-subunit. Nature. 368: 67-70, 1994.

Puri, T.S. Gerhardstein, B.L. Zhao, X.L. Ladner, M.B. and Hosey, M.M.: Differential effects of subunit interaction on protein kinase A- and C-mediated phosphorylation of L-type calcium channels. Biochemistry. 36: 9605-9615, 1997.

Rios, E., and Pizarro, G.: Voltage sensor of excitation-contraction coupling in skeletal muscle. Physiol. Rev. 71: 849-908, 1991.

Rios, E. Karhanek, M. Ma, J. and Gonzales, A.: An allosteric model of the molecular interactions of excitation-contraction coupling in skeletal muscle. J. Gen. Physiol. 102: 449-481,1993.

Roden, D.M. Lazzara, R. Rosen, M. Schwartz, P.J. Towbin, J. and Vincent,G.M.: Multiple mechanisms in the long-QT syndrome. Current knowledge, gaps, and future directions. Circulation. 94: 1996-2012, 1996.

Rosenberg, A.H. Goldman, E. Dunn, J.J. Studier, F.W. and Zubay, G.: Effects of Consecutive AGG Codons on Translation in *Escherichia coli*, Demonstrated with a Versatile Codon Test System. J. of Bacteriol. 175: 716-722, 1993.

Saito, A. Seiler, A. Chu, A. and Fleischer, S.: Preparation and Morphology of Sarcoplasmic Reticulum Terminal Cisternae from Rabbit Skeletal Muscle. J. Cell. Biol. 99: 875-885, 1984.

Sasaki, T., Inui, M., Kimura, Y., Kuzuya, T., and Tada, M.: Molecular mechanism of regulation of Ca^{2+} pump ATPase by phospholamban in cardiac sarcoplasmic reticulum. J. Biol. Chem. 267: 1674-1679, 1992.

Sather, W.A. Yang, J. Tsien, R.W. Tang, S. Mikala, G. Bahinski, A. Yatani, A. Varadi, G. and Schwartz, A.: Structural basis of ion channel permeation and selectivity: Molecular localization of ion selectivity sites within the pore of a human L-type cardiac calcium channel. Curr. Opin. Neurobiol. 268: 13026-13029, 1993.

Schneider, M.F. and Chandler, W.K.: Voltage dependent charge movement in skeletal muscle. Nature 242: 244-246, 1973.

Schulman, H. Hanson, P.I. and Meyer, T.: Decoding calcium signals by multifunctional CaM kinase. Cell. Calcium. 13: 401-411, 1992.

Schulman, H. The multifunctional calcium/calmodulin-dependent protein kinases. Current Opinion in Cell Biology. 5: 247-253, 1993.

Schulman, H. and Lou, L.L.: Multifunctional Ca2+/calmodulin-dependent protein kinase: domain structure and regulation. Trends in Biochem Sciences. 14: 62-6, 1989.

Schworer, C.M. Rothblum, L.I. Thekkumkara, T.J. Singer, H.A.:Identification of novel isoforms of the delta subunit of Ca2+/calmodulin-dependent protein kinase II. Differential expression in rat brain and aorta. J. Biol. Chem. 268: 14443-14449, 1993.

Scott, J.D.: Dissection of protein kinase and phosphatase targeting interactions. Soc. Gen. Physiol. Ser. 52: 227-239, 1997.

Silverman, H.S., Di Lisa, F., and Hui, R.C. et al.: Regulation of intracellular free Mg2+ and contraction in single adult mammalian cardiac myocytes. Am. J. Physiol. 266: C222-233, 1994.

Simmerman, H.K. and Jones, L.R.: Phospholamban: protein structure, mechanism of action, and role in cardiac function. Physiol. Rev. 78: 921-947, 1998.

Singer, D. Biel, M. Lotan, I. Flockerzi, V. Hofmann, F. Dascal, N.: The roles of the subunits in the function of the calcium channel. Science. 253: 1553-1557, 1991.

Singer-Lahat, D. Gershon, E. Lotan, I. Hullin, R. Biel, M. Flockerzi, V. Hofmann, F. and Dascal, N.: Modulation of cardiac Ca^{2+} channels in *Xenopus* oocytes by protein kinase C. FEBS Lett. 306: 113-118, 1992.

Siv, G. Andersson, E. and Kurland, C.G.: Codon Preferences in Free-Living Microorganisms. Microbiol. Rev. 54: 198-210, 1990.

Spanjaard, R.A. and Van Duin, J.: Translation of the sequence AGG-AGG yields 50% ribosomal frameshift. Proc. Natl. Acad. Sci. USA. 85: 7967-7972, 1988.

Spanjaard, R.A. Chen, K. Walker, J.R. and Van Duin, J.: Frameshift suppression at tandem AGA and AGG codons by cloned tRNA genes: assigning a codon to argU tRNA and T4 $tRNA^{Arg}$. Nuc. Acid. Res. 18: 5031-5036, 1990.

Srinivasan, M. Edman, C.F. and Schulman, H. Alternative splicing introduces a nuclear localization signal that targets multifunctional CaM kinase to the nucleus. J. Cell. Biol. 126:839-852, 1994.

Striessnig, J.: Pharmacology, Structure and Function of Cardiac L-Type Ca^{2+} Channels. Cell. Physiol. Biochem. 9: 242-269, 1999.

Stull, J.T. Lin, P.J. Krueger, J.K. Trewhella, J. Zhi, G.: Myosin light chain kinase: functional domains and structural motifs. Acta. Physiol. Scand. 164: 471-482, 1998.

Suko, J. Maurer-Fogy, I. Plank, B. Bertel, O. Wyskovsky, W. Hohenegger, M. and Hellman, G.: Phosphorylation of serine 2843 in ryanodine receptor-calcium release channel of skeletal muscle by cAMP-, cGMP- and CaM-dependent protein Kinase. Biochem et Biophys Acta. 1175: 193-206, 1993.

Sun, P. Lou, L. and Maurer, R.A.: Regulation of activating transcription factor-1 and the cAMP response element-binding protein by Ca2+/calmodulin-dependent protein kinases type, I, II, and IV. J. Biol. Chem. 271: 3066-3073, 1996.

Tanabe, T. Mikami, A. Numa, S. and Beam, K.G.: Cardiac-type excitation-contraction coupling in dysgenic skeletal muscle injected with cardiac dihydropyridine receptor cDNA. Nature. 344: 451-453, 1990a.

Tanabe, T. Beam, K.G. Adams, B.A. Nidome, T. and Numa, S.: Regions of the skeletal muscle dihydropyridine receptor critical for excitation-contraction coupling. Nature. 346: 567-569, 1990b.

Takahashi, M. Seagar, M.J. Jones, J.F. Reber, B.F.X and Catterall, W.A.: Subunit structure of digydropyridine-sesitive calcium channels from skeletal muscle. Proc. Natl. Acad. Sci. USA. 84: 5478-5482, 1987.

Takasago, T. Imagawa, T. Furukawa, K. Ogurusu, T. and Shigekawa, M.: Regulation of the Cardiac Ryanodine Receptor by Protein Kinase-Dependent Phosphorylation. J. Biochem. 109: 163-170, 1991.

Takuwa, N. Shou, W. and Takuwa, Y.: Calcium, calmodulin and cell cycle progression. Cell. Signal. 7: 93-104, 1995.

Thomas, J.W. Boerner, E.B. Knight, W.B. White, G.C. 2nd and Schaller, M.D.: SH2- and SH3-mediated interactions between focal adhesion kinase and Src. J. Biol. Chem. 273: 577-583, 1998

Timerman, A.P. Ogunbumni, E. Freund, E. Wiederrecht, G. Marks, A.R. and Fleischer, S. J. Biol. Chem 268 22992-22999 1993.

Tombes RM, Krystal GW.: Identification of novel human tumor cell-specific CaMK-II variants. Biochim. Biophys. Acta. 1355: 281-292, 1997.

Toyofuku, T. Curotto, K.K. Narayanan, N. and MacLennan, D.H.: Identification of Ser38 as the site in cardiac sarcoplasmic reticulum Ca(2+)-ATPase that is phosphorylated by a Ca2+/calmodulin-dependent protein kinase. J. Biol. Chem. 269: 26492-26496, 1994.

Tu, Y. Kucik, D.F. and Wu, C.: Identification and kinetic analysis of the interaction between Nck-2 and DOCK-180. FEBS Lett 491: 193-199, 2001.

Tuana, B.S. and MacLennan, D.H.: Isolation of the calmodulin-dependent protein kinase system from rabbit skeletal muscle sarcoplasmic reticulum. FEBS Lett. 235: 219-223, 1988.

Tuana, B.S., Murphy, B.J., and Schwarzkopf, C.: A calmodulin dependent protein kinase activity associated with rabbit heart sarcolemma. Molecular & Cellular Biochemistry 78, 47-54, 1987.

Ulrich Bayer, K. Harbers, K. and Schulman H.: αKAP is an anchoring protein for a novel CaM kinase II isoform in skeletal muscle. EMBO J. 17: 5598-5605, 1998.

Uriquidi, V. and Ashcroft, S.J.: A novel pancreatic beta-cell isoform of calcium/calmodulin-dependent protein kinase II (beta 3 isoform) contains a proline-rich tandem repeat in the association domain. FEBS Lett. 358: 23-26, 1994.

Vander, A.J. Sherman, J.H. and Luciano, K.S.: Human Physiology: The Mechanism of Body Function. McGraw-Hill, New York, 1994.

Vidal, M. Montiel, J.L. Cussac, D. Cornille, F. Duchesne, M. Parker, F. Tocque, B. Roques, B.P. and Garbay, C.: Differential Interactions of the Growth Factor Receptor-bound Protein 2 N-SH3 Domain with Son of Sevenless and Dynamin. J. Biol. Chem. 273: 5343-5348, 1998.

Walaas, S.I. and Greengard, P.: Protein phosphorylation and neuronal function. Pharmacol. Rev. 43: 299-349, 1991.

Wang, Z.M. Messi, M.L. Renganathan, M. and Delbono, O.: Insulin-like growth factor-1 enhances rat skeletal muscle charge movement and L-type Ca2+ channel gene expression. J. Physiol. 516: 331-341, 1999.

Wang, J. and Best, P.M.: Inactivation of the sarcoplasmic reticulum calcium channel by protein kinase. Nature. 359: 739-741, 1992.

Wagenknecht, T., Grassucci, R., Frank, J., Saito, A., Inui, M., and Fleischer, S.: Three-dimensional architecture of the calcium channel/foot structure of sarcoplasmic reticulum. Nature (Lond.) 338: 167-170, 1989.

Wenham, R.M. Landt, M. Walters, S.M. Hidaka, H. and Easom, R.A.: Inhibition of insulin secretion by KN-62, a specific inhibitor of the multifunctional Ca2+/calmodulin-dependent protein kinase II. Biochem. Biophys. Res. Commun. 189: 128-133, 1992.

Wenham, R.M. Landt, M. and Easom, R.A.: Glucose activates the multifunctional Ca2+/calmodulin-dependent protein kinase II in isolated rat pancreatic islets. J. Biol. Chem. 269: 4947-4952, 1994.

Witcher, D.R. Kovacs, R.J. Schulman, H.R. Cefali, D.C. and Jones, L.R.: Unique Phosphorylation Site on the Cardiac Ryanodine Receptor Regulates Calcium Channel Activity. J. Biol. Chem. 2666: 11144-11152, 1991.

Wolin, S.L. and Walter, P.: Ribosome pausing and stacking during translation of eukaryotic mRNA. EMBO J. 7: 3559-3569, 1988.

Woodgett, J.R. Davison, M.T. and Cohen, P.: The calmodulin-dependent glycogen synthase kinase from rabbit muscle. Purification, sub-unit structure and substrate specificity. Eur. J. Biochem. 136: 481-487, 1983.

Xu, A. Hawkins, C. and Narayanan, N.: Phosphorylation and activation of the Ca2+-pumping ATPase of cardiac sarcoplasmic reticulum by Ca2+/calmodulin-dependent protein kinase. J. Biol. Chem. 268: 8394-8397, 1993.

Xu, A., Hawkins, C., and Narayanan, N.: Ontogeny of Sarcoplasmic Reticulum Protein Phosphorylation by Ca^{2+} Calmodulin-dependent Protein Kinase. J. Mol Cell Cardiol. 29: 405-418, 1997.

Yang, J. Ellinor, P.T. Sather, W.A. Zhang, J.F. and Tsien, R.W.: Molecular determinants of Ca^{2+} selectivity in L-type Ca^{2+} channels. Nature 366: 158-161, 1993.

Yu, H. Chen, J.K. Feng, S. Dalgarno, D.C. Brauer, A.W. and Schreiber, S.L.: Structural Basis for the Binding of Proline-Rich Peptides to SH3 Domains. Cell. 76: 933-945, 1994.

Yuan, A. Pardy, R.L. and Chia, C.P.: Nonspecific interactions alter lipopolysaccharide patterns and protein mobility on sodium dodecyl sulfate polyacrylamide gels. Electrophoresis 20: 1946-1949, 1999.

Zahradnikova, A. Minarovic, I. Venema, R.C. and Meszaros, L.G.: Inactivation of the cardiac ryanodine receptor calcium release channel by nitric oxide. Cell. Calcium. 22: 447-454, 1997.

Zong, S. Zhou, J. and Tanabe, T.: Molecular determinants of calcium-dependent inactivation in cardiac L-type calcium channels. Miochem. Biophys, Res. Commun. 201: 1117-1123, 1994.

Zorzato, F. Fujii, J. Otsu, K. Phillips, M. Green, N.M. Lai, F.A. Meissner, G. and MacLennan, D.H.: Molecular cloning of cDNA encoding human and rabbit forms of the Ca^{2+} release channel (ryanodine receptor) of skeletal muscle sarcoplasmic reticulum. J. Biol. Chem. 265: 2244-2256, 1990.

Zuhlke, R.D. and Reuter, H.: Ca sesitive inactivation of L-type Ca channels depends on multiple cytoplasmic amino acid sequences of the alpha 1C subunit. Proc. Natl. Acad. Sci. USA 95: 3287-3294, 1998.

Zuhlke, R.D. Pitt, G.S. Deisseroth, K. Tsien, R.W. and Reuter, H.: Calmodulin supports both inactivation and facilitation of L-type calcium channels. Nature. 399: 159-162, 1999.